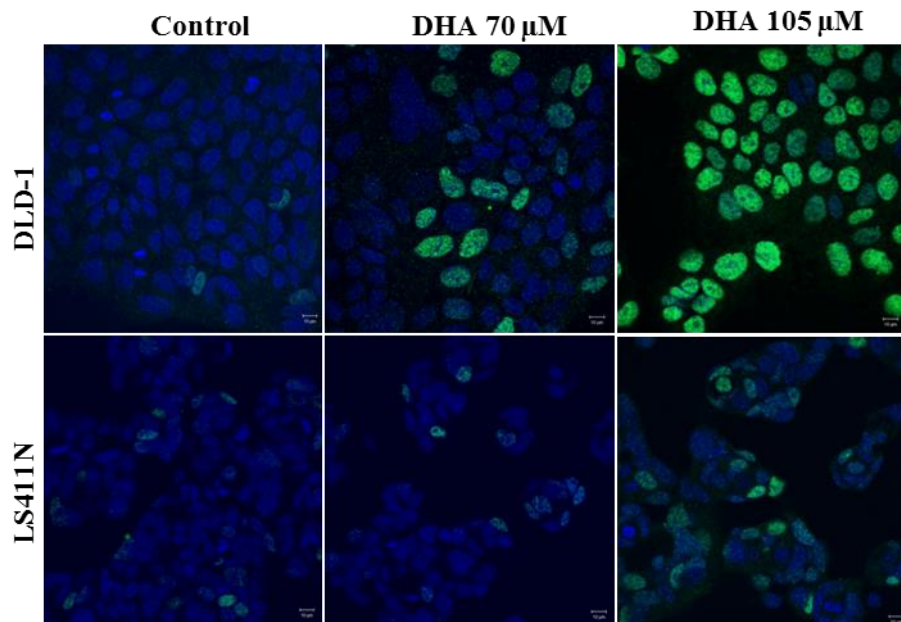Helle Samdal

# Effect of DHA on growth of two human colon cancer cell lines
# - the role of ER stress and unfolded protein response

Master thesis in Molecular Medicine

Trondheim, Spring 2014

# Contents

# Acknowledgements

# Abstract

Docosahexaenoic acid (DHA; 22:6n-3) is an essential omega-3 polyunsaturated fatty acid important to human health. DHA has been shown to have anticancer properties by reducing cancer cell proliferation, inducing apoptosis and differentiation, and inhibiting tumor cell invasion, angiogenesis and metastasis. Several mechanisms have been proposed to explain the effect of DHA in cancer. In colon cancer DHA may cause oxidative stress, changes in membrane composition or function, alterations in eicosanoid synthesis, signal transduction and regulation of gene expression. We have previously shown that DHA induces ER stress and growth arrest in some human cancer cell lines. The aim of this study was to investigate the molecular mechanisms involved in DHA anticancer properties, especially the role of endoplasmic reticulum (ER) stress, in human colon cancer cell lines with different DHA sensitivity.

Two colon cancer cell lines, grown in the same culture medium, were selected based on their differences in sensitivity towards DHA. Cell growth response after DHA treatment was measured by cell counting and MTT viability assay, showing that DLD-1 cells were sensitive to DHA (70 µM) with about 50 % growth inhibition after 48 h, while LS411N cells were considered insensitive with almost no growth inhibition at the same conditions. RT-PCR and western blotting were used to measure transcript and protein levels of ER stress and unfolded protein response (UPR) mediators, like activating transcription factor 4 (ATF4), which was found to be induced. Confocal imaging was done to investigate the localization of proteins of interest, like ATF4 that had an increased signal in the nucleus after DHA (70 and 105 µM) treatment. The role of ATF4 in DHA-mediated growth inhibition in DLD-1 cells was investigated using siRNA. DLD-1 cells transfected with siRNA against ATF4 showed a clear reduction in both ATF4 protein level and cell growth compared to cells transfected with non targeting siRNA. However, the ATF4 knockdown did not affect the DHA-mediated growth inhibition, suggesting that ATF4 alone is not responsible for the DHA-mediated effect. Preliminary results also indicated a possible increase in autophagic flux in DLD-1 cells after treatment with DHA (70 µM). In the LS411N cells, the UPR was slightly induced at later timepoints, while there was no change in autophagic flux. The role of lipid peroxidation was also studied by co-incubating both cell lines with vitamin E and DHA. Vitamin E did not conteract DHA-mediated growth inhibition in DLD-1 cells, indicating that lipid peroxidation is not the main cause of DHA-mediated cytotoxicity.

# Abbreviations

| | |
|---|---|
| AA | arachidonic acid (20:4 n-6) |
| AKT | v-Akt murine thymoma viral oncogene homolog 1 |
| ALA | α-linolenic acid (18:3 n-3) |
| ASNS | Aspargine synthetase |
| ASK1 | apoptosis signal regulating kinase |
| ATF | activating transcription factor |
| Atg | autophagy gene |
| AtgL | adipose triglyceride lipase |
| ATP | adenosine triphosphate |
| BAD | BCl-2 antagonist of cell death |
| BAK | BCl-2 antagonist killer |
| BAX | BCl-2-associated X protein |
| BCl-2 | B-cell leukemia/lymphoma 2 |
| BIM | BCl-2-interacting protein |
| BiP/GRP78 | glucose-regulated protein of 78 kDa |
| Ca | calsium |
| CAM-1 | cell adhesion molecule-1 |
| cAMP | cyclic adenosine monophosphate |
| CMA | chaperone mediated autophagy |
| CHOP/GADD153 | C/EBP homologous protein |
| c-myc | v-myc myelocytomatosis viral oncogene homolog |
| CoA | coenzyme A |
| CoAS | CoA synthetase |
| COX | cyclooxygenase |
| CYP | cytochrome P450 monooxygenase |
| DAG | diacylglycerol |
| DHA | docosahexaenoic acid (22:6 n-3) |
| DNA | deoxyribonucleic acid |
| cDNA | complementary DNA |
| E-chaderin | epithelial cadherin |
| EDEM | ER carbohydrate-binding protein |
| EDTA | ethylene diamine tetraacetic acid |
| EFA | essential FAs |
| EGFR | epidermal growth factor receptor |
| eIF2α | eukaryotic translation initiation factor 2, α subunit |
| Elovl | elongation of very long-chain fatty acid |
| EPA | eicosapentanoic acid (20:5 n-3) |
| ER | endoplasmic reticulum |
| ERAD | ER-associated degradation |
| EtOH | ethanol |
| FA | fatty acid |

| | |
|---|---|
| FAS | fatty acid synthase |
| FABP | FA binding protein |
| FAO | Food and Agriculture Organization of the United Nations |
| FFA | free FA |
| FIP200 | 200 kDa FAK-family interacting protein |
| GADD34 | growth arrest and DNA damage gene 34 |
| GRP94 | glucose-regulated protein 94 kDa |
| HMOX1 | heme oxygenase 1 |
| HNF | hepatocyte nuclear factor |
| HSL | hormone-sensitive lipase |
| HSP | heat shock protein |
| JNK | c-Jun amino terminal kinase |
| IRE1 | inositol-requiring enzyme 1 |
| JNK | cJUN NH2-terminal kinase |
| LA | linoleic acid (18:2 n-6) |
| LC3 | microtubule-associated protein 1 light chain 3/ATg8 |
| LOX | lipoxygenase |
| LXR | liver X receptor |
| MA | macroautophagy |
| MAG | monoacylglycerol |
| MAPK | mitogen-activated protein kinase |
| mTORC1 | mammalian target of of rapamycin complex 1 |
| MUFA | monounsaturated FA |
| N-3 | omega-3 |
| N-6 | omega-6 |
| N-6/n-3 ratio | the ratio between n6 and n-3 PUFAs |
| NADPH | nicotinamide adenine dinucleotide phosphate |
| NFκB | nuclear factor kappa B |
| Nrf2 | nuclear factor (erythroid-2)-related factor 2 |
| NT | non target |
| OA | oleic acid (18:1 n-9) |
| P38 MAPK | p38 mitogen-activated protein kinase |
| P58$^{IPK}$ | 58 kDa inhibitor of PKR |
| P62/ SQSTM1 | sequestosome-1 |
| PA | palmitatic acid (16:0) |
| p-AKT | phosphorylated AKT |
| PBS | phosphate saline buffer |
| p-eIF2α | phosphorylated eIF2α |
| PCR | polymerase chain reaction |
| PDK1 | 3-phosphoinositide dependent protein kinase-1 |
| p-PERK | phosphorylated PERK |
| PERK | double-stranded RNA-activated protein kinase (PKR)-like ER kinase |
| PI3K | phosphatidylinositol-3`-kinase |
| PG | prostaglandin |

| | |
|---|---|
| PIP$_2$ | phosphatidylinositol 4,5-biphosphate |
| PIP$_3$ | phosphatidylinositol 3,4,5-triphosphate |
| PPAR | peroxisome proliferator-activated receptor |
| PTEN | phosphatase and tensin homolog |
| PUFA | polyunsaturated FA |
| Rb | retinoblastoma protein |
| ROS | reactive oxygen species |
| RNA | ribo nucleic acid |
| RT-PCR | reverse transcriptase PCR |
| RXR | retinoid X receptor |
| S1P | site-1 protease |
| S2P | site-2 protease |
| SER | smooth endoplasmic reticulum |
| SERCA | sarcoplasmic/ER-Ca$^{2+}$-ATPase |
| SFA | saturated FA |
| siRNA | small interfering RNA |
| SREBP | sterol regulatory element binding protein |
| TAG | triacylglycerol |
| TE | total energy |
| TF | transcription factor |
| TG | thapsigargin |
| TRAF2 | tumor necrosis factor receptor-associated factor-2 |
| TRIB3 | tribbles-related protein 3 |
| TSP-1 | trombospondin-1 |
| UFA | unsaturated FA |
| ULK | unc-51-like kinases |
| UPR | unfolded protein response |
| VEGF | vascular endothelial growth factor |
| VCP | valosin-containing protein |
| WHO | World Health Organization |
| XBP-1 | X box binding protein-1 |

# 1. Introduction

Early studies done in the 1970`s showed a connection between the high dietary intake of fish and seal rich in n-3 polyunsaturated fatty acids (PUFAs), and low blood levels of cholesterol and triacylglycerol (TAG) among the Inuit population on Greenland. It was speculated if these results could be the reason why there were a low incidence of ischemic heart disease in the population [1]. During the last forty years there has been an increased intake of dietary fat due to a more westernized lifestyle, with a rise in the consumption of saturated animal fat and a decreased dietary intake of unsaturated fat. The high fat and high calorie intake, together with an increased n-6: n-3 ratio, have been found to influence the pathogenesis of many diseases like cardiovascular disease, obesity, diabetes, inflammation, autoimmune diseases and cancers (reviewed in [2]). Several studies have investigated the relationship between the risk of cancer and fish consumption, but many inconsistencies exist among the epidemiological studies. On the contrary, there are many in vitro and in vivo experimental studies showing anti-tumor properties of n-3 PUFAs. The mechanisms by which n-3 PUFAs reduce the growth of tumor cells probably involve the inhibition of cell proliferation, induction of cell death, or a combination of both (reviewed in [3]).

## 1.1. Cancer

### 1.1.1. Carcinogenesis

Cancer is a disease characterized by an imbalance between cell proliferation and cell death. Carcinogenesis can be divided into four main stages: tumor initiation, tumor promotion, malignant conversion, and tumor progression (Figure 1). The process is complex and involves mutational events causing the inactivation of tumor suppressor genes and the activation of protooncogenes. The accumulation of different mutations contributes to the carcinogenesis [4].
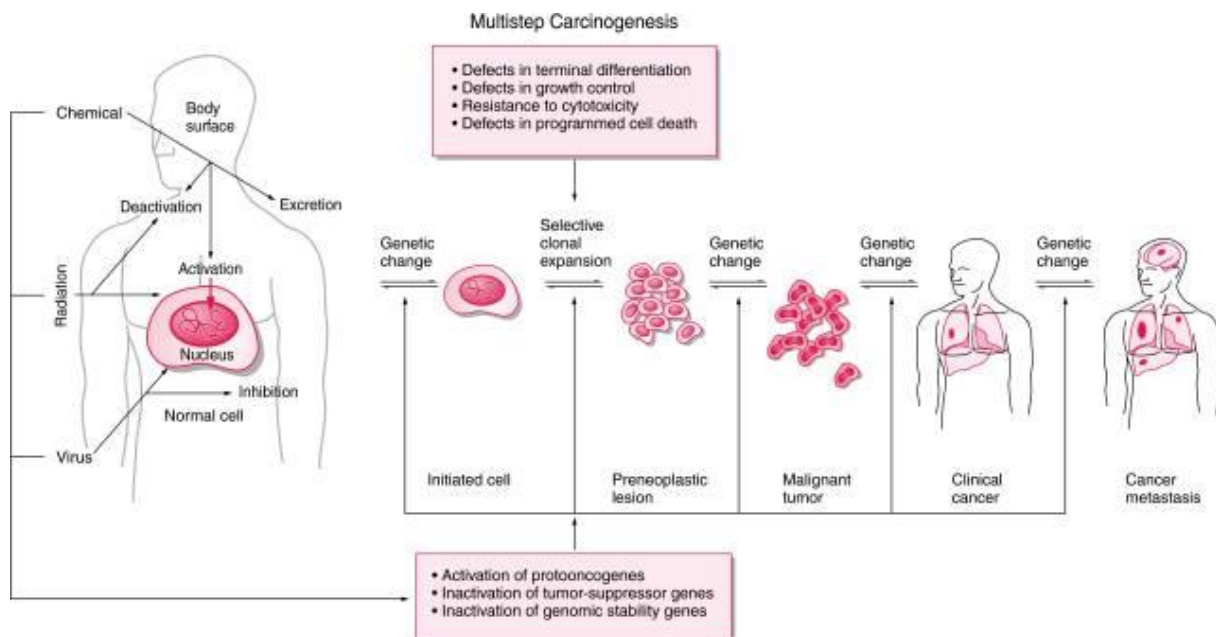
**Figure 1:** The multistep process of carcinogenesis (copied from[4]).

A tumor is composed of multiple different cell types which interact with each other. The tumor is surrounded by recruited normal cells that act as supportive participants in tumor genesis, and form the tumor-associated stroma. To understand the biology of the tumor, the contribution of the tumor microenvironment must be considered. There are different capabilities that enable tumor growth and its ability to metastasize. Hanahan and Weinberg have listed six different cellular alternations that all contributes to malignant growth (Figure 2), and are also suggesting two additional newly emerging hallmarks of cancer (reviewed in [5]).

*Unlimited growth*

The most important trait of cancer cells is their ability to have unlimited proliferation. Cancer cells have several strategies to enable them to sustain continuous proliferation. The tumor can produce its own growth factors and thereby stimulate its own growth. Alternatively the cancer cells can stimulate the normal cells in their microenvironment to supply the cancer cells with growth factors. Another strategy to increase proliferation is to elevate the amount of receptors on the cancer cell surface, which makes the cancer cells hyper responsive to the growth factors present. The cancer cells might also become independent of growth factors if signaling components downstream from these receptors become constitutive active (reviewed in [5]).

*Evading growth suppressors*

Another strategy for cancer cells to enhance proliferation is to evade growth suppressors. Two important tumor-suppressors are Retinoblastoma (RB) and P53 proteins. RB is an important gate keeper, when absent permits constitutive proliferation. P53 function both as a gate keeper and a caretaker of the cell. P53 is able to halt cell cycle progression in response to DNA damage, and if the damage is irreparable it induces apoptosis (reviewed in [5]).

*Escape cell death*

To avoid cell death by apoptosis the cancer cells evolve several different strategies. Loss of P53 is most common, but there are also other strategies like; down-regulating pro-apoptotic signals or avoiding the extrinsic ligand-induced death pathway, by increased expression of anti-apoptotic regulators or of survival signals (reviewed in [5]).

*Induce angiogenesis*

Due to the high requirement of oxygen and nutrients, and the need to remove metabolic waste and carbon dioxide ($CO_2$) in tumors, the development of tumor-associated neovasculature, a process called angiogenesis, addresses these demands. An angiogenic switch is activated in most progressing tumors due to its high requirement for nutrients and oxygen, as well as the need to remove waste products and $CO_2$. This switch is regulated by different inducers and inhibitors, like vascular endothelial growth factor-A (VEGF-A) and thrombospondin-1 (TSP-1), respectively (reviewed in [5]).

*Activate invasion and metastasis*

The invasion and formation of metastasis is a complex multistep process. It starts with local cell invasion to tissue, which eventually enters the nearby blood and lymphatic vessels, spreading to distant tissues, forming micro metastasis, and finally growing into macroscopic tumors (reviewed in [5]).

*Replicative immortality*

Normal cells can only pass through a limited number of divisions before entering senescence or crisis, while cancer cells require unlimited growth to generate macroscopic tumors. Immortalization is achieved when cells emerge from a population in crisis having the potential to unlimited replication. The limited proliferation in normal cells is caused by the

shortening of their telomeres. Most cancer cells have an increased amount of telomerase, a DNA polymerase that adds telomere repeat segments to the telomere end of DNA, which is correlated to reduced induction of senescence and crisis (reviewed in [5]).

Hanahan and Weinberg also suggest two additional hallmarks of cancer; reprogramming energy metabolism and evading immune destruction. The cancer reprograms the metabolism to optimize its support to neoplastic growth. The other emerging hallmark, to evade immune destruction, is an important feature to avoid detection by especially B- and T lymphocytes, macrophages and natural killer cells (reviewed in [5]).
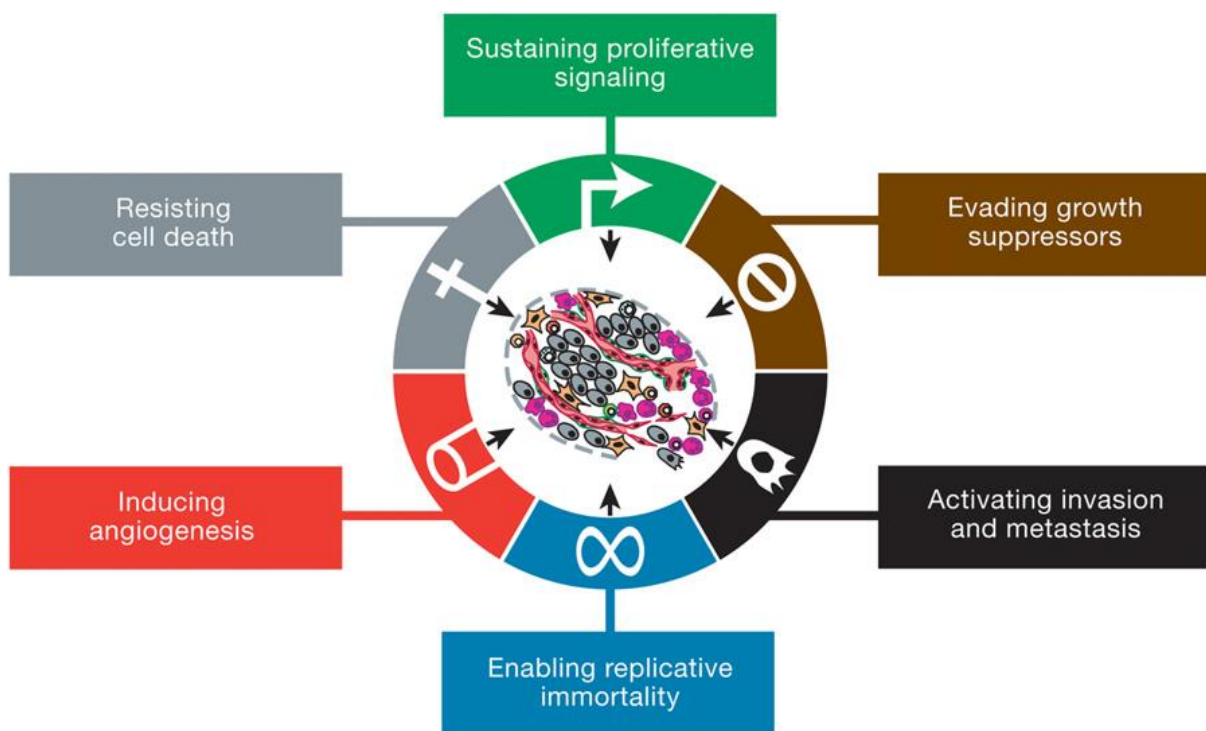


**Figure 2**: Six essential alterations in cell physiology that contribute to malignant growth (Figure is copied from [5]).

### 1.1.2. Colon cancer

According to a report from "Kreftregisteret" 2011, there was a total of 29907 new cases of cancer in Norway, which is an increase from 2010. Colorectal cancer are the forth most frequent cancer among genders, and the second leading cause of cancer related deaths in Norway [6].

The balance between cell production and cell death at the surface of the intestinal epithelium is closely regulated by different physiological endogenous factors. The carcinogenesis of the colon involves mutations in both tumor suppressor genes and oncogenes, and alterations in

gene expression. Life style and environmental factors, especially the diet, are important factors in the pathogenesis of colon cancer (reviewed in [2]).

## 1.2. Fatty acids

### 1.2.1. Classification, structure and nomenclature

Fatty acids (FAs) consist of hydrocarbon chains with a methyl group at one end and a carboxyl group at the other end. The carbon chains are bound together by single and double bonds, and classified as saturated fatty acids (SFA) and unsaturated fatty acids (UFA) respectively. UFA are further divided into monounsaturated fatty acids (MUFAs) and polyunsaturated fatty acids (PUFAs) depending on the number of double bounds [3]. There are several systems of nomenclature for FAs. The International Union of Pure and Applied Chemistry (IUPAC) use a systemic nomenclature based on the number of carbon atoms, the number of double bounds and their position relative to the hydroxyl group. Configuration of double bonds, location of heteroatoms and branched chains, and other structural features are also established by this system. Due to the complexity of the systemic names, trivial names are frequently used on FAs. Although many abbreviations for FAs exist, they all use the form C :D, which designates the number of carbons and double bonds respectively. The Delta ($\Delta$) system is another widely used terminology, and it is based on the number of carbon atoms between the carboxyl carbon and the double bounds closest to the carboxyl group. The cis/trans configuration and the position of the double bounds are also specified. In addition, the "n minus system" is a terminology commonly used, which refers to the position of the double bound closest to the methyl end [7]. The marine fatty acid, docosahexaenoic acid (DHA), has the systemic name cis-4,cis-7,cis-10,cis-13,cis-16,cis-19- docosahexaaenoic acid, but the abbreviation commonly used is 22:6n-3 (Figure 3).



**Figure 3:** Structure of DHA.

### 1.2.2. Biosynthesis of fatty acids

In humans there are little de novo synthesis of FAs as long as sufficient calories are consumed through the diet. When carbohydrates and proteins are consumed in excess of what the body

needs, they will be converted to FAs, mainly in the liver and in lactating mammary glands, where they are stored as TAGs. The de novo synthesis of FAs starts by breaking down the redundant carbohydrates into acetate units. In the FA synthase (FAS) complex the carbons from acetyl coenzyme A (CoA) is combined with a series of malonyl CoA, forming palmitate. This is an energy requiring process utilizing adenosine triphosphate (ATP) and reduced nicotinamide adenine dinucleotide phosphate (NADPH). The incorporation of a two-carbon unit from malonyl CoA is repeated until the end product, Palmitic acid (16:0), is produced. palmitic acid is released from the FAS complex, and can be further elongated and desaturated. Further elongation takes place in smooth ER (SER) by the addition of two carbon units, where malonyl CoA is the donor and NADPH supplies the electrons, a process aided by the action of different enzymes [8]. The desaturases in humans are not able to introduce double bonds between carbon atoms beyond carbon-9 and the methyl end. Hence, α- linolenic acid (ALA; 18:3n-3) and linoleic acid (LA; 18:2n:6), precursors of n-3 PUFA and n-6 PUFA family of FAs, respectively, are essential FAs that have to be supplied through diet. LA and ALA may be further elongated and desaturated to produce long chain PUFAs like eicosapentaenoic acid (EPA) and DHA, a process which is not very effective in humans. For that reason EPA and DHA are termed conditionally essential (reviewed in [7] [9]).

### 1.2.3. Uptake, transport and metabolism of fatty acids

Most of the fat consumed by humans is TAG. TAGs are being degraded by different acid-stable lipases to free FAs (FFAs) and glycerol. In the small intestine, the lipids are emulsified due to their hydrophobic nature and forms micelles together with vitamins before absorption in intestinal mucosal cells. The FFAs are re-esterified to TAGs, cholesterylesters and phospholipids in the intestinal mucosa cells and transported as part of chylomicrons through lymphatic vessels before entering the blood circulation. Due to their hydrophobic character the FAs are transported bound to albumin, as a part of lipoproteins and as chylomicrons in the circulation [10]. FAs are hydrolyzed from the chylomicrons and lipoproteins before they are transported through the capillary wall into cells as an energy-source or into the adipocytes to be stored as fat. A part of the FFAs binds to albumin and are cleared by the liver (reviewed in [7]).

In the cell the FAs are esterified into TAGs by two different pathways; the monoacylglycerol (MAG) pathway, which takes place in SER, and the *sn*-glycero-3-phosphate pathway, which takes place in the rough ER (reviewed in [7]). The TAGs are stored in lipid droplets controlled by perilipin-1. During basal conditions the perilipin promotes storage of TAGs.

The mobilization of FAs and TAG`s increases when the energy demand is high, yielding FFAs and glycerol through a process called lipolysis. Lipolysis is controlled by three lipases: hormone-sensitive lipase (HSL), adipose triglyceride lipase (Atgl) and MAG lipase (reviewed in [11]).

FAs are degraded to produce energy mainly in the mitochondria, in a process called β-oxidation. By mitochondrial β-oxidation, the FFAs are converted to acetyl-CoA molecules. The acetyl-CoA-molecules are oxidized in the tricarboxylic cycle to $CO_2$ and water, and release energy. Due to the hydrophobic character of the FAs, the β-oxidation is not an efficient process because it requires all FAs longer than 12 cabons to be transported into the mitochondria through the carrier carnitine, which is the rate limiting process (reviewed in [7]). The oxidation of short and long FAs are performed by mitochondrial β-oxidation, while very long FAs undergoes a preliminary β-oxidation in the peroxisomes, before the shortened FA enters the mitochondria for further oxidation [8]. The metabolism of FAs is summarized in Figure 4.
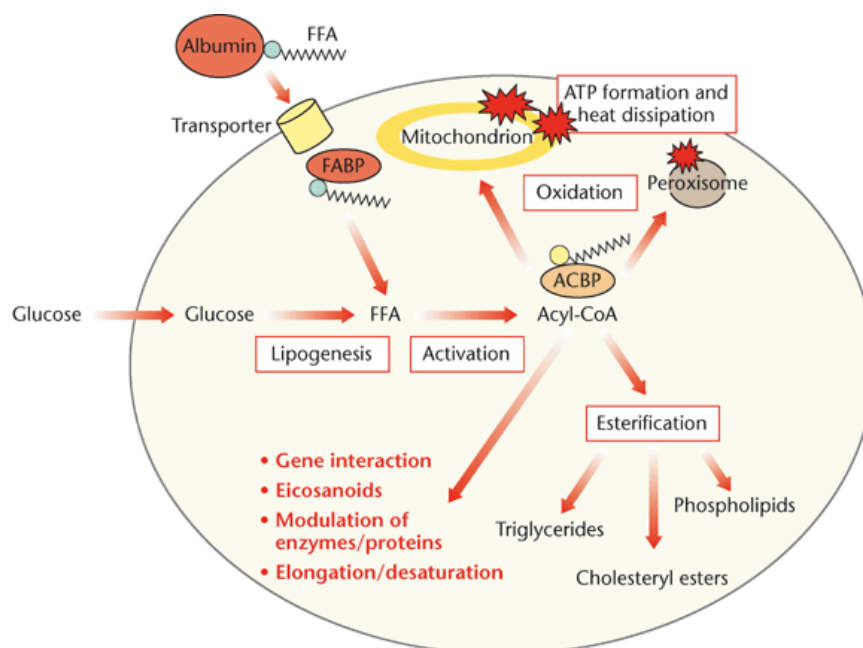


**Figure 4:** Metabolism of fatty acids (figure copied from [10]).

### 1.2.4. n-3 PUFAs

The n-3 and n-6 families of PUFAs are the most important PUFAs related to occurrence, and human diet and health [7]. The precursor for long chain n-3 PUFAs is ALA, and its main metabolic products are EPA and DHA. ALA is produced by many land plants and is a common constituent of human diet through seeds and leaves of some plants and their oils,

while EPA and DHA are abundantly present in oily fish, fish oil, liver of non-oily fish and, in lower amounts, from the flesh of non-oily fish (reviewed in [9]).

DHA and EPA are crucial for correct fetal development, especially retinal, neural, and immune function. Both have been shown to have an effect in management of patients with different chronic diseases, like coronary heart disease, rheumatoid arthritis, depression and dementia (reviewed in [12]).

According to the last report from the food and agriculture organization (FAO) of the united nations, a total intake of n-3 PUFAs can range between 0.5-2% of the total energy consumption. 0.5 % is the minimum requirement for ALA and is considered sufficient to prevent deficiency symptoms in adults. There is evidence that both DHA and EPA contribute in the prevention of coronary heart disease, and probably other degenerative diseases associated with aging. A daily intake of about 0.250 g  of EPA plus DHA is recommended for adult men and non-pregnant/non-lactating females [13].

### 1.2.5. Mechanisms of action

FAs and their derivates play a number of central roles in metabolism, as essential parts of membranes, signal molecules and as gene regulators, and can by several mechanisms influence biological systems (Figure 5). Eicosanoids are important signal molecules derived from PUFAs with 20 carbon atoms, and these signaling molecules are important for cellular functions like platelet aggregability, cell growth and chemotaxis (reviewed in [10]). Different types of eicosanoids are produced in different cells based on their biological function. There has recently been discovered new EPA- and DHA derived lipid mediators, the E- and D series of resolvins, respectively (reviewed in [14]). Membrane fluidity increases with the amount of n-3PUFAs incorporated into membrane phospholipids. The altered physical characteristics of the membrane may influence the function of different membrane proteins, thereby affecting signaling pathways. FAs have different substrate specificity to receptors and enzymes, based on their structure. The preferred substrate specificity for certain enzymes is the reason why EPA and DHA often are found in certain phospholipids. Another important mechanism of FAs and their derivates is that they can function as transcription factors (TF) by interacting with nuclear receptor proteins and altering their transcription, thereby having the ability to influence metabolism, cell proliferation and cell death. The acetylation of proteins is important for protein folding and the anchoring of some proteins in membranes. Proteins are more commonly acetylated by SFAs than by PUFAs. One of the main concerns regarding

intake of PUFAs is lipid peroxidation and the production of lipid radicals, which might cause cell damage. The degree of lipid peroxidation increases with the degree of unsaturation in lipids (reviewed in [10]).
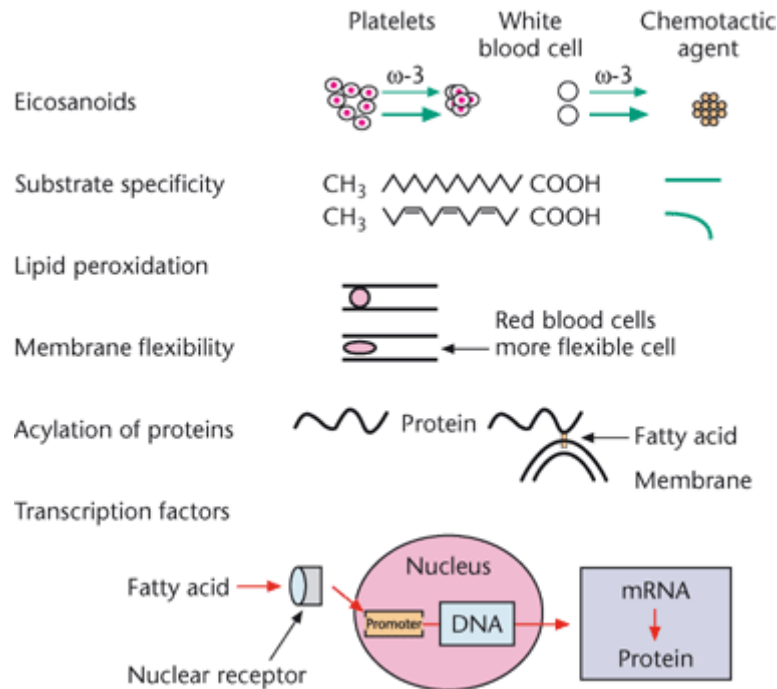


**Figure 5:** The different mechanisms by which FAs are able to influence biological systems (figure copied from [10]).

## 1.3. Cancer and PUFAs

### 1.3.1. Anticancer properties of PUFAs

The anticancer property of n-3 PUFAs are supported by in vitro and in vivo experiments, as well as by some epidemiological studies. Several experimental and clinical studies have shown that DHA can be used in the management of some types of cancers and increases the response to anticancer therapy, including radiation, hypothermia, some chemotherapeutic drugs and photodynamic therapy (reviewed in [2]).

DHA has a complex effect of both cellular and molecular mechanisms, including changes in cellular membranes, redox balance, the regulation of signaling pathways, the production of different metabolites, TFs and gene expression (reviewed in [2]).

PUFAs have been shown to interact with transcription mediators such as nuclear peroxisome proliferator-activated receptors (PPARs), the hepatocyte nuclear factor (HNF)-4α, the retinoid X receptor (RXR) alpha, the liver X receptor (LXR), sterol regulatory element-binding

proteins (SREBP`s) and the nuclear factor kappa-light-chain-enhancer of activated B cells (NF-κB)(reviewed in [2]). Impaired activity of the PPAR family members PPARβ and PPARγ are associated with colon cancer. Especially the activation of PPARγ is reported to be important in the anticancer property of n-3 PUFAs [15]. DHA inhibits the activation of NF-κB, which reduces the production of pro-proliferative eicosanoids from cyclooxygenase-2 (COX-2) and decreases the production of cancer promoting cytokines induced by NF-κB (reviewed in [2]). Different n-3 PUFAs have been shown to modulate expression of proteins involved in apoptosis and cell cycle control in colon cancer cells both in vitro and in vivo [16-18]. DHA has been found to induce cell cycle arrest and downregulate both SREBP1 and SREBP2, indicating a possible connection between cell cycle arrest and the intrusion of lipid homeostasis (reviewed in [2, 19]). An n-3 PUFA induced expression of pro-apoptotic proteins, like Bak, and decreased expression of anti-apoptotic proteins such as Bcl-2 and Bcl-XL, have been reported in several studies (reviewed in [19]). There has also been shown that n-3 PUFAs influence the expression of molecules involved in neoangiogenesis, invasion and metastatic spreading of colon cancer, where the downregulation of angiogenetic factors like VEGF, adhesion molecules (E-cadherins and CAM-1), and some proteolytic enzymes seem to be of importance (reviewed in [19]).

Oxidative stress has been proposed to cause the direct anti-cancer effect of DHA, and colon cancer cells are more susceptible to oxidative stress than normal cells (reviewed in [20]). The oxidative degradation of lipids is referred to as lipid peroxidation, a reaction consisting of three steps: initiation, propagation and termination. Free radicals remove an electron from the methylene group in lipids, causing the production of lipid radicals. The lipid radical reacts with oxygen forming a FA peroxyl radical, which can attack other FAs in the cell membrane, causing cell damage [3]. FAs are highly peroxidisable, producing reactive oxygen species (ROS) involved in cell cycle and apoptosis in tumor cells. Cancer cells have in general a lower anti-oxidative defense, and the apoptotic and anti-proliferative effects of n-3 PUFAs have been associated with increased oxidative stress (reviewed in [14]).

PUFAs that are released from phospholipid membranes are metabolized to eicosanoids by three main pathways; the COX pathway, the lipoxygenase (LOX) pathway and the cytochrome p450 monooxygenase pathway. EPA competes, with a higher affinity, for the same enzyme as the n-6 FA arachidonic acid (AA), reducing the amount of AA derived metabolites, such as the COX-2 product prostaglandin (PG) $E_2$. $PGE_2$ is proinflammatory and is associated with colorectal carcinogenesis (reviewed in [2, 14]). DHA can inhibit the

activity of COX-2, which often is found overexpressed in colon cancer cells, where it has an anti-apoptotic role. DHA can also directly inhibit $PGE_2$ (reviewed in [2]). Vascular endothelial growth factor (VEGF) is correlated to angiogenesis, and is considered a marker for poor clinical outcome (reviewed in [19]). Both EPA and DHA have been shown to downregulate VEGF through the COX-2 pathway in both colon cancer and breast cancer cells transplanted into animals [17, 21].

Incorporation of PUFAs into membranes affects the fluidity, function and structure of lipid rafts or calveoale. The localization of cell surface receptors, such as EGFR and Ras, in lipid rafts is considered to be important for the downstream signaling controlling proliferation and apoptosis. The incorporation of n-3 PUFAs can change the localization of these receptors, thereby modulating the signaling pathways (reviewed in [14, 19]). DHA has been shown to suppress the activation of Ras, an oncogene often found mutated in human cancers, by limiting its localization to the cell membrane (reviewed in [2]).

Both EPA and DHA are the precursors of the recently discovered anti-inflammatory lipid mediators: resolvins, docosatriens, and protectins, but their role in anti-cancer activity is yet not clear [3].

## 1.4. Endoplasmic Reticulum stress response

The main functions of Endoplasmic Reticulum (ER) is to maintain $Ca^{2+}$ homeostasis, bio-synthesis of lipids and sterols, synthesis of membrane- and secretory proteins and protein folding. ER stress is induced by perturbation of any of these functions, causing accumulation of unfolded or misfolded proteins in the ER lumen and subsequent activation of the Unfolded Protein Response (UPR) (Figure 6) (reviewed in [22]). The balance of influx of unfolded proteins and the efflux of folded proteins, and the proteolytic degradation of misfolded or slowly folding proteins by ER-associated degradation (ERAD), is important in maintaining ER homeostasis. Different Heat shock proteins (HSPs) are induced by different type of cellular stress. HSPs act as molecular chaperones which promote protein folding and prohibit aggregation of unfolded proteins by binding the hydrophobic surface areas of unfolded proteins (reviewed in  [23]). There are different families of molecular chaperones in the ER, where HSP27 and HPS70 are the chaperones most strongly induced after cellular stresses. Both HSP27 and HSP70 are being abundantly expressed in cancer cells compared to normal cells, which might make them potential prognostic factors (reviewed in [24]). Several types of cancers rely on ER to ensure proper structure of important proteins. Due to the high metabolic

rate sustained through the activation of signaling pathways in rapidly proliferating tumors, the ER is filled with proteins that need to be processed. If the amount of proteins exceeds the folding capacity of ER, unfolded proteins will accumulate and cause ER stress in cancer cells. The environment in solid tumors is low in pH, hypoxic and low in nutrients, which are all factors that may induce ER stress. Activating transcription factor 4 (ATF4) is found upregulated in several tumors, and causes adaptive responses in cells by regulating the expression of target genes involved in metastasis, amino acid synthesis, oxidative stress, differentiation, angiogenesis and drug resistance (reviewed in [25]). Several cancers have adapted different strategies to avoid ER stress associated cell death, which make ER stress-induced signaling pathways, like the UPR, potential targets in anti-cancer therapy (reviewed in [26]).

### 1.4.1. ER stress and UPR

The UPR is mediated by the three ER transmembrane proteins: activating transcription factor 6 (ATF6), double-stranded RNA-activated protein kinase (PKR)-like ER kinase (PERK) and inositol requiring 1 (IRE1). ATF6, IRE1 and PERK are normally bound to a member of the HSP70 family of chaperones, the heavy chain binding protein/glucose-regulated protein of 78 kDa (Bip/GRP78), which keeps them in an inactive state. When unfolded proteins accumulates in the ER lumen, Bip detaches from the three ER stress sensors and bind to the unfolded proteins (reviewed in [22]). Thapsigargin (TG) is often used to induce ER stress by inhibiting the sarcoplastic/endoplasmic $Ca^{2+}$-ATPase, causing depletion of $Ca^{2+}$ in ER (reviewed in [27]).

**PERK** is activated upon dissociation of Bip, which leads to its dimerization and auto-phosphorylation, and subsequent phosphorylation of eukaryotic translation initiation factor 2 α (eIF2α). The phosphorylation of eIF2α halts the global protein translation, decreasing the influx of proteins into the ER. After reducing the general protein burden of ER, the clearance of unfolded protein by ER associated degradation (ERAD) increases. The attenuation of translation is not absolute; some genes with a specific regulatory sequence in their 5`untranslated region can bypass the translational block mediated by phosphorylated eIF2α (reviewed in [22]). ATF4 is the most studied of the proteins escaping the translational stop. ATF4 is found upregulated in tumors, and causes adaptive responses in cells by regulating the expression of target genes involved in metastasis, amino acid synthesis, oxidative stress, differentiation, angiogenesis and drug resistance (reviewed in [25]). Not all genes targeted by ATF4 are associated with cell survival, like the TF C/EBP homologous protein (CHOP)

which is an important mediator of ER stress induced apoptosis (reviewed in [22, 24]). ATF4 induces the transcription of growth arrest and DNA damage gene 34 (GADD34), which dephosphorylates eIf2α, thereby allowing protein translation to resume (reviewed in [25]).TRIB3 is a pseudokinase induced by interaction with ATF4, and is known to modulate several signaling pathways, including the phosphatase and tensin homolog (PTEN) pathway by interacting with v-Akt murine thymoma viral oncogene homolog 1 (AKT) [28], and to negatively regulate the ATF4/CHOP pathway [29]. TRIB3 promotes ubiquitination-dependent degradation of proteins, thereby regulating cell growth, differentiation, oogenesis and metabolism. TRIB3 is often found overexpressed in colorectal cancers, where its expression is correlated with high risk of recurrence and low survival, and is therefore suggested as a novel marker for prognosis [28]. TRIB3 has also been associated with CHOP-dependent cell death during ER stress [30].

Although the activation of PERK has a pro-survival role, this turns into a pro-apoptotic signal if the ER stress is to severe or profound (reviewed in [24]). PERK activates the transcription factor, nuclear factor (erythroid-derived 2)-related factor 2 (NRF2), by phosphorylation [31]. The phosphorylation promotes its dissociation from Keap1, allowing Nrf2 to translocate to the nucleus, where it induces the transcription of genes involved in the anti-oxidative defense (reviewed in [24]). P62 is another regulator of Nrf2, which inhibit the association between Nrf2 and Keap1 by directly interacting with Keap1. This will cause the release of Nrf2, and further translocation into nucleus where it induces transcription of cytoprotective genes, including p62, creating a positive regulatory feedback loop [32].

**ATF6** is a bZIP transcription factor, which appear in two isoforms; ATF6α and ATF6β. ATF6 is transported to the Golgi upon Bip dissociation, where it is cleaved by serine protease site-1 protease (S1P) and metalloprotease site-1 (S2P), producing a 50 kDa transcriptional domain. This domain translocates into the nucleus where it transcribes genes with ATF/cAMP response element and ER stress responsive element. ATF6 is shown to induce the transcription of ER chaperone proteins such as Bip, and the transcription factors X box binding protein-1 (XBP1) and CHOP (reviewed in [22, 24, 33]).

**IRE1** has a dual role by transmitting both pro-survival and pro-apoptotic signals. IRE1 is activated by dimerization and auto-phosphorylation after dissociation from Bip. The subsequent activation of its RNAase domain leads to a translational frameshift and the cleavage of XBP1 mRNA, generating a 41 kDa variant XBP1s. XBP1s is a transcription factor, and regulates genes involved in protein folding and degradation. It also upregulates 58

kDa inhibitor of PKR (P58 IPK), which negatively regulate PERK activity (reviewed in [22]). IRE1 kinase signaling can also activate pro-death signaling by binding tumor necrosis factor receptor-associated factor-2 (TRAF2), thereby activating c-Jun amino terminal kinase (JNK), which is known to phosphorylate and inactivate members of the anti-apoptotic Bcl-2 family [24].
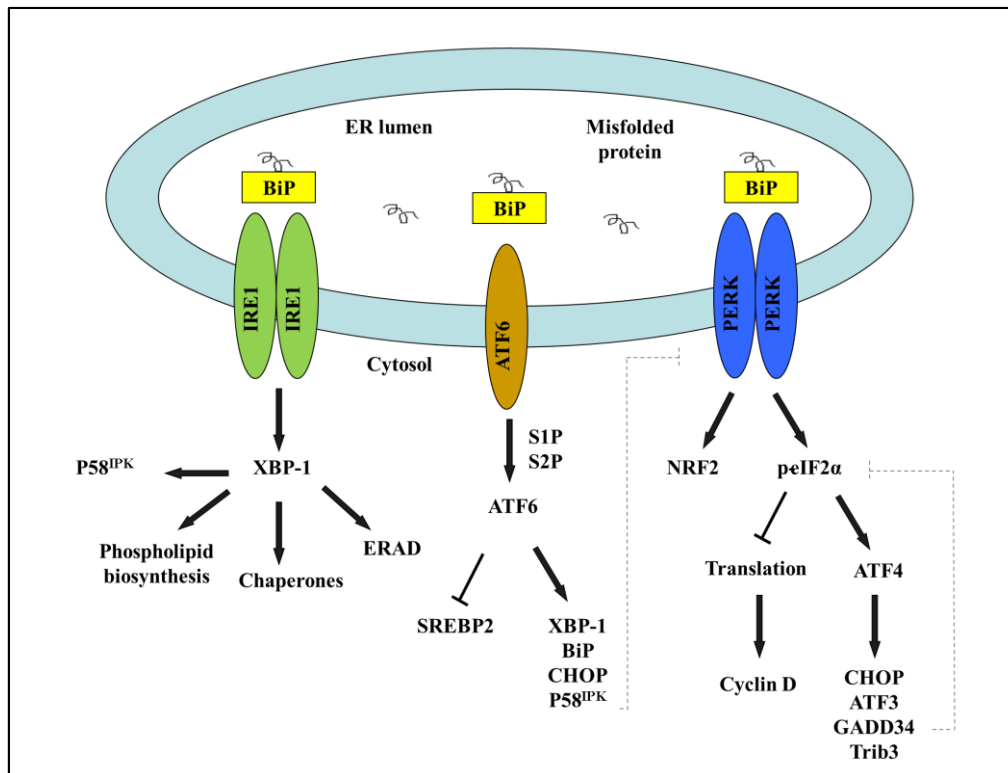


**Figure 6:** The ER stress pathway (copied from [34]).

### 1.4.2. ER stress associated degradation, autophagy and apoptosis.

Autophagy and proteasomal degradation are the two main processes responsible for protein clearance in stressed cells. ERAD is the main mechanism responsible for the clearance of unfolded and misfolded proteins during ER stress, but when the amount of proteins marked for degradation exceeds the capacity of ER, autophagy can be activated as a secondary response. Persistent stress can turn the protective functions of UPR and autophagy into cytotoxic signals and activation of cell death programs (reviewed in [35]).

### a. ER associated degradation (ERAD)

A quality control system ensures that only correctly folded proteins leave the ER. During ER stress, ERAD remove misfolded and unfolded proteins from ER by the help of protein retrotranslocation into the cytosol, followed by ubiquitination and proteasomal degradation

14

(reviewed in [35]). The IRE1/XBP1 pathway induces many genes required for induction of ERAD, one of these being EDEM, which is involved in the recognition and targeting of unfolded proteins for proteosomal degradation (reviewed in [36]). If ERAD does not function properly, proteins accumulate in the ER lumen and induce apoptosis (reviewed in [35]).

**b. Autophagy**

Autophagy is a highly regulated degradation process (Figure 7). A high induction of autophagy can cause cell death possibly through the activation of apoptosis, or as a result of the cell being unable to survive the non-specific degradation of high amounts of its cytoplasmic components (reviewed in [37]). The clearance of damaged or unneeded cellular components at basal levels is necessary to maintain cellular homeostasis.  If autophagy does not function properly, it can contribute to several diseases, including cancer, diabetes, neurodegenerative diseases, muscle atrophy and infectious diseases (reviewed in [27]). Autophagy is stimulated by several stress signals, such as nutrient deprivation and anticancer agents. There are three types of autophagy; macroautophagy (MA), chaperone mediated autophagy (CMA) and microautophagy (reviewed in [27, 38]). Both micro- and macroautophagy can envelope large structures through selective and non-selective mechanisms, while CMA just degrade soluble proteins (reviewed in [37]). MA is the degradation process for most cytoplasmic components, with the formation of double-membrane vesicles called autophagosomes, which engulf long-lived proteins, damaged organelles and some pathogens. The formation of an autophagosome membrane is a multistep process involving vesicle nucleation, elongation, fusion with lysosomes and degradation of its cargo by lysosomal hydrolases as the last step (reviewed in [35, 38]).

More than 30 autophagy-related genes (Atg) have been identified, first discovered in yeast. The formation of autophagosomes is a complex process and involves the formation of different complexes. The UNC-51-like kinases (ULK) complex regulates early stages of autophagosome formation by associating with the autophagy isolation membrane upon activation. It also functions as a sensor of nutrient status in the cell, and initiates autophagy by recruiting autophagy proteins to the autophagosomes (reviewed in [27]).

In mammals, the different classes of phosphatidylinositol-3`-kinases (PI3Ks) are involved in the signaling pathways controlling MA. Initiation of autophagy requires formation of a complex between class III PI3k (PI3KC3), Beclin1 and the myristylation protein kinase p150 [39]. When activated by recruitment to the cell surface by growth receptor tyrosine kinases,

PI3K catalyzes the conversion of phosphatidylinositol 4,5-biphosphate ($PIP_2$) to phosphatidylinositol 3,4,5-triphosphate ($PIP_3$), a process inhibited by phosphatase and tensin homolog (PTEN), a tumor suppressor often found mutated in human cancers. $PIP_3$ function as a docking site for several proteins, including AKT serine/threonine kinase, and for the 3-phosphoinositide dependent protein kinase-1 (PDK1). AKT is activated by PDK1, and phosphorylates many target proteins, and is found to regulate cell proliferation, survival and motility. Phosphorylated AKT can activate mammalian target of of rapamycin (mTOR), thereby inhibiting autophagy [40].

Further elongation of the autophagosome requires two ubiquitin-like conjugation systems, where one of them converts microtubule-associated protein-1 light-chain 3 (LC3) from its free form, LC3-I, to a phosphatidylethanolamine(PE)-conjugated form, LC3-II. The amount of LC3-II is closely connected to the number of autophagosomes, and commonly used as an indicator of autophagosome formation ([39], reviewed in [27]). The protein p62 is a selective substrate for autophagy by binding ubiquitin and LC3, thereby regulating the formation of aggregates [32, 41].
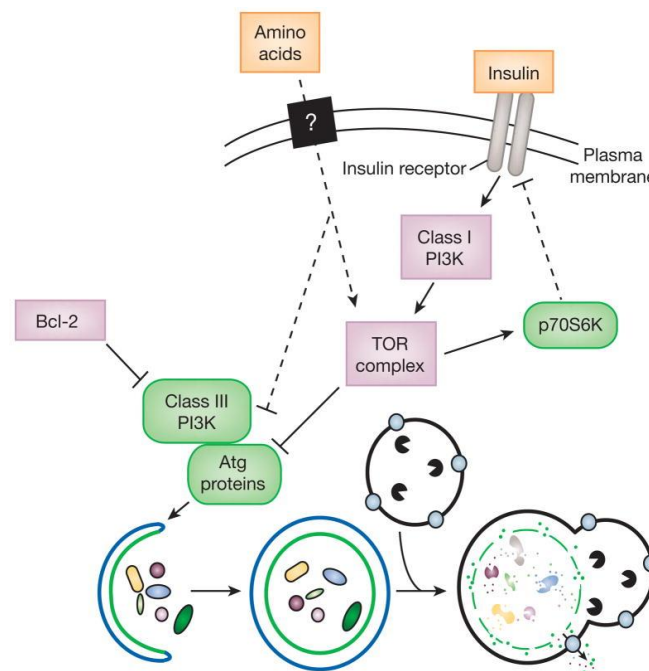


**Figure 7:** A simplified figure of the regulation of autophagy, where the protein in green and pink are stimulatory and inhibitory, respectively (copied from [37]).

Autophagy can be a protective or death inducing pathway, and can either help cells to manage ER stress, or contribute to ER stress induced cell death. Different types of ER stresses have

been shown to stimulate autophagy. Autophagy can be activated through the release of $Ca^{2+}$ from ER, and by two of the UPR pathways, IRE1α and PERK-eIF2α (reviewed in [35]). Activation of the IRE1/TRAF2/JNK arm of ER stress seems to regulate autophagy through Bcl-2 phosphorylation, preventing its association with, and inhibition of, Beclin-1. Beclin-1 is required for the initiation of the formation of the autophagosome, and is now free to bind to class III phosphoinositide-3-kinase (PI3K), promoting vesicle nucleation (reviewed in [35] [38]). Several studies have shown that the phosphorylation of eIF2α plays an important role in the ER stress induced activation of autophagy. PERK contributes to the induction of autophagy by phosphorylation of eIF2α, followed b the activation of ATF4 which induce the expression of Atg12, while activated CHOP induces the transcription of Atg5 (reviewed in [35]). Another way of stimulating ER stress associated autophagy, is through ATF4 and the stress regulated protein p8, which upregulate TRIB3, leading to the inhibition of the Akt/mTORC1 axis, thereby reducing the negative regulation on autophagy. mTORC1 is a protein complex that plays an important role in protein synthesis, cell growth and proliferation. It also seems to inhibit the activity of Atg1, Atg13-Atg17/FIP200 complex. By the inhibition of mTOR, ULK1 and ULK2 are activated, and phosphorylate Atg13 and FIP200, which are essential for autophagy activity (reviewed in [35, 38]) Baf A1is commonly used to inhibit autophagosome-lysome fusion (reviewed in [42]).

## c. Apoptosis

Apoptosis, also called programmed cell death, is characterized by cell shrinkage, blebbing of the membrane, chromatin condensation and fragmentation into apoptotic bodies. There are two main pathways; the extrinsic pathway and the intrinsic pathway. The extrinsic pathway is mediated by death receptors, which transduce extracellular signals into the cell. The intrinsic pathway, also called the mitochondrial pathway, is initiated by different stimuli such as genetic damage, high $Ca^{2+}$ concentration, hypoxia and oxidative stress within the cell (reviewed in [43]). The initiation is followed by the release of pro-apoptotic molecules, like cytochrome-c, into the cytoplasm. The intrinsic pathway is regulated by pro-apoptotic (e.g. Bak, Bax and Bad) and anti-apoptotic (e.g. Bcl-2) proteins of the Bcl-2 family. Both the intrinsic- and extrinsic pathway lead to a common pathway, the execution phase of apoptosis, which involves the activation of several caspases (reviewed in [43]). A third less known initiation pathway is the intrinsic ER pathway, which is induced by prolonged or severe ER stress (reviewed in [43]). CHOP and JNK are reported to play important roles in induction of the ER stress associated apoptosis. The PERK/eIF2α induction of CHOP may cause the

17

switch from pro-survival to pro-apoptotic signaling, by the regulation of TRIB3, the Bcl2 family and growth arrest and DNA damage inducible protein 34 (GADD34) (reviewed in [44]) . CHOP releases the translational suppression through the induction of GADD34 which dephosphorylates eIF2α, thereby increasing the protein load in the ER lumen [45]. CHOP is also thought to upregulate pro-apoptotic proteins of the Bcl-2 family and downregulate anti-apoptotic members of the same family, causing the release of cytochrome c form the mitochondria into the cytosol (reviewed in [35]). IRE1 is another promoter of ER-induced apoptosis. By recruiting TRAF2, apoptosis signal regulating kinase (ASK1) is stimulated, which activates JNK and P38 MAPK. JNK inactivates Bcl-2 and activates Bim by phosphorylation, while P38 MAPK promotes apoptosis by activation of CHOP. Both ER stress induced apoptotic pathways eventually activates the caspase cascade mediated by caspase-9 and caspase-3, resulting in ER stress induced cell death (reviewed in [35] [44]).

## 1.5. Aim of study

The aim of this study was to elucidate molecular mechanisms involved in DHA mediated anticancer properties in human colon cancer cell lines. Recent work from our group has shown that endoplasmic reticulum (ER) stress-related genes and proteins are induced after DHA treatment in the colon cancer cell line SW620 [16]. This study aims at investigating whether differences in the induction of the ER stress response in DHA sensitive vs. non-sensitive human colon cancer cell lines grown in the same culture medium could explain some of the differences in sensitivity.

# 2. Materials and methods

## 2.1. Cell culture

### 2.1.1. Cell lines

LS411N is a human colorectal carcinoma cell line, isolated from a primary Dukes` type B tumor, while DLD-1 is a human colorectal adenocarcinoma cell line, from a Dukes` type C tumor. Both DLD-1 and LS411N were obtained form the American Type Culture Collection (ATCC, USA).

### 2.1.2. Cell subcultivation, supplementation and treatment of cells for experiments

**a. Subcultivation**

DLD-1 and LS411N were grown in 75 cm² cell culture flasks incubated at 37 °C in a humid atmosphere of 5 % $CO_2$ and 95 % air. Both cell lines were grown in RPMI 1640 medium from Gibco, supplemented with fetal bovine serum (10 % FBS) and Gentamicin (45 mg/l). All solutions and equipment used during cell handling are listed in Appendix A. During cell subcultivating, all growth medium was removed and the cells were washed with phosphate saline buffer (PBS, 2 x 5 ml). Cells were enzymatically detached by incubating the cells with Trypsin (1 ml) with ethylene diamine tetraacetic acid (EDTA) for 8 minutes. After detachment, the cells were re-suspended in fresh growth medium, counted using the Moxi Z cellcounter (Orflo technologies, USA) and added to a new culture flask. All solutions used when handling the cells were preheated in a water bath (37 °C).

**b. Thawing**

Cells were retrieved from the $N_2$ container and thawed in a 37 °C water bath for about 5 minutes, before resuspended and added to a 15 ml tube containing 9 ml growth medium. The cells were centrifuged at 125 g for 7 minutes, and the supernatant was discarded to remove DMSO from the cryoprotective media. The cell pellet was re-suspended in 4 ml preheated growth medium, and transferred to a 25 cm² flask. The flask was incubated at 37°C and 5 % $CO_2$, and sub-cultivated when the cells were about 70 % confluent.

**c. Treatments and supplementation**

Different treatments were used, including ethanol (EtOH) as control, oleic acid (OA, 1770 mM), docosahexaenoic acid (DHA, 761 mM), vitamin E (α-tocopherol, 400 mM),

19

Bafilomycin A1 (BafA1, 0.16 mM) or TG (650.75 g/mol). Stock dilutions were prepared in absolute EtOH and stored at -20°C.

The cells were seeded 24 hours (h) before treatment, before the medium was discarded and replaced with the supplemented growth medium. The different treatments were added to the growth medium in wanted concentrations using a syringe. The supplemented growth medium was vortexed for 30 seconds, covered with aluminimum, incubated in a 37°C water bath for 15 minutes, and then vortexed for 30 seconds before use. The same protocol was used for the FAs, EtOH and TG.

*Vitamin E treatment*

The medium was replaced 24 h after seeding by medium with different treatments for pre-incubation. Some of the cells received regular medium with no supplements, while others were pre-incubated with EtOH or vitamin E. The pre-incubation medium was replaced after 24 h with medium supplemented with Vitamin E + DHA, EtOH + DHA, EtOH + Vitamin E, DHA, EtOH or vitamin E. All treatments were added to medium according to the above protocol.

*Bafilomycin A1 treatment*

The medium was replaced 24 h after seeding by medium with different treatments; EtOH (70 µM), DHA (70 µM), BafA1 (100 nM), or DHA + BafA1. All treatments were added to medium as described above, and total protein was isolated according to protocol (chapter 2.6.1).

## 2.2. Cell counting

The effect of DHA supplementation was investigated by comparing untreated and treated cells grown under the same conditions in the time intervals of 24, 48 and 72 h after seeding. Cells were seeded in 12 well plates, using 3 parallels per treatment. 24 h after the cells were seeded, the growth medium was removed, and growth medium supplemented with DHA, OA or EtOH, were added. Every 24 h after supplementation, the growth medium was discarded and the cells were washed with PBS (2 x 1 ml), detached from the wells using Trypsin (0.15 ml) and re-suspended in growth medium (1 ml) before counting the cells with Moxi z, using the type S cassette.

## 2.3.  MTT cell viability assay

The growth effect of DHA in the DLD-1 and LS411N cells were evaluated using the MTT assay. The MTT assay is developed by Mosmann [46], and is commonly used to measure cytotoxicity, proliferation or activation in cells after treatment with different substrates. The activity of the mitochondrial enzyme succinate dehydrogenase, which cleaves the tetrazole ring of the yellow substrate MTT (3-(4.5-dimetylthiazol-2-yl) 2.5-diphenyl tetrazolium bromide) in the oxidation of succinate to fumarate in the citric acid cycle, forms a dark blue formazan product. The formazan product is only generated in living cells and the absorbance at 500 nM, measured spectrophotometrically, is directly proportional to their mitochondrial activity [46].

The cell survival of both cell lines was measured using 96-well microtitre dishes, and 3000 LS411N cells and 1500 DLD-1 cells were seeded per well. The dishes were incubated for 4 h to ensure attachment of the cells, before culture medium was replaced with medium supplemented with DHA (35, 70 or 105 µM) or EtOH (70 µM) as control, according to treatment protocol (chapter 2.1.2.c). The plates were incubated for 0-96 h before supplemented medium was replaced with 100 µl medium containing MTT (stock solution 5 mg/ml in PBS diluted 1:10 in growth medium). After 4 h incubation, 50 µl of the medium containing MTT was replaced with 100 µl isopropanol containing HCl (3.3 ml/l) to solubilize the MTT-formazan, and the dishes were placed on a shaker for 30 minutes at room temperature. The absorbance was measured on a Titertek Multiscan Plus$^R$ Reader at 570 nm.

## 2.4.  Isolation, quality assessment and quantification of total RNA

For total RNA isolation, $1.24 \times 10^6$ DLD-1 cells were seeded in 15 cm plates. 24 h after seeding the medium was removed and treatments were added according to protocol (chapter 2.1.2.c.). Cells were harvested 3, 6, 12, and 24 h after treatments. The growth medium was removed and the cells were washed with ice cold PBS, before they were scraped in 6 ml cold PBS and collected in a pre-cooled 15 ml tube. The cell suspension was centrifuged at 4 °C for 10 minutes at 2000 rpm and the supernatant was discarded before the pellet was re-suspended in 1 ml cold PBS and transferred to a pre-cooled Eppendorf tube. The suspension was again centrifuged at 4 °C for 10 minutes at 2000 rpm, the supernatant was removed and the pellet stored at -80 °C.

### 2.4.1. Total RNA-isolation

Total RNA-isolation was performed in a RNase free/pre-PCR room. Working area and equipment was washed with RNase Away (VWR) and sterile, RNase-free disposable equipment was used. Total RNA was isolated using the RNA easy mini kit (Qiagen) according to manufactures protocol. In short, cells were lysed and passed through a QiaShredder coloumn to homogenize the sample. The flow through was added absolute EtOH for precipitation of RNA and then applied to a quick spin column. The columns were centrifuged, before washing and DNase I treatment to remove DNA (RNase free DNase set, Qiagen). After additional washing steps, total RNA was eluted in RNase free water. Total RNA was stored at -80 $^{\circ}$C.

### 2.4.2. Quality assessment and quantification of total RNA

RNA quality was evaluated using BioAnalyzer (Agilent Technologies). RIN value should be above 7 for cell line samples. The electrophoresis should show specific bands for 28S and 18S ribosomal RNA and rRNA ratio (28S/18S) should be about 2, indicating intact and pure RNA. The concentration and quality of total RNA was also measured using the NanoDrop$^R$ ND-1000 Spectrophotometer (ND-1000, NanoDrop technologies). The absorbance was measured using 2 µl total RNA. The RNA to protein ratio (260/280) of about 2.0 is generally accepted as "pure" for RNA, indicating low protein contamination. The RNA to chemical contaminants ratio (260/230) should be in the range 1.8-2.2, where a lower ratio may represent the presence of co-purified contaminants, such as guanidinetriphosphate. ND-1000 is a full-spectrum (220-750nM) spectrophotometer that measures the consentration and quality of 1-2 µL sample placed on a light-absorbing fiber cable. Another fiber cable is then placed on top of the sample, creating a liquid bridge between the optic ends. A pulsed xenon flash sends light through the sample, and a spectrophotometer using a Charge Coupled Device (CCD) analyzes the light after passing through the sample [47].

## 2.5. Real time reverse transcriptase polymerase chain reaction

### 2.5.1. RT-PCR

The effect of DHA on different ER stress pathway related genes in DLD-1 was investigated using real time reverse transcriptase (RT) polymerase chain reaction (PCR). The quantification of mRNA was performed using RT$^R$ Profiler PCR Array (Qiagen) according to manufactures protocol. In short, 500 ng total RNA from the samples was reverse transcribed into cDNA using the RT$^2$ First Strand Kit (Qiagen). Then the cDNA were mixed with a

fluorescent dye to allow detection using the RT$^2$ SYBR$^R$ Green ROX$^{TM}$ qPCR Mastermix (Qiagen). The components were dispensed into the PCR array applying 25 µl of the sample mix in each well before sealing it with an optical adhesive film. The PCR array was analyzed by using the real-time cycler AB1 StepOnePlus$^R$ instrument (Applied Biosystems) following the recommended protocol. The PCR array of 96 wells in total, contain 84 wells which assay UPR pathway specific genes, 5 different housekeeping genes for normalization, and controls that evaluate quality of the sample and the reaction [48].

### 2.5.2. Data analysis RT PCR

The threshold cycle (Ct) for each well was calculated using the real time cycle software. First the baseline was set automatically before manually defining the threshold by considering the log view of the amplification plots. The threshold was set to the same value for PCR arrays that were to be compared, by choosing a signal within the lower third of the linear phase, but above the background signal. The Ct values were exported to excel and further analyzed in the SABioscience's web-based PCR Array Data Alaysis Software (www.SABiosciences.com/pcrarraydataanalysis.php). The link "from Ct to fold change in minutes/web-based" was opened, then choosing standard RT$^2$ PCR array type PAHS-089Y before uploading the excel file with the Ct values.

## 2.6. Cell harvesting and protein isolation

1.24 x10$^6$ cells of DLD-1 were seeded in 15 cm plates and 3.6 x 10$^6$ cells of LS411N in 10 cm plates, and the growth medium was replaced after 24 h with growth medium supplemented with different treatments: DHA (70 µM), EtOH (70 M), OA (70 µM) as a negative control and Tg (1 µM) as a positive control. The cells were harvested after 3, 6, 12 and 24 h of incubation. As a control of DHA sensitivity, cells from the same cell-suspension used for protein harvesting, were seeded in a 12 well tray for counting after 48 h receiving the same treatment.

### 2.6.1. Total cell extract

The medium was removed and the cells were washed with ice cold PBS with 1mM EDTA (2x10 ml), before scraping in 6 ml cold PBS and collecting in a pre-cooled 15 ml tube. The cell suspension was centrifuged at 4$^°$C for 10 minutes at 2000 rpm, and the supernatant was discarded before the pellet was re-suspended in 1 ml cold PBS and transferred to a pre-cooled Eppendorf tube. The suspension was again centrifuged at 4$^°$C for 10 minutes at 2000 rpm, and the supernatant was removed. Urea lysis buffer (2 x packed cell volume) was added, before vortexing for 30 seconds, followed by 30 seconds incubation on ice. This was repeated twice

before centrifuged at 4 °C for 15 minutes at 13 000 rpm. The supernatant was transferred to new cold Eppendorf tubes, frozen in liquid nitrogen, and stored at -20°C.

### 2.6.2. Cell extract for phosphorylated proteins

The medium was removed and the cells were washed with ice cold PBS with 1mM EDTA and phosphatase inhibitors (2x10 ml), before they were scraped in 6 ml cold PBS and collected in a pre-cooled 15 ml tube. The suspension was centrifuged at 4°C for 10 minutes at 2000 rpm, and the supernatant was discarded before the pellet was re-suspended in lysis buffer (Appendix B) and transferred to a pre-cooled Eppendorf tube. The suspension was Incubated 10 minutes on ice before centrifuged at 4°C for 15 minutes at 13200 rpm. The supernatant was transferred to a cold 1.5 ml tube, before frozen in liquid nitrogen and stored at -20°C.

## 2.7.  Quantification of protein

The protein concentrations were determined by using the Bio-Rad assay, containing Coomassive Brilliant Blue G-250 dye, which changes color when binding to aromatic and basic protein residues. Absorbance measured at 595 nM will be higher in samples with higher protein concentrations [49]. The Biorad concentrate was diluted in MQ water in a ratio of 1:5. Two parallels from each protein extract were made by adding 1 μl sample to 999 μl diluted Biorad, before measured on the spectrophotometer on 595 nM 15 minutes after sample preparation. The respective lysis buffer served as blank measurement. The protein concentration for each sample was calculated based on the measured absorbance and a premade standard curve, following formula 1.

Protein concentration (μg/μl): Absorbance 595 x 22.02 x dilution.         **Formula 1**

## 2.8.  Western blotting

### 2.8.1.  Preparation of samples

The samples used in SDS-polyacrylamide gel electrophoresis were prepared by diluting the protein extracts in Tris-HCL (10mM, pH 8,0) to achieve an equal concentrations of proteins. After the samples were diluted, NuPAGE LDS buffer (Life Technologies, USA) and dithiothreitol (DTT)(Sigma Aldrich,USA) were added. The prepared samples hold 70 % diluted proteins, 25 % NuPAGE LDS 4x sample buffer and 5 % DTT. The samples were heated on 80°C for 15 min, spun down and put on ice before they were loaded on the gel.  A

standard containing Odyssey protein molecular weight marker 928-40000 (Li-cor Biosciences, USA) (Appendix E) and loading mix (75%) were prepared.

### 2.8.2. SDS-polyacrylamide gel electrophoresis

For total protein extracts a 10 % NuPAGE Novex Bis-Tris 10- or 12 well gels (acrylamide) (Life Technologies) were used. For the phosphorylated proteins, both 10 % and 4-12 % 10 and 12 well gels were used. The gels were run in Xcell SureLock Mini-Cell (Life Technologies) according to the NuPage Technical guide. NuPage MOPS running Buffer (Appendix B) was added in both inner and outer chamber of the Mini-Cell, and 500 µl of NuPAGE antioxidant was added to the inner chamber to keep the proteins in a reduced state. The proteins were separated at 200 V for about 1 h.

### 2.8.3. Blotting

The gels were placed in the XCell TM blot module according to the NuPage Technical guide and transferred to the XCell SureLock TM Mini-Cell following the XCell Surelock TM Minicell user manual. NuPAGE Transfer Buffer (Appendix B) was added to the inner chamber before it was placed on ice. Blotting was carried out at 30 V for 1 hour, and the proteins were transferred to an Immobilion Transfer Membrane (Merck Millipore, USA).

### 2.8.4. Hybridization and detection

The membrane was rehydrated by leaving it for 20 seconds in Methanol (MeOH), followed by 30 seconds in Tris Buffered Saline with tween (TBST) (Appendix B). After rehydration the membrane was placed with the protein side facing inwards in a 50 ml tube with 3 ml Odyssey blocking buffer (Li-cor Biosciences, USA). The membrane was then put on a roller for 1 h at room temperature.

The membranes were incubated with primary antibodies (Table 1) diluted in Odyssey blocking buffer (3 ml) and left on a roller at room temperature for 1 h, before washing 3 x 10 minutes with TBST (5 ml). Secondary antibodies (Table 2) were diluted in Odyssey blocking buffer (5 ml) and added to the 50 ml tubes containing the membranes, and incubated for 1 h in room temperature in a dark room, due to the light-sensitivity of the secondary antibodies. After the incubation the membranes were washed 3 x 10 minutes with TBS (Appendix B).

The Odyssey Infrared Imaging System (Li-cor Biosciences) was used to detect the proteins on the membrane

**Table 1.** Primary antibodies used in western blotting experiments.

| Antigen | Primary antibody | Manufacturer (catalogue no.) | Dilution |
|---|---|---|---|
| AKT | Rabbit polyclonal | Cell signaling (9272) | 1:1000 |
| ATF4 | Rabbit monoclonal | Cell Signaling (11815) | 1:1000 |
| CHOP | Mouse monoclonal | Thermo Fisher Scientific (MA1-250) | 1:333 |
| eIF2α | Mouse monoclonal | abcam (ab5369) | 1:500 |
| GRP78 | Rabbit monoclonal | abcam (ab108613) | 1:1000 |
| LC3 | Rabbit monoclonal | Cell signaling (3868) | 1:1000 |
| Nrf2 | Rabbit polyclonal | Santa Cruz biotechnology (sc:13032) | 1:500 |
| P62 | Guinea pig polyclonal | Progen (GP-62C) | 1:1000 |
| p- AKT | Rabbit monoclonal | Cell signaling (4060) | 1:2000 |
| p- eIF2α | Rabbit monoclonal | Cell Signaling (3398) | 1:200 |
| PERK | Mouse polyclonal | abcam (ab105929) | 1:500 |
| p-PERK | Rabbit monoclonal | Sante Cruz Biotechnology (sc-32577) | 1:100 |
| PTEN | Rabbit polyclonal | Life Technologies (18-0256) | 1:1000 |
| TRIB3 | Rabbit monoclonal | Sigma-Aldrich (R05388) | 1:200 |
| β-actin | Mouse monoclonal | Abcam (Ab6276) | 1:10000 |

**Table 2.** Secondary antibodies used in western blotting experiments.

| Antigen | Secondary antibody | Manufacturer | Dilution |
|---|---|---|---|
| AKT anti rabbit | IRDye 700 CW conjugated donkey anti rabbit IgG | Licor Odyssey | 1:20000 |
| Rabbit anti ATF4 | IRDye 700 CW conjugated donkey anti rabbit IgG | Licor Odyssey | 1:20000 |
| Mouse anti ATF6 | IRDye 700 CW conjugated donkey anti mouse IgG | Licor Odyssey | 1:20000 |
| Mouse anti CHOP | IRDye 800 CW conjugated donkey anti mouse IgG | Licor Odyssey | 1:5000 |
| Mouse anti eIF2α | IRDye 800 CW conjugated donkey anti mouse IgG | Licor Odyssey | 1:5000 |
| Rabbit anti GRP78 | IRDye 700 CW conjugated donkey anti rabbit IgG | Licor Odyssey | 1:20000 |
| Rabbit anti LC3 | IRDye 800 CW conjugated donkey anti rabbit IgG | Licor Odyssey | 1:5000 |
| Rabbit anti Nrf2 | IRDye 700 CW conjugated donkey anti rabbit IgG | Licor Odyssey | 1:20000 |
| Rabbit anti p-AKT | IRDye 800 CW conjugated donkey anti rabbit IgG | Licor Odyssey | 1:5000 |
| Rabbit anti p- eIF2α | IRDye 700 CW conjugated donkey anti rabbit IgG | Licor Odyssey | 1:20000 |
| Mouse anti PERK | IRDye 800 CW conjugated donkey anti mouse IgG | Licor Odyssey | 1:5000 |
| Rabbit anti p-PERK | IRDye 700 CW conjugated donkey anti mouse IgG | Licor Odyssey | 1:20000 |
| Rabbit anti PTEN | IRDye 700 CW conjugated donkey anti rabbit IgG | Licor Odyssey | 1:20000 |
| Guinea pig anti p62 | IRDye 800 CW conjugated donkey anti guinea pig  IgG | Licor Odyssey | 1:5000 |
| Mouse anti TRIB3 | IRDye 700 CW conjugated donkey anti mouse IgG | Licor Odyssey | 1:20000 |
| Mouse anti β-actin | IRDye 700 CW conjugated donkey anti mouse IgG | Licor Odyssey | 1:20000 |

### 2.8.5.  Statistics

The band signals from the membranes were quantified using the Image Studio Lite version 3.1 software. The signals were normalized to their respective loading controls before calculating fold change values of treated samples versus controls. Significance was calculated in the excel software using t-test (paired, one-tailed distribution). P-values below 0.05 were considered statistically significant from control.

## 2.9.   Measuring autophagic flux

$4,4 \times 10^5$ cells of DLD-1 and $3,6 \times 10^6$ cells of LS411N were seeded in 10 cm plates , and the growth medium were replaced 24 hour after seeding with growth medium supplemented with DHA (70 µM) , Ethanol (70 µM), BafA1 (100 nM), or BafA1 and DHA. The cells were harvested 12 h and 24 h after supplementation, and total proteins were isolated according to protocol (chapter 2.6.1.).

## 2.10.  Confocal Microscopy

Cells were seeded in 8 well confocal plates (Nunc, Germany) and supplemented with DHA (70 µM/105 µM), TG (1 µM)  and EtOH (70 µM) according to treatment protocol (2.1.2.c), before fixated and stained with primary- and secondary antibodies for visualization. DRAQ5 was used as nuclear staining.

### 2.10.1. Fixation

The fixation solution was made by dissolving 16 % para-formaldehyde (Alfa Aesar, Germany) in 2 x PBS (Appendix B) to get the wanted concentration of 8%. 200 µl fixation solution (8%) were then added to each well without removing the medium (200 µl), which gave the wanted concentration of para-formaldehyde at 4%. After 10 minutes of fixation at room temperature all solution were removed from the wells, before washing with 200 µl cold PBS. The wells were filled with 400 µl PBS, wrapped in foil, and stored at 4°C until blocking and hybridization with antibodies were performed.

### 2.10.2. Permeabilization, blocking and immunofluorescent staining

PBS were removed from the confocal wells and 200 µL cold methanol (-20°C) were added to each well. After 10 minutes of incubation on ice the methanol was removed and 200 µl PBS were added. The PBS was removed and the blocking solution was added (Appendix C) and left on a shaker at room temperature for 1 h. The blocking solution was removed and 100 µL of primary antibody solution (Table 3, Appendix C) were added to each well and incubated on a shaker at room temperature for 1 h.  Then the cells were washed with 200 µl PBS 3x5 minutes. After washing, the cells were incubated with 100 µl secondary antibody solution (Table 4, Appendix C) on a shaker at room temperature for 30 minutes. The cells were washed with 400 µl PBS 5x5 minutes after the incubation.

DRAQ5 is a highly cell permeable DNA-interactive agent, with fluorescence signature extending into the infra-red region of the spectrum. It is used for nuclear staining of cells. Since no washing step is required, DRAQ5 will usually be the final staining procedure, after any cell treatment or labelling, and immediately prior to analysis. DRAQ 5 was first diluted to 5 µM with cold PBS, and covered with foil to avoid light exposure. The PBS was removed from each of the confocal wells and 100 µl DRAQ5 was added to the wells. After 5 minutes of incubation on a shaker at room temperature, the DRAQ5 solution was replaced with cold PBS.

**Table 3.** Primary antibodies used in immunofluorescent staining.

| Antigen | Primary antibody | Manufacturer (cat. no.) | Dilution |
|---------|-----------------|------------------------|----------|
| ATF4 | Rabbit monoclonal | Cell Signaling (D4B8) | 1:1000 |
| CHOP | Mouse monoclonal | Thermo Fisher Scientific (MA1-250) | 1:333 |
| Nrf2 | Rabbit polyclonal | Santa Cruz biotechnology (sc:13032) | 1:500 |
| TRIB3 | Rabbit  monoclonal | Abcam (ab5369) | 1:500 |

**Table 4**. Secondary antibodies used in immunofluorescent staining.

| Antigen | Secondary antibody | Manufacturer (cat. no.) | Dilution |
|---------|-------------------|------------------------|----------|
| Rabbit anti ATF4 | Alexa Fluor 488 goat anti rabbit igG | Life Technologies (A11008) | 1:5000 |
| Mouse anti CHOP | Alexa Fluor 488 goat anti rabbit igG | Life Technologies (A11008) | 1:5000 |
| Rabbit anti Nrf2 | Alexa Fluor 488 goat anti rabbit igG | Life Technologies (A11008) | 1:5000 |
| Rabbit anti TRIB3 | Alexa Fluor 488 goat anti rabbit igG | Life Technologies (A11017) | 1:5000 |

### 2.10.3. Imaging

Subcellular localization of proteins was imaged using an Axiovert 200 microscope with confocal module LSM 510 Meta and a 63x1.2 W objective (Carl Zeiss), and analyzed using the Zeiss LSM Image Examiner Software version 4.2.0.121.

## 2.11.  siRNA

ATF4 mRNAs were knocked down in the DLD-1 cells using small interfering RNAs (siRNAs)(Qiagen), and the effect of siATF4 on DHA-mediated growth inhibition was investigated by cell counting. Western blotting and confocal imaging were also used to explore the protein expression of ATF4 in response to siATF4.

### 2.11.1. Transfection with siRNA

DLD1 cells were transfected with pre-validated siRNAs towards ATF4 using the Lipofectamine RNAiMax transfection reagent (Life Technologies) and final concentration of 10 and/or 20 nM siRNA. The following siRNAs were used: ATF4 (#SI03019345, Qiagen), AllStars Hs Cell Death control (positive transfection control), (#1027298, Qiagen), AllStars Negative Control (#1027280, Qiagen) and SignalSilence control siRNA (Fluorescein conjungate, #6201, Cell Signaling). During initial testing, 300 000 cells/well were transfected for 48 h in 6 well plates using 2.5 ml growth media and 5 µl transfection buffer, according to

manufacturer's protocol (Life Technologies). In short, reverse transfection was performed by diluting 6 or 12 pmol siRNA (negative control and ATF4 siRNAs) in 500 µl Opti-MEM I medium without serum, before mixing it with 5 µl transfection buffer and incubation for 20 minutes at room temperature and added to the wells. Cells were diluted in 2500 µl growth medium without antibiotics and added to the wells with prediluted siRNA/transfection buffer. The plated cells were left in an incubator at 37°C and 5% $CO_2$ for 48 h. The cells were washed 2 x2 ml with ice cold PBS before scraping in 1 ml ice cold PBS and transferred to precooled Eppendorf tubes. The cells were centrifuged at 1500 rpm for 5 minutes before pipetting of the supernatant, isolating total proteins and performing western blotting according to above protocols. The fluorescein conjugated and positive control siRNAs were used for transfection in an 8 well confocal tray, by scaling down the components used during transfection in 6 well trays. The confocal tray was fixated, stained and imaged in a confocal microscope according to above protocols. The results from the confocal imaging of the controls were used to estimate transfection efficiency.

For treatment with DHA and TG, DLD-1 cells were seeded in 2x6 well plates (proteins) with 200 000 cells per well, 2x12 well plates (counting) with 40 000 cells per well and 3x8 well plates (confocal imaging) with 16 842 cells per well. Transfection was performed as described above using a final concentration of 20 nM. After 48 h of incubation, the culture medium was replaced with growth medium supplemented with EtOH (70 µM), DHA (70 µM) or TG (1 µM), and left for incubation at 37°C and 5% $CO_2$. Total proteins were harvested and isolated from the 6 well plates 6 h after incubation as described above, and western blotting was performed according to protocol (chapter 2.8.). The 8 well plates were fixated according to protocol (chapter 2.10.1.) 6 h after incubation, and a plate with controls of cells with siATF4, NT-siRNA, lipofectamine or no treatment were fixated 48 h post transfection. To investigate the effect of siATF4 on DHA induced growth inhibition, the 12 well plates were left for 48 h of incubation after treatments were added before counting.

# 3. Results

## 3.1. Different cell growth response to DHA in the human colon cancer cell lines DLD-1 and LS411N

The effect of DHA on growth of the human colon cancer cell lines DLD-1 and LS411N, both cultivated in the same growth medium, was investigated by cell counting. The results from cell counting shows that the DLD-1 cells is DHA sensitive with about 50 % growth inhibition 48 h after treatment with DHA (Figure 8A and B), while the LS411N cells are insensitive with no growth inhibition after the same treatment (Figure 8C and D). OA, which is an n-9 PUFA, was used as a control.
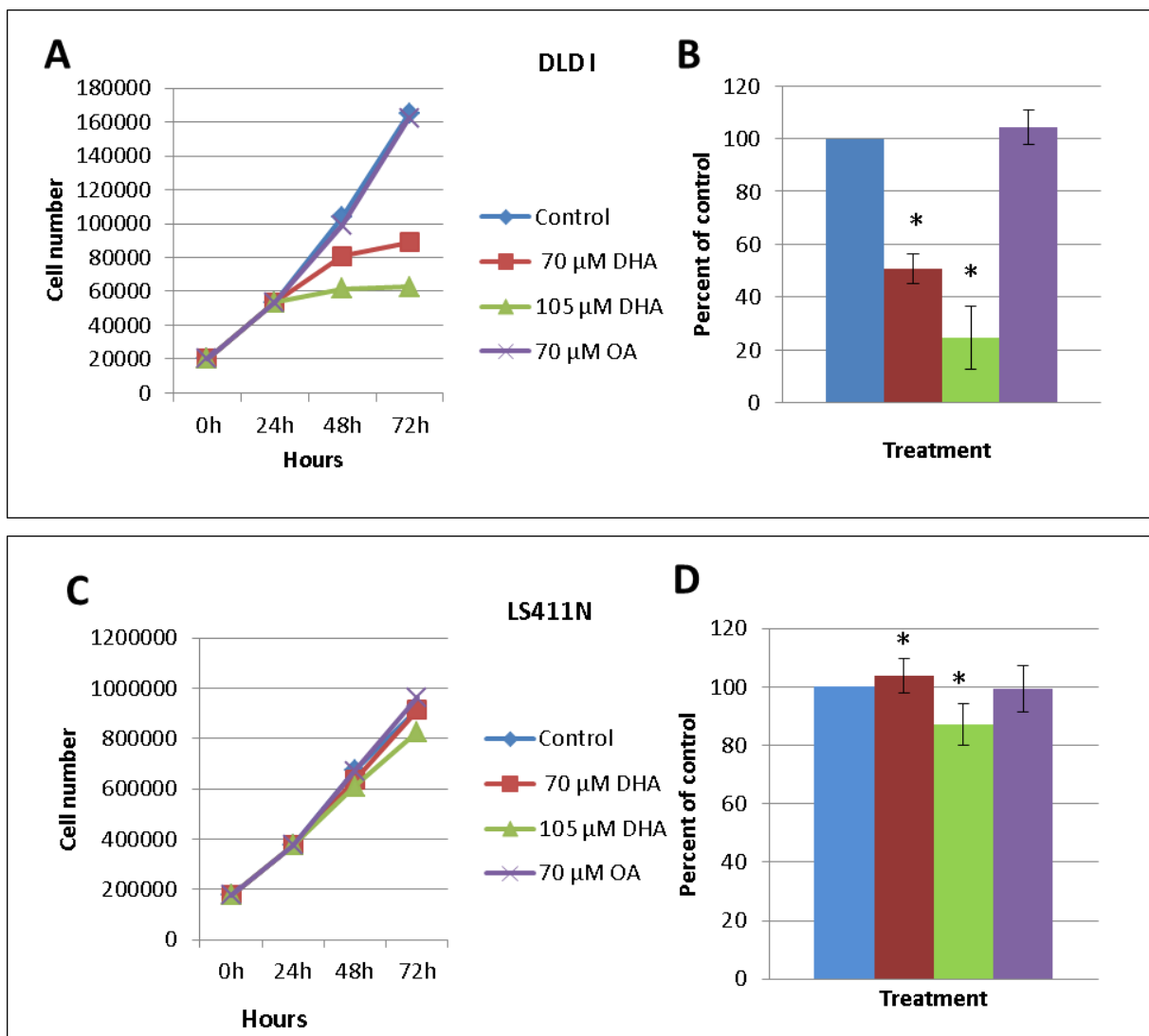
**Figure 8:** The effect of DHA (70 µM) and OA (70 µM) on cell growth of DLD-1 and LS411N cell lines. Cells were added EtOH, DHA or OA 24 h after seeding, and the cells were counted 24 h and 48 h after treatment of DLD-1 **(A)** and LS411N **(C)**. Mean and standard deviations are based on four and three independent experiments from DLD-1 **(B)** and LS411N **(D)**, respectively, shown as percent growth inhibition 48 h after treatment compared to control. *Significantly different from control (p<0.05).

Effect of DHA on cell viability was monitored on both cell lines over 4 days using the MTT viability assay. In agreement with results from cell counting presented above, DLD-1 is the most sensitive towards DHA, although the response to DHA (70 µM) was first seen after 72 h (20 %) and 96 h (50%). The LS411N cells were less sensitive when treated with DHA (70 µM) after 72 h and 96 h, with 5 % and 13 % growth inhibition respectively. A more profound response was found using DHA (105 µM) for both cell lines, with a growth reduction of 40% at 24 h, 55% at 48 h, 72% at 72 h, and 79 % at 96 h in the DLD-1 cells. With the same treatment in LS411N, a growth reduction was first seen at 72 h and 96 h, with 29 % and 38 %, respectively (Figure 9).
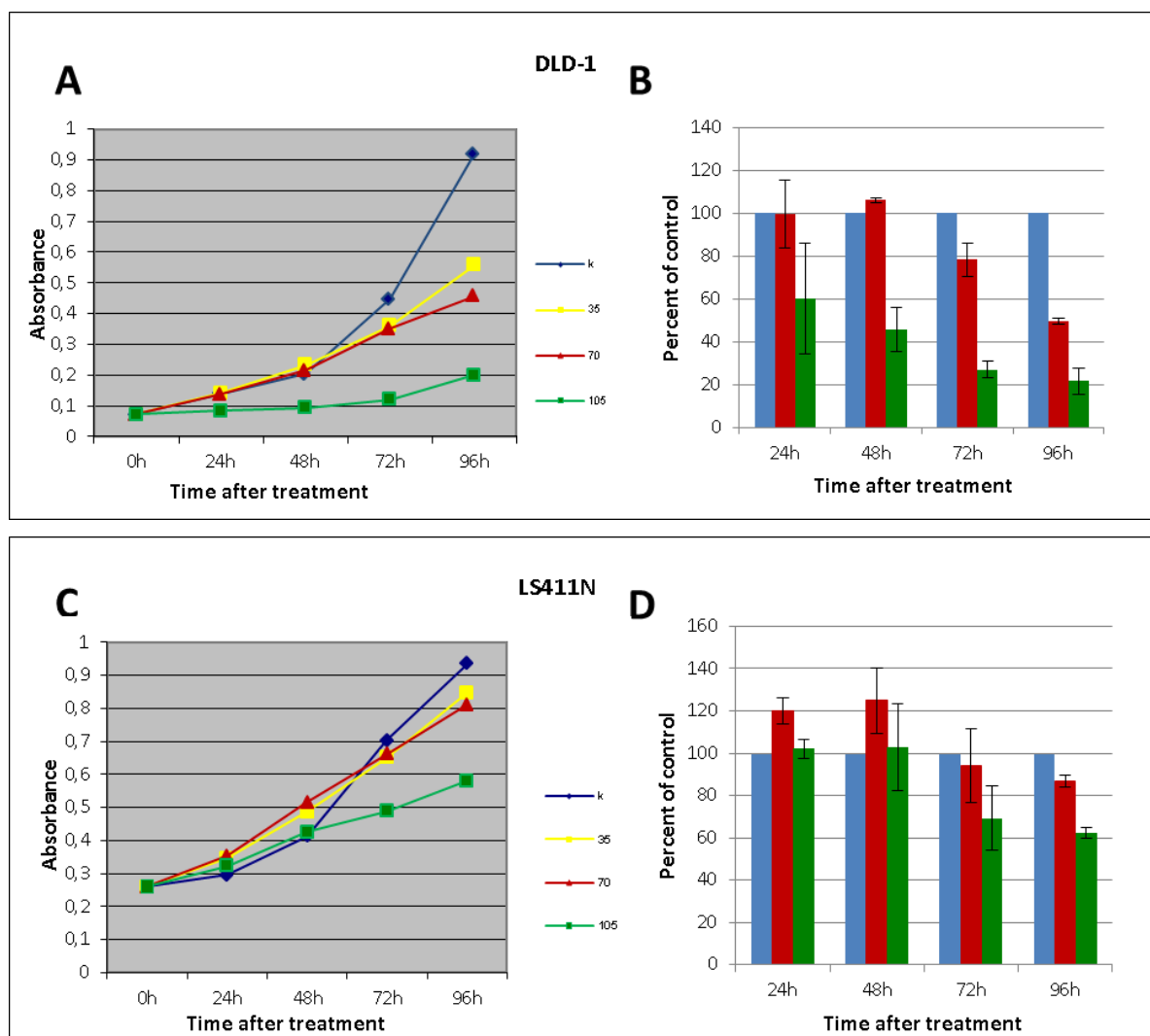
**Figure 9:** The effect of DHA (35, 70 or 105 μM) on cell viability was measured by MTT assay in DLD-1 **(A)** and LS411N **(C)** cells. Mean and standard deviation are based on two independent experiments, shown as the percent growth inhibition compared to control per timepoint for DLD-1 **(B)** and LS411N **(D)**.

## 3.2.    Isolation of total RNA

It is important to use RNA with high quality for reliable gene expression data, and the quality of total RNA for RT-PCR experiments was assessed by measuring the RIN values using the BioAnalyzer (Agilent Technologies). The RIN values were all between 7.4 and 10, as expected for cell lines. The electrophoresis showed specific bands for 28S and 18S ribosomal RNA and a ratio (28S/18S) above 2 for all samples from 3, 6 and 12 h. For the 24 h DHA and TG treated samples the rRNA ratio (28S/18S) was below 2 and the electrophoresis picture shows sign of slightly degraded RNA (Figure 10). At the 24 h timepoint, the cells incubated with DHA and TG where about 20 % growth inhibited, which might explain the lower RNA quality in treated compared to non-treated at the last timepoint. Results from the Nanodrop show that the RNA to protein ratio (260/280) and RNA to chemical contaminants ratio (260/230) were all above 2.0, indicating low protein and chemical contamination. The resulting concentrations, RIN values, 28S/18S ratio, $A_{260}/A_{280}$ ratio and $A_{260}/A_{230}$ ratio are presented in Appendix D.
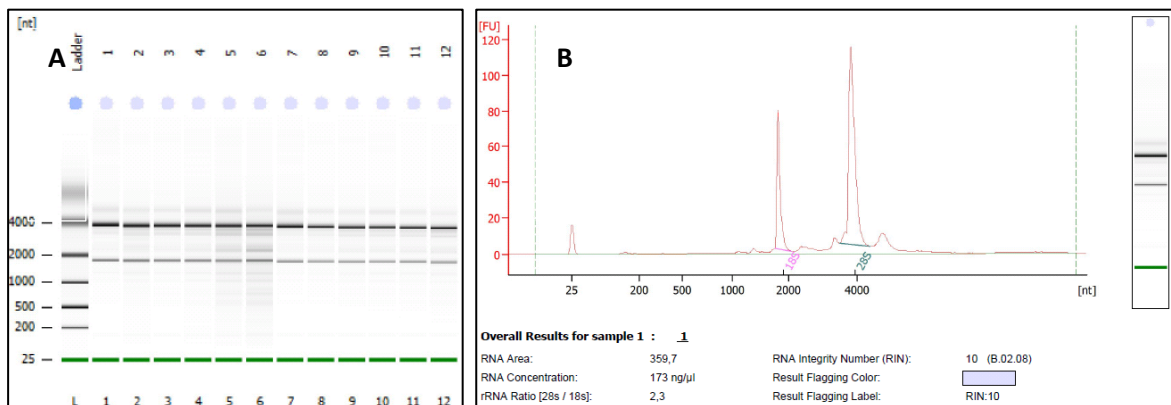


**Figure 10:** Quality assessment of total RNA by measuring RIN values and rRNA ratios **A.** The electrophoresis shows specific bands for 28S and 18S ribosomal RNA. Samples 5 and 6, representing 24 h incubation with DHA (70 μM) and TG (1μM), show signs of some degradation with rRNA ratio 1.5 and 1.3, respectively. **B**. An electropherogram summary of the 12 h control with RIN value 10, and rRNA ratio 2.3.

## 3.3.    Quantification of ER stress-related mRNA in the DLD-1 cells

ER stress-related transcripts have previously been found to be upregulated in the DHA sensitive colon cancer cell line SW620 by Jakobsen et al. (2008) [16]. RT-PCR was used to

quantify mRNA involved in the UPR-pathway in the DLD-1 cells. The mRNA from cells incubated with DHA (70 µM) for 6 h, were compared to controls, to investigate the effect on 84 different UPR related genes. The results were sorted to give a list of transcripts induced or reduced more than 1.4 fold (Table 5). Total RNA was also isolated from DLD-1 cells for 3, 12 and 24 h, but was stored for later use.

**Table 5:** Quantification of mRNA from DLD-1 cells incubated with DHA (70 µM) for 6h using RT-PCR. Transcripts that are increased or decreased more than 1.4 fold compared to control are included. The results are based on one experiment only. FC= fold change.

| Gene Symbol | FC DHA/C | Unigene | Refseq | Gene name |
|---|---|---|---|---|
| HSPA1B | 4,3 | Hs.719966 | NM_005346 | Heat shock 70kDa protein 1B |
| HSPH1 | 2,6 | Hs.743267 | NM_006644 | Heat shock 105kDa/110kDa protein 1 |
| VIMP | 2,2 | Hs.32148 | NM_203472 | Selenoprotein S |
| SLC17A2 | 1,8 | Hs.591802 | NM_005835 | Solute carrier family 17 (sodium phosphate),member 2 |
| HPRT1 | 1,8 | Hs.412707 | NM_000194 | Hypoxanthine phosphoribosyltransferase 1 |
| ATF4 | 1,7 | Hs.496487 | NM_001675 | Activating transcription factor 4 |
| UFD1L | 1,7 | Hs.474213 | NM_005659 | Ubiquitin fusion degradation 1 like (yeast) |
| TCP1 | 1,7 | Hs.363137 | NM_030752 | T-complex 1 |
| TOR1A | 1,7 | Hs.534312 | NM_000113 | Torsin family 1, member A (torsin A) |
| EDEM1 | 1,7 | Hs.224616 | NM_014674 | ER degradation enhancer, mannosidase alpha-like 1 |
| SERP1 | 1,7 | Hs.713956 | NM_014445 | Stress-associated endoplasmic reticulum protein 1 |
| RNF5 | 1,6 | Hs.731774 | NM_006913 | Ring finger protein 5 |
| UBXN4 | 1,6 | Hs.591242 | NM_014607 | UBX domain protein 4 |
| MANF | 1,6 | Hs.436446 | NM_006010 | Mesencephalic astrocyte-derived neurotrophic factor |
| PFDN5 | 1,6 | Hs.655327 | NM_002624 | Prefoldin subunit 5 |
| ADM2 | 1,6 | Hs.743540 | NM_024866 | Adrenomedullin 2 |
| BAX | 1,6 | Hs.624291 | NM_004324 | BCL2-associated X protein |
| GINS2 | 1,6 | Hs.433180 | NM_016095 | GINS complex subunit 2 (Psf2 homolog) |
| ERN1/IRE1 | 1,5 | Hs.700027 | NM_001433 | Endoplasmic reticulum to nucleus signaling 1 |
| INSIG2 | 1,5 | Hs.7089 | NM_016133 | Insulin induced gene 2 |
| AMFR | 1,5 | Hs.295137 | NM_001144 | Autocrine motility factor receptor |
| HSPA4L | 1,5 | Hs.135554 | NM_014278 | Heat shock 70kDa protein 4-like |
| DNAJB9 | 1,5 | Hs.741182 | NM_012328 | DnaJ (Hsp40) homolog, subfamily B, member 9 |
| RRM2 | 1,5 | Hs.226390 | NM_001034 | Ribonucleotide reductase M2 |
| B2M | 1,5 | Hs.534255 | NM_004048 | Beta-2-microglobulin |
| MAPK8/JNK | 1,5 | Hs.522924 | NM_002750 | Mitogen-activated protein kinase 8 |

| | | | | |
|---|---|---|---|---|
| **CEBPB** | 1,5 | Hs.719041 | NM_005194 | CCAAT/enhancer binding protein (C/EBP), beta |
| **CREB3** | 1,5 | Hs.522110 | NM_006368 | CAMP responsive element binding protein 3 |
| **DERL1** | 1,5 | Hs.241576 | NM_024295 | Der1-like domain family, member 1 |
| **USP14** | 1,5 | Hs.707058 | NM_005151 | Ubiquitin specific peptidase 14 |
| **NPLOC4** | 1,5 | Hs.464333 | NM_017921 | Nuclear protein localization 4 homolog (S. cerevisiae) |
| **PPIA** | 1,5 | Hs.356331 | NM_021130 | Peptidylprolyl isomerase A (cyclophilin A) |
| **DNAJC10** | 1,5 | Hs.744512 | NM_018981 | DnaJ (Hsp40) homolog, subfamily C, member 10 |
| **ASNS** | 1,5 | Hs.489207 | NM_183356 | Asparagine synthetase (glutamine-hydrolyzing) |
| **ATXN3** | 1,4 | Hs.532632 | NM_004993 | Ataxin 3 |
| **DNAJC3** | 1,4 | Hs.59214 | NM_006260 | DnaJ (Hsp40) homolog, subfamily C, member 3 |
| **SYVN1** | 1,4 | Hs.75859 | NM_172230 | Synovial apoptosis inhibitor 1, synoviolin |
| **HSPA5** | 1,4 | Hs.743241 | NM_005347 | Heat shock 70kDa protein 5 |
| **GADD34** | 1,4 | Hs.631593 | NM_014330 | Growth arrest and DNA-damage-inducible gene 34 |
| **SEC63** | 1,4 | Hs.26904 | NM_007214 | SEC63 homolog (S. cerevisiae) |
| **VCP** | 1,4 | Hs.529782 | NM_007126 | Valosin containing protein |
| **ERO1L** | 1,4 | Hs.592304 | NM_014584 | ERO1-like (S. cerevisiae) |
| **GANAB** | -1,4 | Hs.595071 | NM_198334 | Glucosidase, alpha; neutral AB |
| **BEX2** | -1,6 | Hs.398989 | NM_032621 | Brain expressed X-linked 2 |
| **SREBP1** | -1,6 | Hs.733635 | NM_004176 | Sterol regulatory element binding transcription protein1 |
| **CREB3L3** | -3,2 | Hs.247744 | NM_032607 | CAMP responsive element binding protein 3-like 3 |

The average Ct Positive PCR control (PPC) values should be around 20+/-2 [48], but are lower on both arrays from 6 h (15.85 for Control array and 15.76 for DHA array 6 h). However this depends on the sensitivity of the real time cycler and is acceptable as long as the average Ct PPC values does not vary more than 2 between arrays compared. The RT efficiency and genomic DNA contamination controls passed the quality control test. The Ct values were normalized using the GAPDH housekeeping gene, which had a difference in Ct value below 1 between arrays compared, as recommended.

### 3.4. The expression of ER stress-related proteins are upregulated at early timepoints in the DLD-1 cells, but not to the same extent in the LS411N cells

Based on data from the RT-PCR analysis presented in the previous section, showing that UPR-pathway-related transcripts are induced by DHA in the DLD-1 cells, we speculated whether differences in the induction of the UPR pathway could explain differences in the PUFA-sensitivity of the DLD-1 and LS411N cell lines. In order to investigate this further, we

analyzed the expression of different ER stress-related proteins after DHA treatment for different time periods in DLD-1 and LS411N cells; considered DHA sensitive and insensitive cell lines, respectively. The protein levels were measured by western blotting, and confocal microscopy was used to detect the localization of some central ER stress/UPR proteins. TG, which is known to induce ER stress, was used as a positive control for both cell lines.

Due to the central role of ATF4 in the UPR and its upregulation at mRNA level, the protein expression of the PERK-eIF2α-ATF4 arm of the UPR pathway was investigated. PERK is one of the three ER stress sensors, and when misfolded/unfolded proteins accumulate in the ER lumen Bip is released and PERK is activated by autophosphorylation. PERK and phosphorylated PERK were found upregulated in both cell lines, although phosphorylated PERK was more induced in the DLD-1 cells after the 3 and 6 h treatment with DHA (Figure 11)
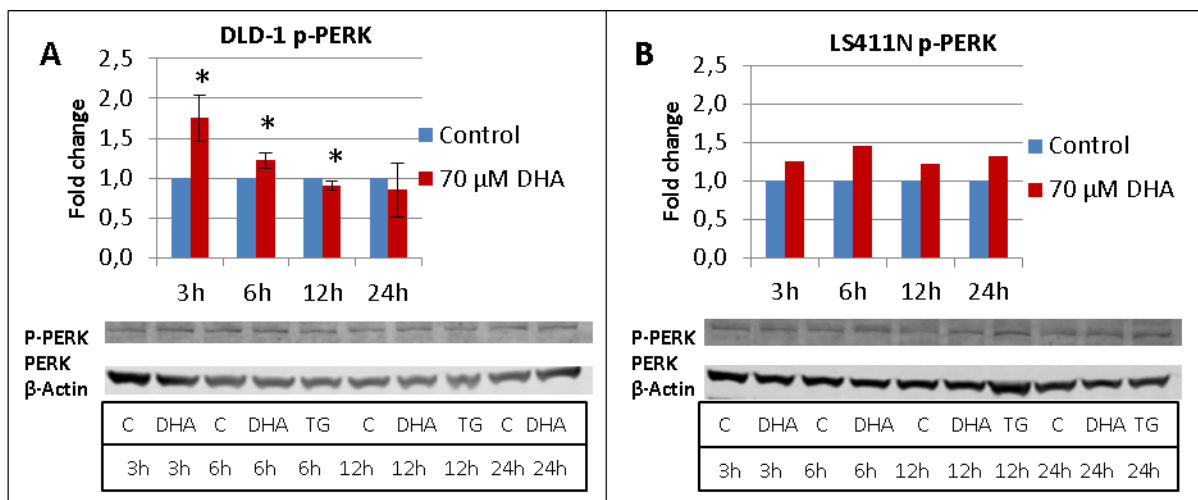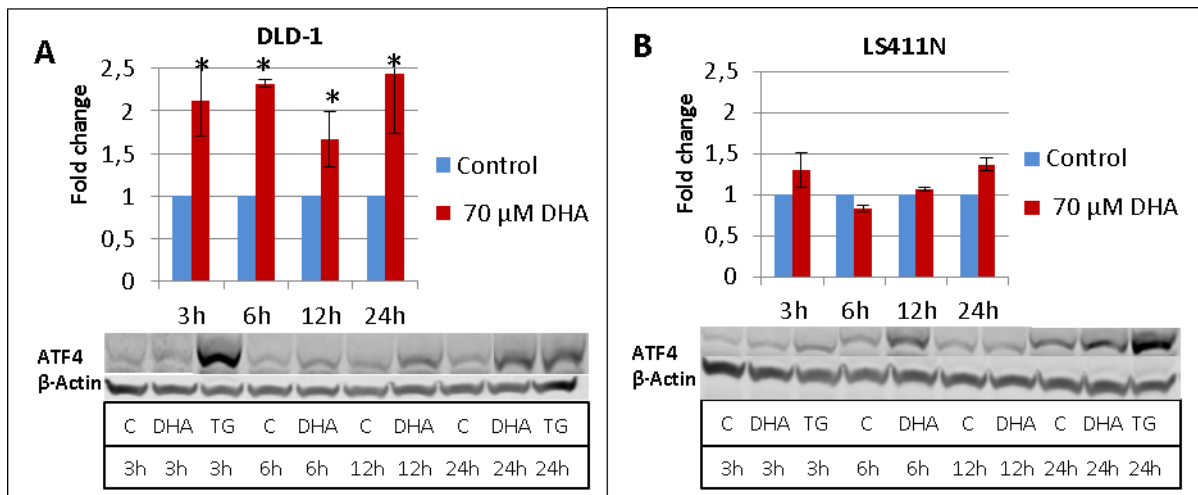


**Figure 11:** The protein expression level of total- and phosphorylated PERK at different timepoints in the DLD-1 cells (**A**) and the LS411N cells (**B**) treated with EtOH (70 μM), DHA (70 μM) and TG (1 μM). The fold change value of p-PERK is correlated to β-actin. The results from the DLD-1 cells and the LS411N cells are based on three and one independent experiments, respectively. *Significantly different from control ($p < 0.05$).

Activated PERK phosphorylates eIF2α, thereby halting the global protein translation. By reducing the protein load in the ER lumen it gives the cell time to deal with the unfolded proteins. Phosphorylated eIF2α was induced at earlier timepoints, and to a higher degree, by DHA (70 μM) in the DLD-1 cells than in the LS411N cells (Figure 12).
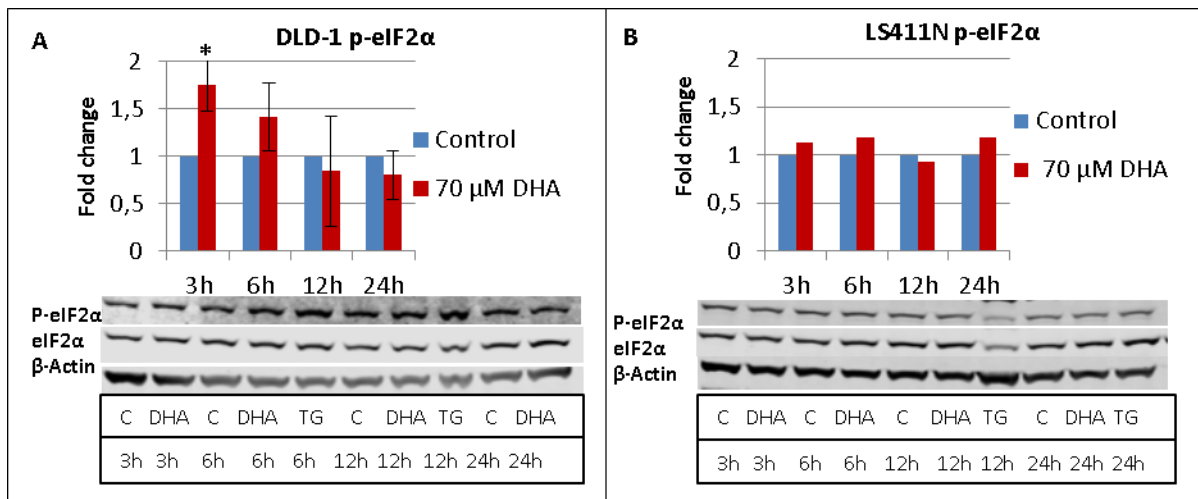
**Figure 12:** The protein expression level of total- and phosphorylated eIF2α at different timepoints in the DLD-1 cells **(A)** and the LS411N cells **(B)** treated with EtOH (70 µM), DHA (70 µM) and TG (1 µM). The fold change of p-eIF2α is correlated to β-actin. The results from the DLD-1 cells and the LS411N cells are based on three and one independent experiments, respectively. *Significantly different from control (p<0.05).

While the phosphorylation of eIF2α stops most of the protein translation, it increases the transcription/translation of others, such as ATF4. The protein expression of ATF4 was upregulated at all timepoints after incubation with DHA (70 µM) in the DLD-1 cells, but only after 24 h and to a lower extent in the LS411N cells (Figure 13).



**Figure 13:** The protein expression level of ATF4 at different timepoints in the DLD-1 cells **(A)** and the LS411N cells **(B)** treated with EtOH (70 µM), DHA (70 µM) and TG (1 µM). The results from the DLD-1 cells and the LS411N cells are based on three and two independent experiments, respectively. *Significantly different from control (p<0.05).

The early upregulation of ATF4 in the DLD-1 cells was confirmed by confocal microscopy which showed that ATF4 was increased in the nucleus in DLD-1 cells after 3 and 6h, especially when treated with the highest concentration of DHA (105 µM), while remaining unchanged compared to control in the LS411N cells. ATF4 was strongly induced in the nucleus in both cell lines when treated with TG (Figure 14A and B).

**A**
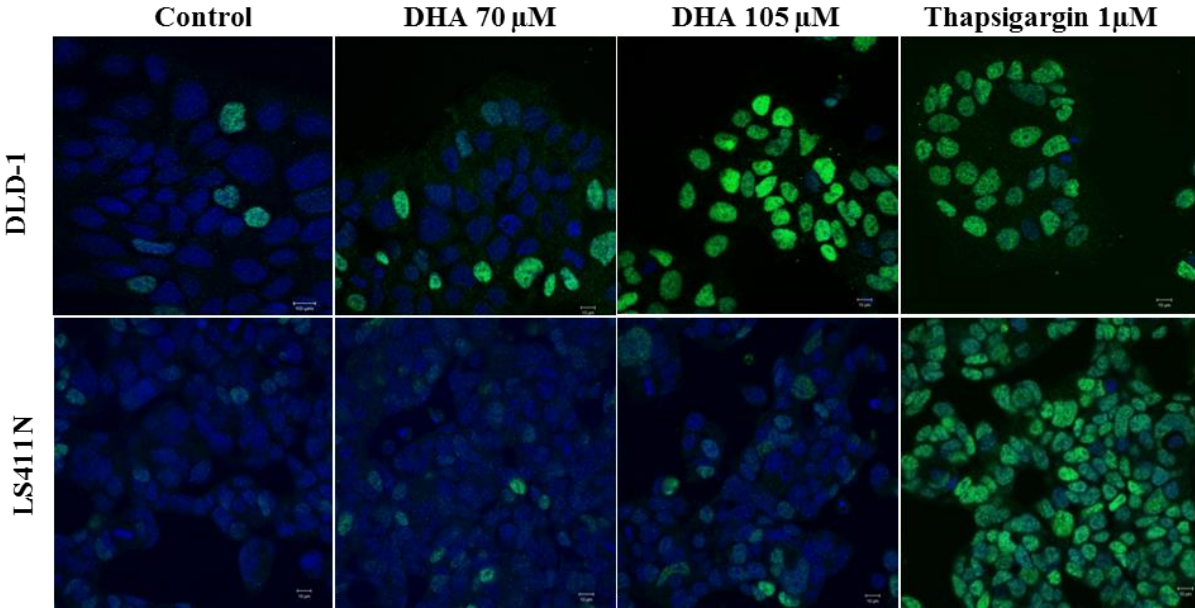


**B**
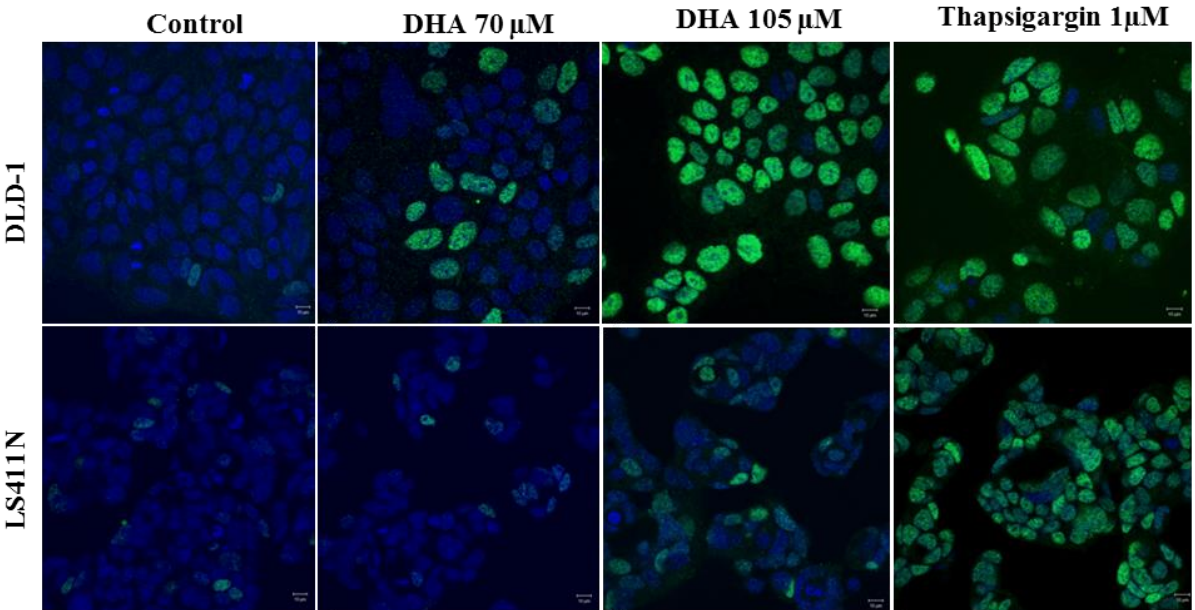


**Figure 14:** Cellular localization of ATF4 in DLD-1 and LS411N cells 3h **(A)** and 6h **(B)** after EtOH (70 µM), DHA (70 and 105 µM) and TG (1 µM) treatment. DHA induced ATF4 in the nucleus in the DLD-1

cells, but not to the same extent in the LS411N cells. Both cell lines are stained with ATF4 (green) and Draq5 (blue). Results are based on three independent experiments.

ATF4 is a transcription factor, and CHOP is one of its downstream targets. CHOP is induced at all timepoints in the DLD-1 cells, but only after 24 h of incubation with DHA and to a less extent, in LS411N (Figure 14).
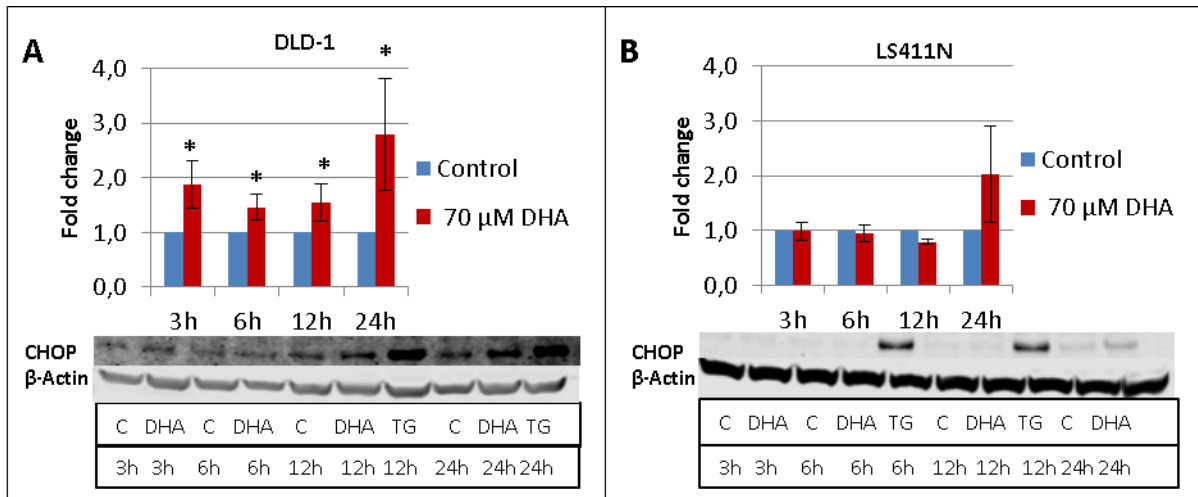


**Figure 14**: The protein expression level of CHOP in DLD-1 **(A)** and LS411N **(B)** cells after treatment with EtOH (70 µM), DHA (70µM) and TG (1µM) for different timeperiods. The results from DLD-1 and LS411N are based on three and two independent experiments, respectively. *Significantly different from control (p<0.05).

CHOP is a transcription factor, and was found induced in the nucleus after 12 h of incubation with DHA in DLD-1 cells, but not in LS411N cells. The difference in expression level of CHOP between DLD-1 cells and LS411N cells was even more evident after treatment with DHA 105 µM. CHOP was strongly induced in the nucleus in both cell lines when treated with TG (Figure 15).
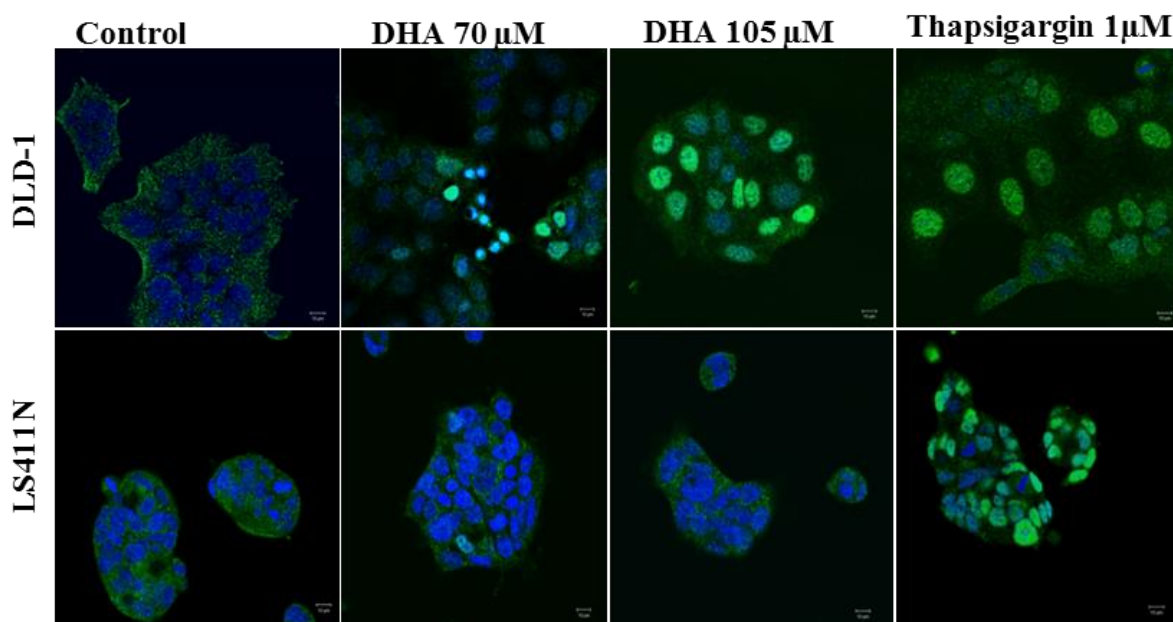
**Figure 15:** Cellular localization of CHOP in DLD-1 and LS411N cells after 12 h treatment with EtOH (70 μM), DHA (70 and 105 μM) and TG (1 μM). Both cell lines were stained with CHOP (green) and Draq5 (blue). Results are based on one experiment.

TRIB3 is induced by CHOP/ATF4, and represses its own induction by downregulating CHOP/ATF4 functions, and its upregulation is implicated in CHOP-dependent cell death during ER stress. TRIB3 is also known to negatively regulate the AKT pathway, thereby reducing the activation of mTOR, a negative regulator of autophagy. The protein level of TRIB3 was found to be upregulated in response to DHA treatment at all timepoints in the DLD-1 cells, but only at the 24 h timepoint, and to a less extent, in the LS411N cell line (Figure 16).
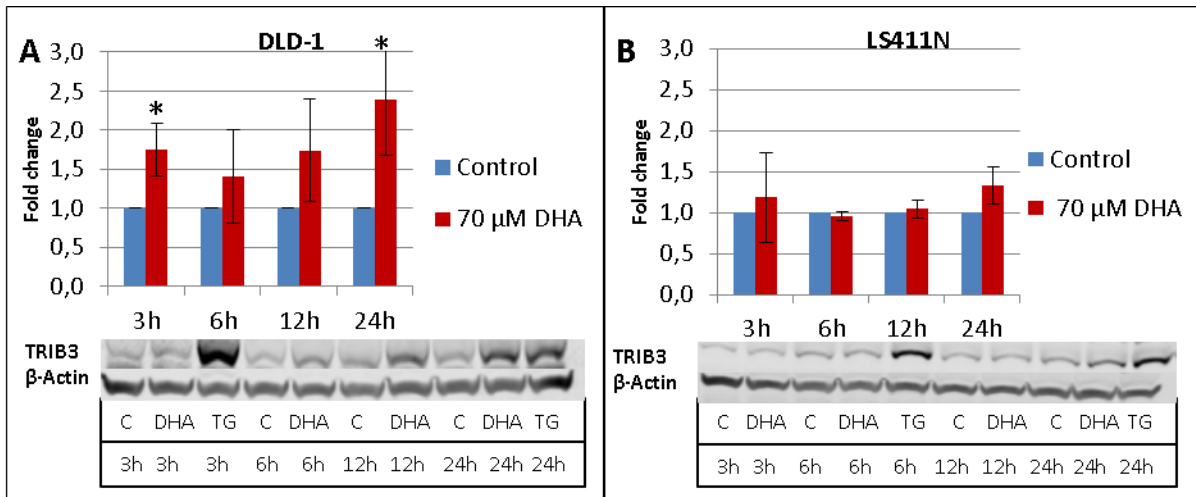
**Figure 16**: The protein expression of TRIB3 in DLD-1 and LS411N cells after treatment with EtOH (70 μM), DHA (70 μM) and TG (1 μM). The results from DLD-1 **(A)** and LS411N **(B)** cells are based on three and two independent experiments, respectively. *Significantly different from control (p<0.05).

The upregulation of TRIB3 was confirmed using confocal imaging. The protein level was higher in the nucleus after DHA treatment in DLD-1 cells, especially by the highest concentration DHA (105 μM) used, but not in the LS411N cells. TRIB3 was highly increased in the nucleus in both cell lines when treated with TG (Figure 17).
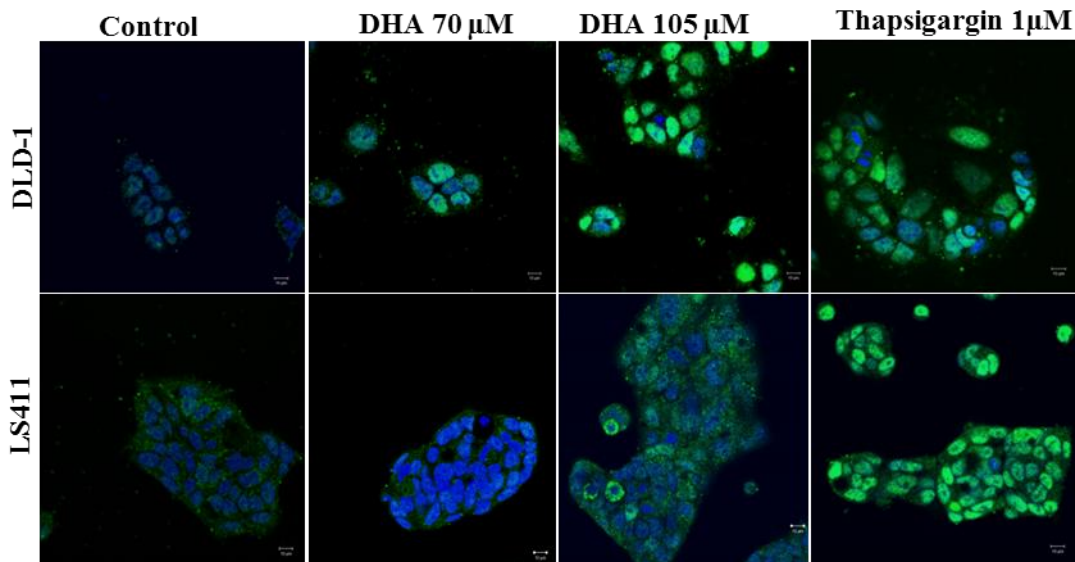


**Figure 17:** Cellular localization of TRIB3 in the DLD-1 and LS411N cells after 12 h treatment with different concentration of EtOH (70 μM), DHA (70 and 105 μM) and TG (1 μM). Both cell lines are stained for TRIB3 (green) and Draq5 (blue). Results are based on one experiment.

Nrf2 may be activated upon phosphorylation by PERK, which leads to the transcription of genes involved in the oxidative defense system. Nrf2 is induced in both cell lines, but is more upregulated after 6, 12 and 24 h in the DLD-1 cells (Figure 18).
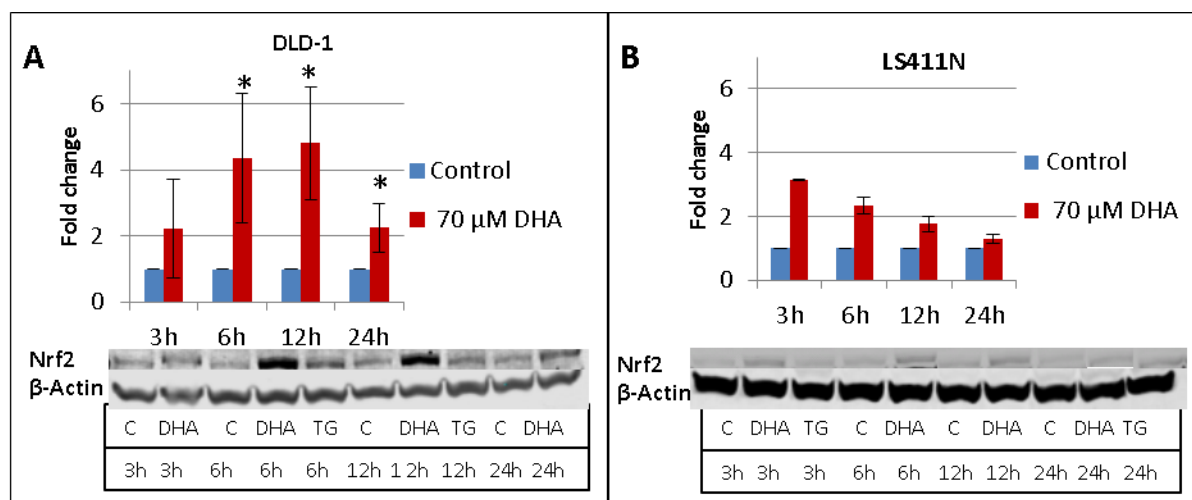


**Figure 18**: Protein expression of Nrf2 in DLD-1 (A) and LS411N (B) cells after treatment with DHA (70 μM) and TG (1 μM). The results from DLD-1 and LS411N are based on three and two independent experiments, respectively. *Significantly different from control ($p<0.05$).

To summarize; the examined ER stress-related proteins in the PERK-eIF2α-ATF4 branch of the UPR were all upregulated already 3h after DHA treatment in DLD-1 cells, while induced at later timepoints and to a lesser extent, in the DHA-insensitive LS411N cell line. A summary of the UPR pathway, and which proteins that were found upregulated by DHA treatment in DLD-1 cells (Figure 19).
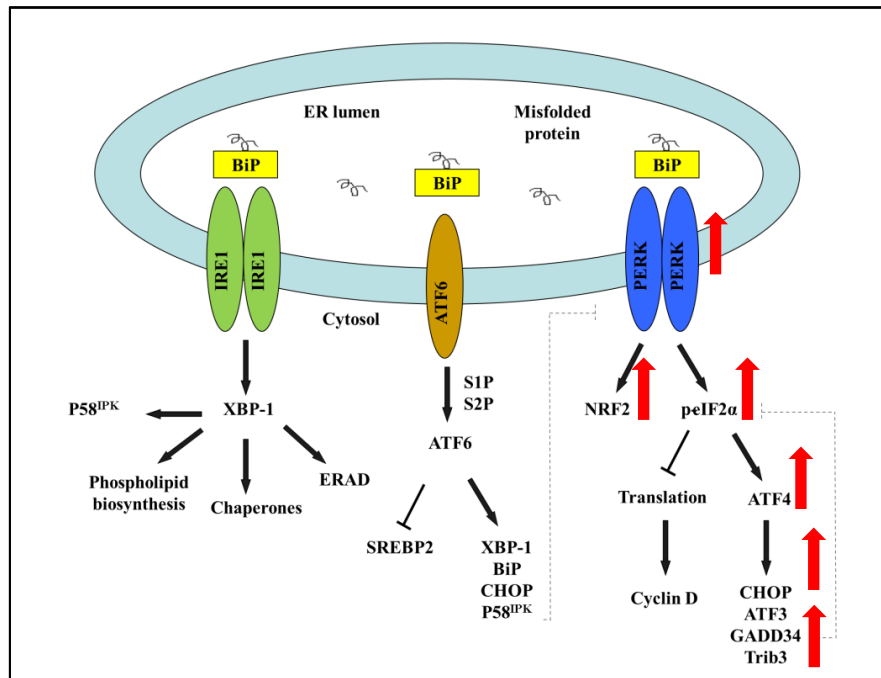
**Figure 19:** DHA-treatment (70 μM) of DLD-1 cells induces ER stress response, indicated by increased protein expression of ATF4, CHOP, TRIB3 and Nrf2, and induction of p-eIF2α and p-PERK (Modified from[34])

## 3.5. DHA increases autophagic flux in DLD-1 cells, but not in LS411N cells

Several research groups have found a connection between ER stress and autophagy [50-53], although a lot remains unclear about the exact mechanism of the regulation between the pathways. The PERK-eIF2α pathway has been shown to induce autophagy [54, 55], and findings by Matsumoto et al. (2013) indicate that the change-over switch between ER-induced apoptosis and autophagy is located between ATF4 and CHOP [56].

We wanted to test whether differences between the two cell lines in the ability to induce autophagy could explain the difference in DHA-sensitivity. Both cell lines were incubated with DHA (70 μM), and BafA1 (100 nM) was added to inhibit the lysosomal degradation of proteins. The lipidated form of LC3B, LC3B II, is present on the autophagosome, and the amount is closely correlated to the number of autophagosomes, which is why LC3B II is commonly used as an indicator of autophagic flux. All results presented in this section are preliminary. DHA-treatment lead to an increase in LC3B II after 24 h in DLD-1 cells as compared to control and the amount of LC3B II further accumulated in the presence of BafA1 at the same timepoint. This may indicate increased autophagic flux in response to DHA in these cells (Figure 20A). In contrast, we see no accumulation of LC3B II in LS411N after

DHA-treatment for 12 and 24 h compared to control, and there were no further accumulation of LC3B II in the presence of Baf A1 at either timepoints (Figure 20B).

Autophagic flux may also be detected by measuring degradation of p62 (SQSTM1) (reviewed in [42]). P62 binds LC3 thereby serving as a selective substrate for autophagy. In line with previous results, we see that DHA potentiated BafA1-induced increase in p62 levels in DLD-1 cells after 12 and 24 h treatment, suggesting DHA induced autophagic flux in these cells. An increase in p62 level is also seen in LS411N cells after the same treatment, although not to the same extent (Figure 20A and B).

Phosphorylated AKT activates mTOR, which in turn negatively regulates autophagy. In the LS411N cells phosphorylated AKT was upregulated after 12 h of incubation with DHA, which correlates with the reduced amount of LC3B II at the same timepoint (Figure 20 B). The protein level of phosphorylated AKT remains unchanged in DLD-1 cells after 12 h treatment with either DHA and/or BafA1. After 24 h treatment, the level of p-AKT seems to decrease slightly compared to control in both cell lines after treatment with DHA, and DHA and BafA1 (Figure 20A). PTEN dephosphorylates $PIP_3$ to $PIP_2$, inhibiting the activation of AKT, thereby counteracting the negative regulation of autophagy. PTEN was found downregulated at 12 h in DLD-1 cells treated with both DHA and Baf A1, while it remains unchanged at 24 h (Figure 20A). In LS411N cells PTEN was found downregulated by DHA at 12 h, and by DHA and Baf A1 at both timepoints (Figure 20B).
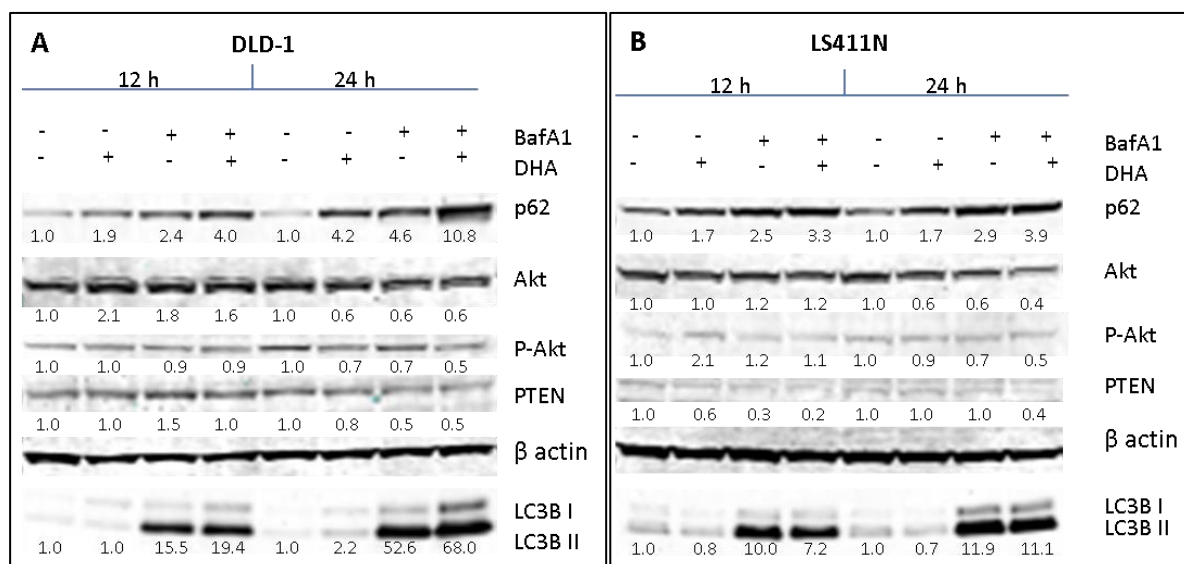


**Figure 20:** Different response in autophagy to DHA treatment in DLD-1 and LS411N cells **A.** DLD-1 cells treated with EtOH (70 µM), DHA (70 µM), Baf A1 (100 nM) or DHA and Baf A1**. B.** LS411N cells treated with DHA (70 µM), Baf A1 (100 nM) or DHA and Baf A1**.** The results from 24 h on LC3B, PTEN and p62 are based on two independent experiments, while the remaining are from one experiment.

## 3.6. siRNA

ATF4 is found upregulated in several tumors where it promotes cell survival in cancer microenvironments by inducing genes involved in autophagy, redox homeostasis and angiogenesis (reviewed in [25, 57]). To further investigate the role of ATF4 in DHA-induced cytotoxicity, siRNA was used to knock down ATF4 mRNA in DLD-1 cells. Initial testing of the knockdown effect of the siRNA was performed, with a clear reduction in protein expression of ATF4 of about 80 % (Figure 21).
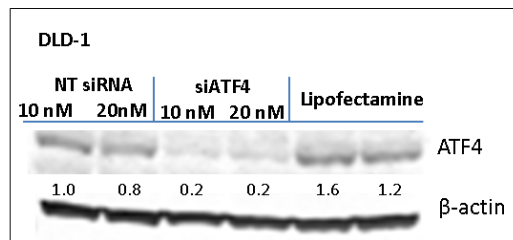


**Figure 21:** Initial testing of the knockdown effect of siATF4 (10/20 nM) by measuring protein levels using western blotting. NT=non target. Initial testing was performed once.

The effect of the siATF4 used here has previously been validated in cell line experiments with high knock down efficiency ([56]).

The transfection efficiency was monitored using SignalSilence control siRNA (Fluorescein conjungate) and a positive transfection control (AllStars Hs Cell Death control)(Figure 22). The pictures clearly show that the cells have been transfected due to the green fluorescensing color in the left picture and the highly reduced cell density in the right picture. The green fluorescence in the right picture is probably autofluorescence caused by apoptosis.
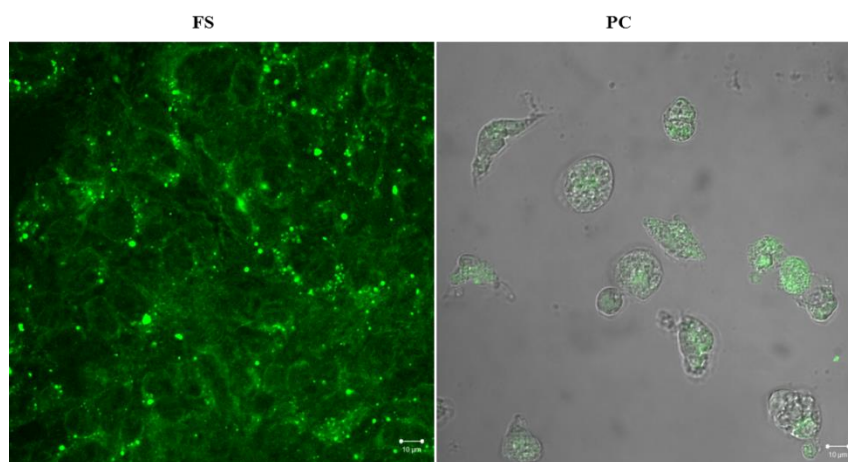


**Figure 22:** The effect of siATF4 transfection was evaluated using SignalSilence control siRNA and positive transfection control. FS= Fluorescent PC= Positive control. The experiment was performed once.

Results from western blotting showed that the knock down of ATF4 seem to be high, about 90 %, when comparing NT-siRNA control with siATF4 control (Figure 23A). When comparing NT siRNA to siATF4, both treated with DHA or TG, a clear decrease in ATF4 was found in the samples transfected with siATF4 (Figure 23A). Effects on growth in DLD-1 cells transfected with siATF4 and incubated with DHA or TG for 48 h, were explored by cell counting. DLD-1 cells transfected with siATF4 were 37 % growth inhibited compared to NT-siRNA control, while the growth inhibition of DHA and TG did not seem to be affected by the siATF4 transfection. Results from cell counting from NT-siRNA and siATF4 are presented in figure 23B. DLD-1 cells transfected with only lipofectamine and untreated cells were also counted, and were consistent with previous results, but not included in this figure.
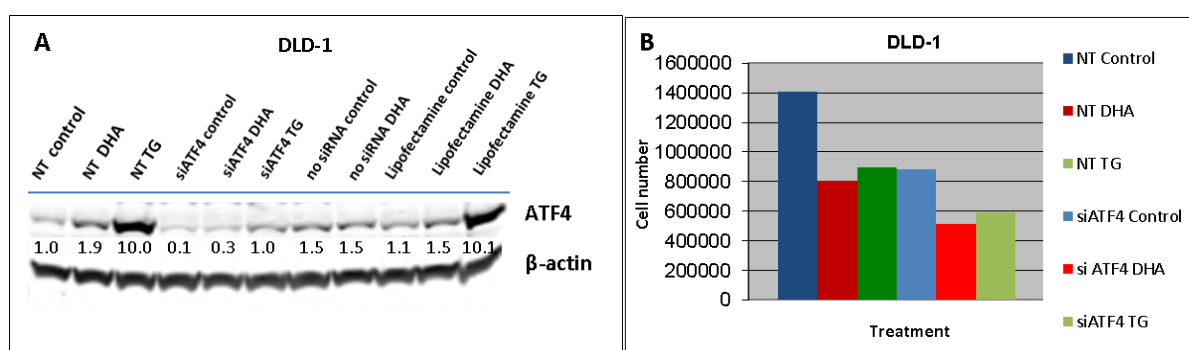


**Figure 23:** The effects of knockdown using siATF4 (20 nM) in DLD-1 cells treated with EtOH (70 μM), DHA (70 μM) or TG (1 μM) **A.** Protein expression of ATF4 after 6 h of incubation with respective treatments was measured using western blot **B.** The effect on growth inhibition was measured by cell counting 48 h after incubation with DHA (70 μM) or TG (1 μM). These results are based on only one experiment.

Confocal imaging was performed after 6 h treatment. The results in figure 24 show that transfection with siATF4 reduced the signal of ATF4 to a high extent, especially evident in the DHA- and TG-treated cells.
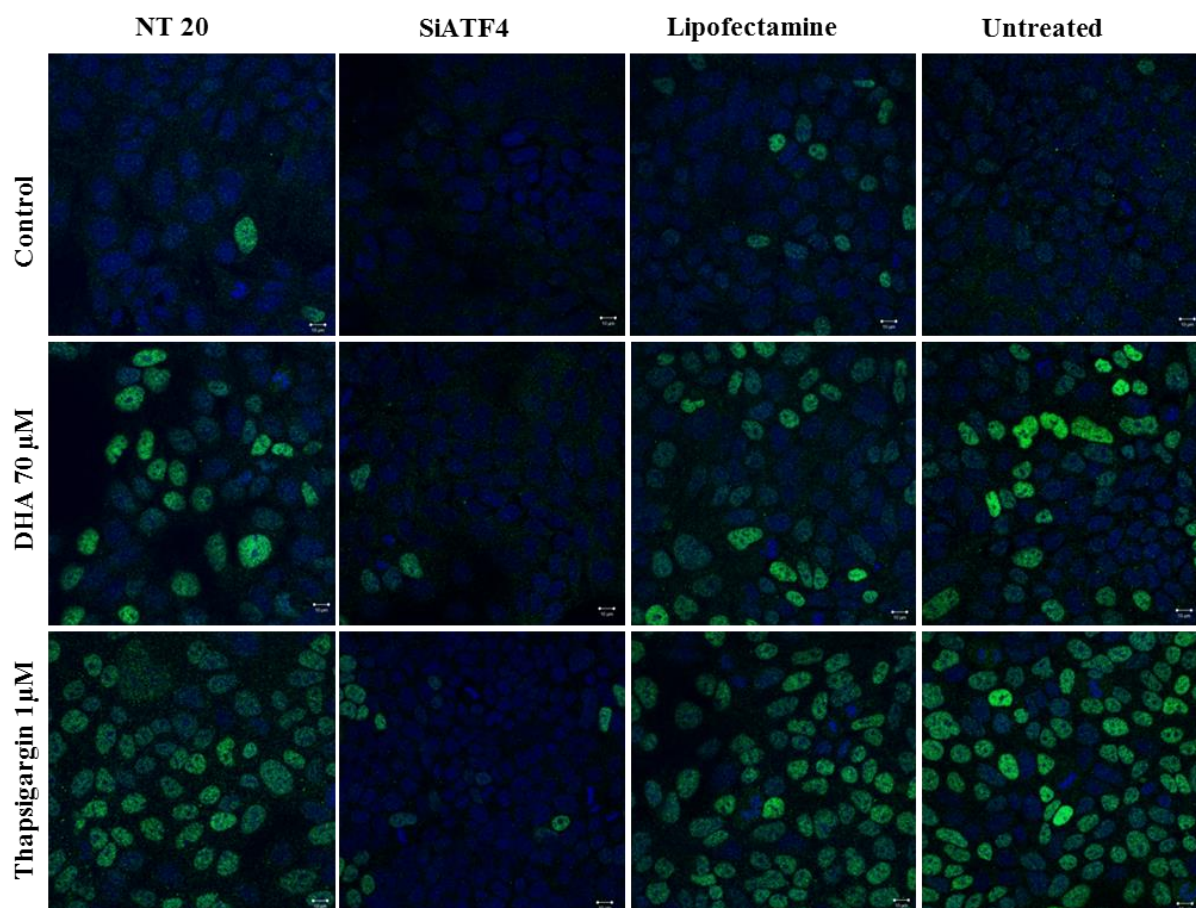
**Figure 24:** The effect of EtOH (70 µM), DHA (70 µM) and TG (1 µM) on DLD-1 cells transfected with siATF4 (20 nM), NT-siRNA (20 nM), Lipofectamine or not transfected were observed using confocal imaging. Cells were stained with ATF4 (green) and Draq5 (blue). Results are based on one experiment.

## 3.7. Vitamin E treatment does not influence the growth inhibitory effect of DHA

Oxidative stress has by several studies been proposed as an important anticancer mechanism of DHA [58] [59-61]. In addition, DHA-induced ROS have been implicated in the activation of both autophagy and apoptosis in cancer cells by inhibition of the AKT-mTOR pathway [58], which led us to further explore if the DHA-induced growth inhibition could be abolished by co-incubating the cells with an antioxidant. Vitamin E is a lipid soluble antioxidant that scavenges lipid peroxyl radicals inhibiting chain propagation. To investigate whether lipid peroxidation could be involved in mediating the growth-inhibitory effect of DHA, both cell lines were co-incubated with vitamin E and DHA. The effect of vitamin E treatment on the growth inhibition was assessed by cell counting. Co-incubation of DHA treated cells with vitamin E did not affect the DHA-mediated growth inhibition in DLD-1 cells. The growth rather seemed to be inhibited when supplemented with vitamin E only, with as much as 21 %

when pre-incubated with vitamin E (Figure 25A). Also, the growth of the DHA-resistant cell line LS411N seemed to be inhibited by both vitamin E supplementation alone and in combination with DHA (Figure 25B). These results may indicate that lipid peroxidation is not the main cause for DHA-mediated cytotoxicity in DLD-1 cells.
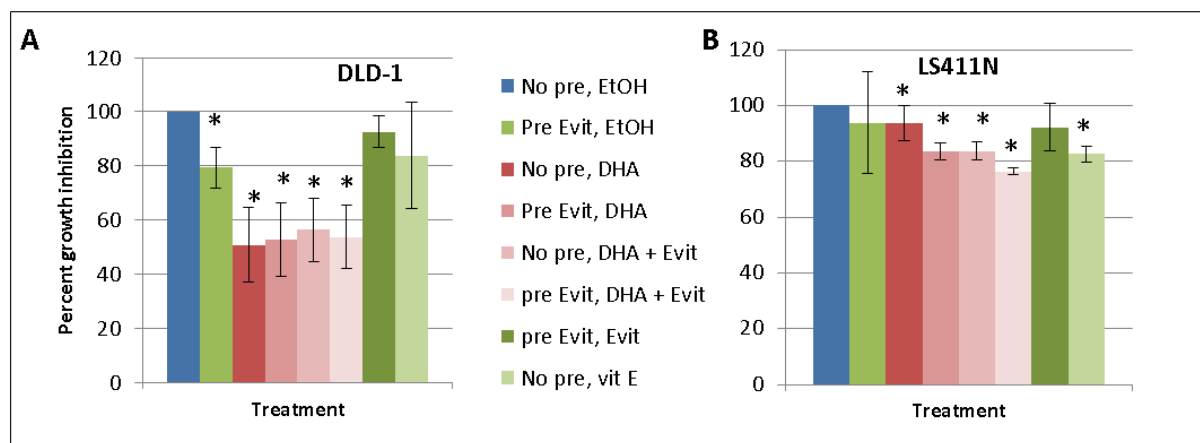


**Figure 25:** The effect of vitamin E (50 µM) on DHA (70 µM)-mediated growth inhibition measured by cell counting. Mean and standard deviation are based on three independent experiments, shown as the percent growth inhibition 48 h after respective treatments compared to control for DLD-1 (**A**) and LS411N (**B**) cells. *Significantly different from control (p<0.05).

Both ER stress and oxidative stress have been reported to be induced by DHA in different human cancer cell lines. Nrf2 is a redox sensitive factor that provides defense against cytotoxic ROS and may be induced by both ER-stress and oxidative stress. We wanted to explore whether the protein expression level of Nrf2 and ATF4 could be influenced by vitamin E. We found an up-regulation of both ATF4 and Nrf2 in DLD-1 cells after co-treatment with vitamin E and DHA. ATF4 was also upregulated when supplemented with vitamin E only, which had no effect on the expression level of Nrf2 (Figure 26A). The expression level of Nrf2 was also upregulated in LS411N cells when co-incubated with DHA and vitamin E, although ATF4 was only slightly increased (Figure 26B).
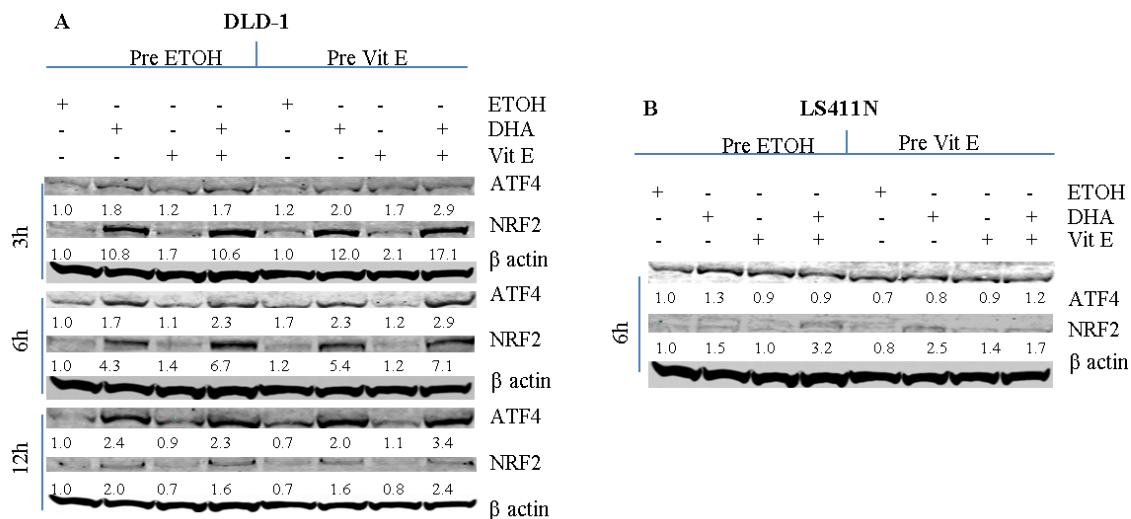
**Figure 26:** The protein expression of ATF4 and Nrf2 in DLD-1 and LS411N cells after incubation with EtOH (70 μM), DHA (70 μM), and/or vitamin E (50 μM). **A.** The protein expression of ATF4 and Nrf2 was measured after 3, 6 and 12 h after incubation with different treatments in DLD-1 cells. **B**. The protein expression of ATF4 and Nrf2 was measured 6h after incubation with respective treatments in LS411N cells. The results from LS411N cells are from only one experiment, while results from DLD-1 cells are based on two independent experiments.

LS411N cells showed 24 % growth inhibition when supplemented with DHA + pre- and co-incubated with vitamin E, and the protein level of Nrf2 was elevated 1.7 fold and ATF4 1.2 fold after the same treatment (Figure 27 and 28).
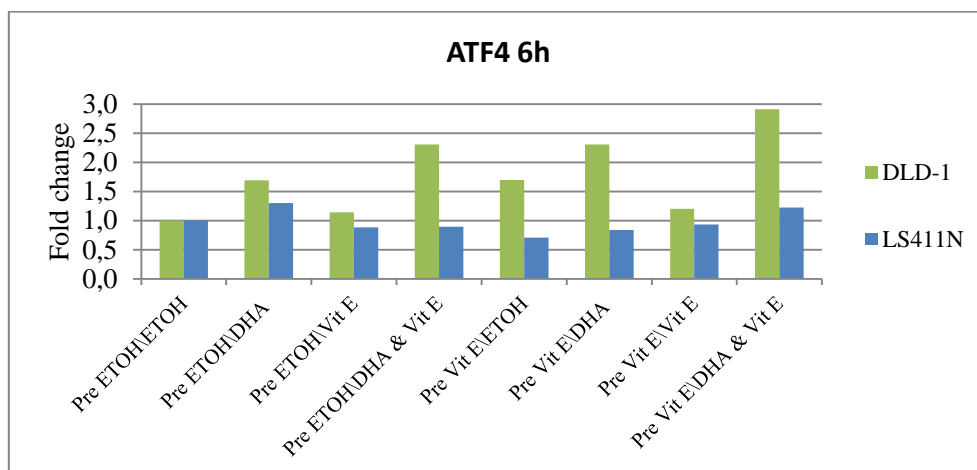


**Figure 27:** Fold change in protein expression of ATF4 in DLD-1 and LS411N cells after incubation with EtOH (70 μM), DHA (70 μM), and/or vitamin E (50 μM) for 6 h. The results from LS411N cells are from only one experiment, while results from DLD-1 cells are based on two independent experiments.
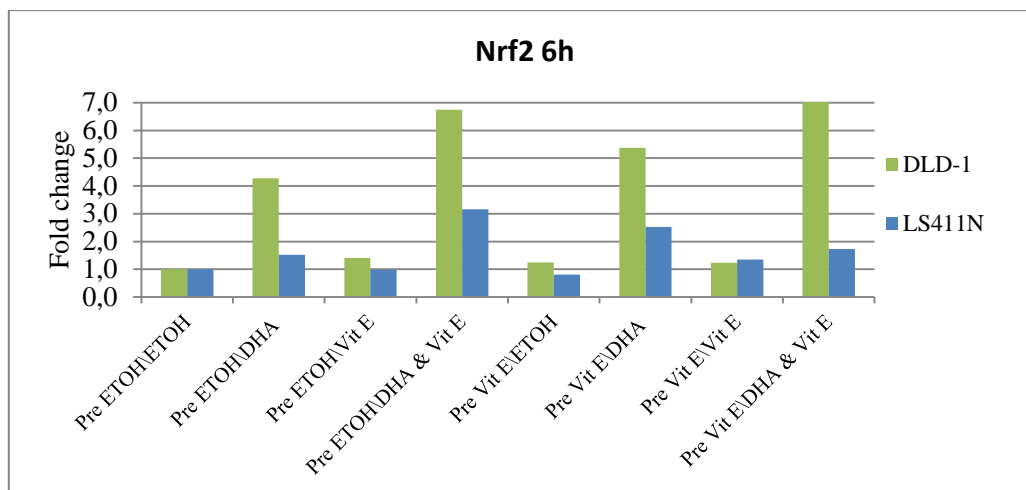
**Figure 28:** Fold change in protein expression of Nrf2 in DLD-1 and LS411N cells after incubation with EtOH (70 µM), DHA (70 µM), and/or vitamin E (50 µM) for 6 h. The results from LS411N cells are from only one experiment, while results from DLD-1 cells are based on two independent experiments

The results presented above were also confirmed by confocal imaging showing that co-incubation of vitamin E and DHA, and vitamin E alone, increases ATF4 expression in the nucleus in DLD-1 cells (Figure 29A). In the LS411N cells, there seemed to be more ATF4 in the nucleus after co-incubation of vitamin E and DHA, and vitamin E alone, but not to the same extent as observed in DLD-1 cells (Figure 29B).

**A**
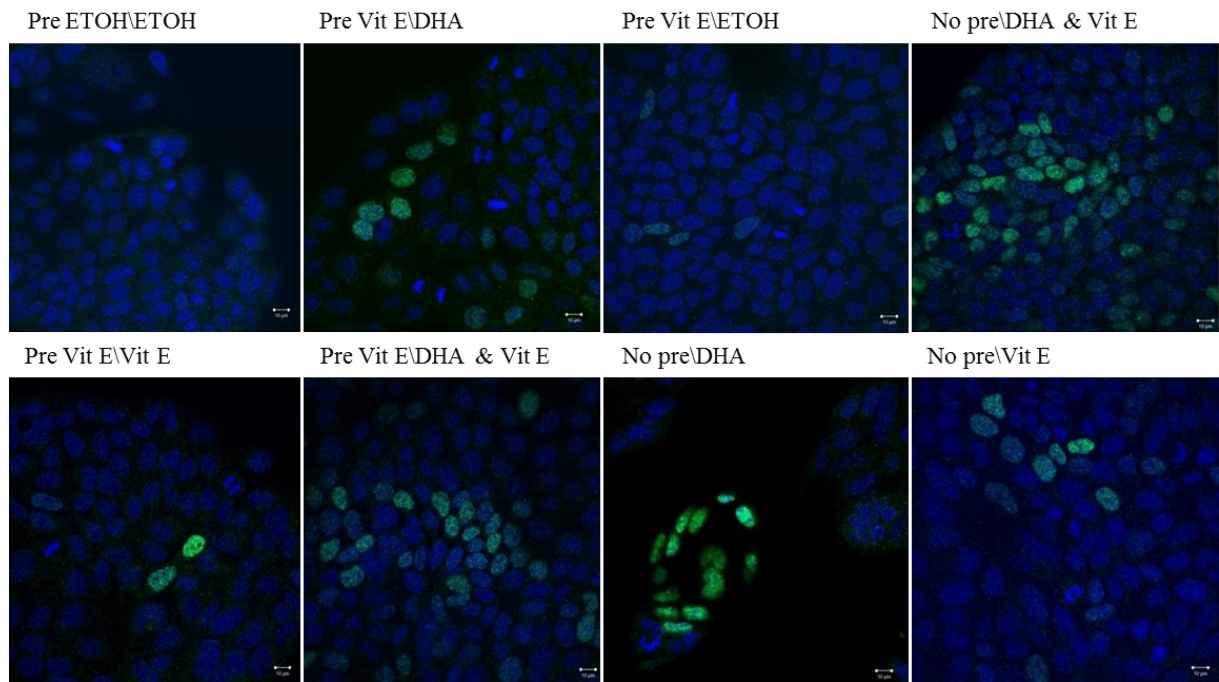


**B**
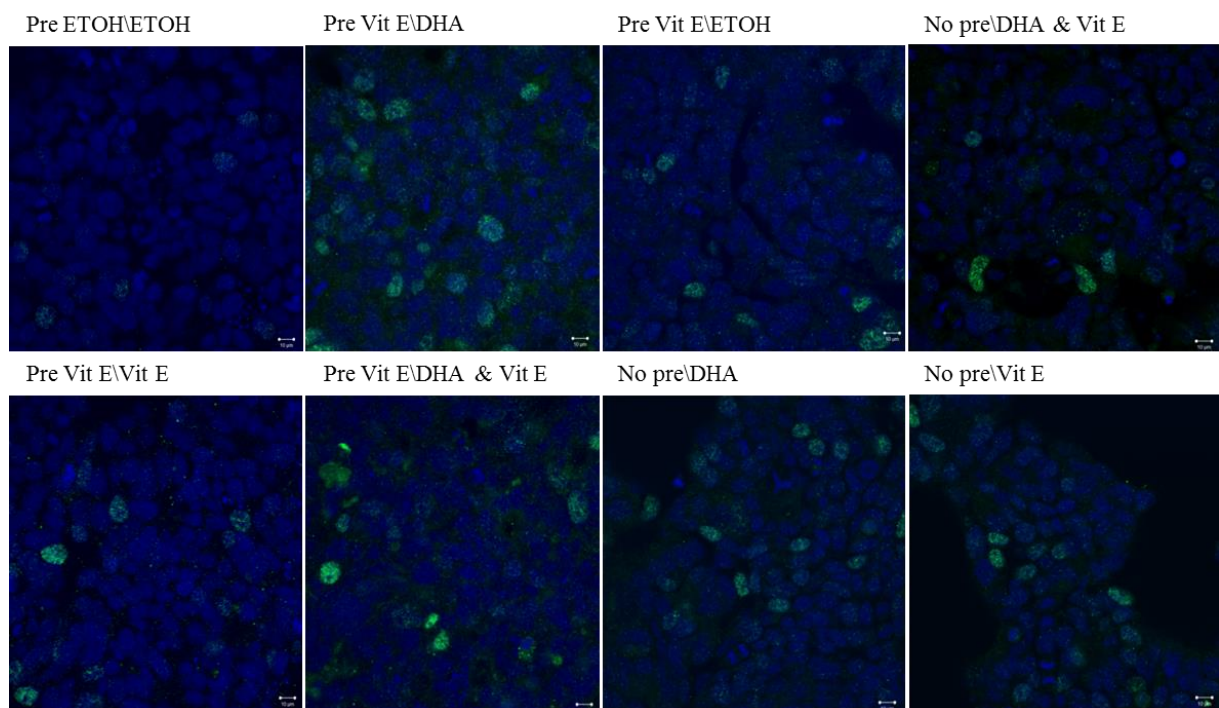


**Figure 29:** Cellular localization of ATF4 in DLD-1 **(A)** and LS411N **(B)** cells after incubation with EtOH (70 µM), DHA (70 µM), and/or vitamin E (50 µM) for 6 h. Both cell lines are stained with ATF4 (green) and Draq5 (blue). Results are based on one experiment, and are therefore not significant.

The Nrf2 protein level was higher in the nucleus of DLD-1 cells after DHA treatment with pre- and co-incubation with vitamin E (Figure 30A), while no change in Nrf2 level was seen with the indicated treatments in LS411N cells (Figure 30B).

**A**



**B**
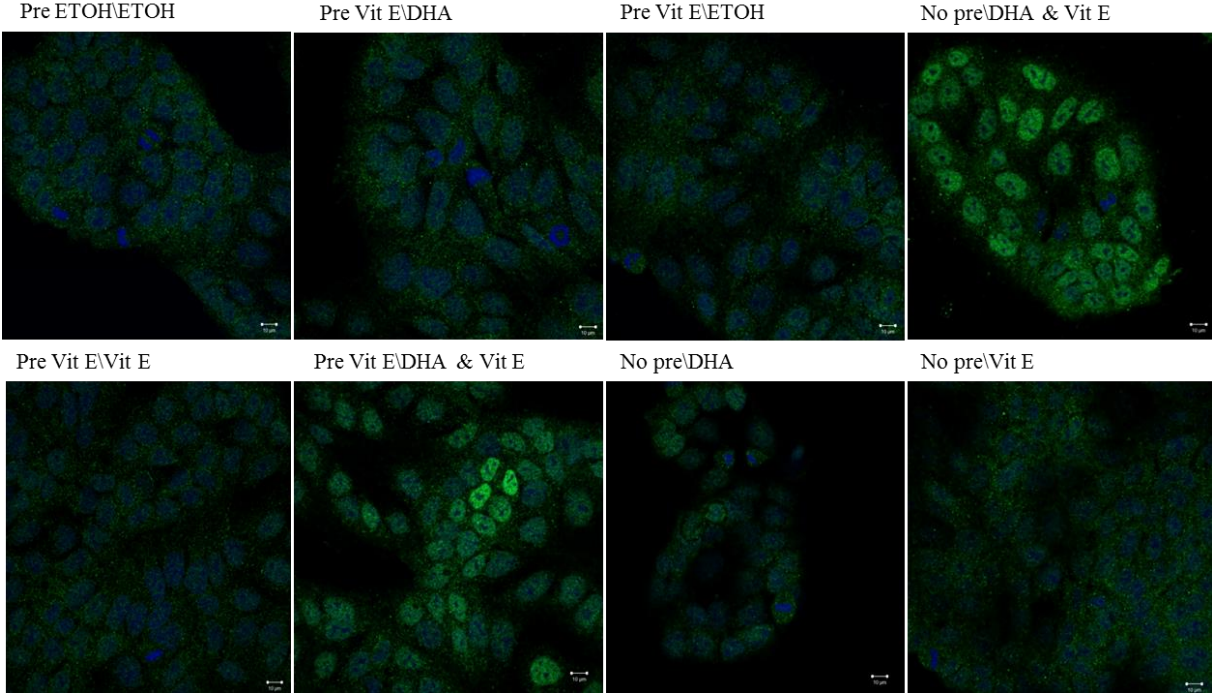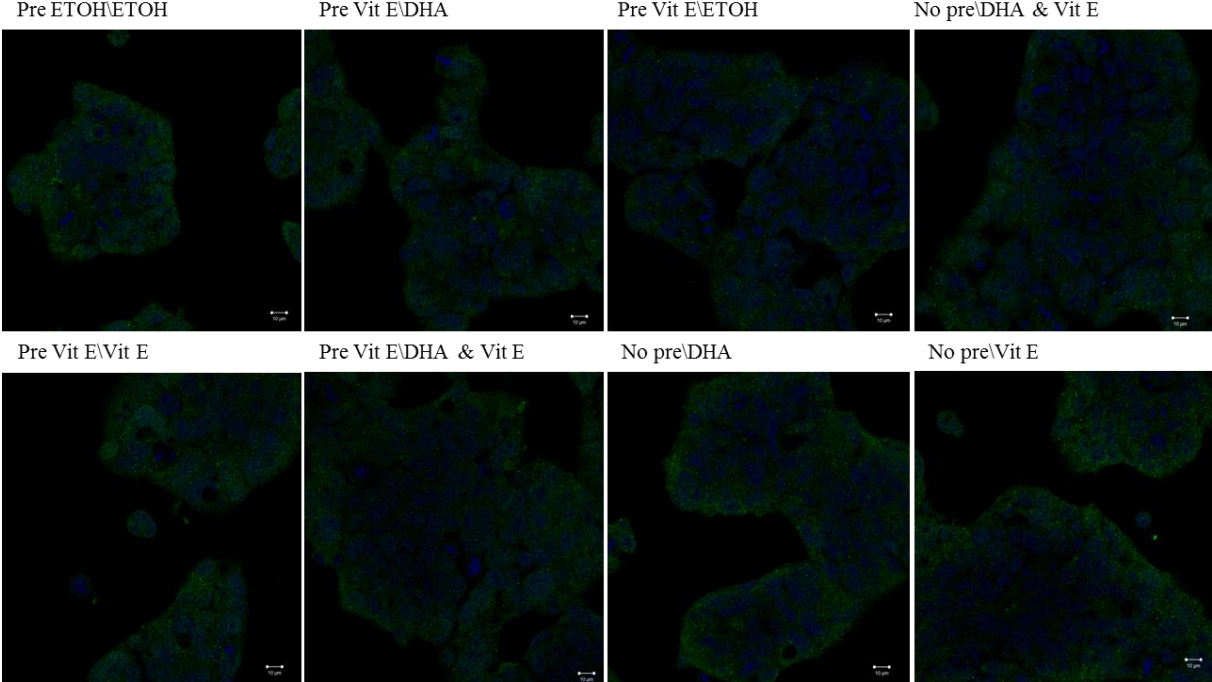
**Figure 30:** Cellular localization of Nrf2 in DLD-1 **(A)** and LS411N **(B)** cells after incubation with EtOH (70 μM), DHA (70 μM), and/or vitamin E (50 μM) for 6 h. Both cell lines are stained with Nrf2 (green) and Draq5 (blue). Results are based on one experiment, and are therefore not significant.

# 4. Discussion

DHA is known to induce different growth responses in cancer cells. The data presented here suggest that DHA causes different stress responses in the two human colon cancer cell lines, DLD-1 and LS411N. The DHA sensitive DLD-1 cell line had an earlier and more pronounced induction of ER-stress and autophagy compared to the less sensitive LS411N cells when treated with DHA. Although ATF4 was upregulated at all timepoints in DHA treated DLD-1 cells, preliminary results indicate that knockdown of ATF4 does not influence the growth inhibitory effect of DHA, suggesting that ATF4 alone is not responsible for the DHA mediated cell cytotoxicity in DLD-1 cells.

## 4.1. DHA induces different growth responses in human colon cancer cell lines

Based on unpublished cell viability data (MTT assay) from our group on different human colon cancer cell lines, and by evaluating the response of these cell lines towards DHA by cell counting, the two cell lines DLD-1 and LS411N were selected for further investigation. The selection was based on their different sensitivity towards DHA and that both cell lines could be cultivated in the same type of growth medium. The DLD-1 cells were clearly sensitive towards DHA with a time and dose dependent growth reduction, while the growth of LS411N cells was not affected under the same condition. This is in agreement with previous studies showing that DHA causes growth inhibition in several human colon cancer cell lines [17, 18, 62]. OA did not influence the growth of any of these cell lines, indicating that n-9 PUFAs don`t have the same anti-cancer properties as DHA. Further experiments should include n-6 PUFAs, to ensure that the growth inhibitory effects are n-3 PUFA specific. The culture medium, especially differences in serum concentrations, may affect cells sensitivity towards DHA [63]. Findings from different groups have shown that serum seems to have a protective effect; cell lines with higher serum concentrations were able to tolerate PUFAs better [64, 65]. By cultivating both cell lines in the same growth medium, the non-PUFA specific effects were reduced. Differences in growth rates are another factor that may affect the response of cells towards DHA, as the cells sensitivity may increase/decrease depending on whether they are in a proliferative or dormant phase (reviewed in [66]). The DLD-1 and LS411N cells have a doubling time of about 22 h and 40 h, respectively, which could influence the differences in sensitivity towards DHA. To make sure that both cell lines were in a proliferative phase, the DHA sensitivity was evaluated at different timepoints, by counting cells 24 and 48 h after

DHA supplementation, and by monitoring the cells 96 h after treatment by the MTT assay. Differences in cell density may also influence the sensitivity towards DHA in some cell lines, where some cells are more sensitive at lower cell densities (reviewed in [66]). Even though the results from cell counting and MTT assay are a bit different, they show the same trend. The MTT assay may depend on several different factors such as the cells ability to metabolize glucose and to form formazan [67].

## 4.2. DHA-supplementation induces ER stress and UPR-related gene- and protein expression in the DHA sensitive DLD-1 cell line

RT-PCR array analysis of DHA-treated DLD-1 cells (70 μM, 6h) indicated upregulation of several UPR-related transcripts. Among these, ATF4 was elevated 1.7 fold, and GADD34 (PPP1R15A), which is known to be induced by ATF4, 1.5 fold. Also induced were several chaperones and heat shock proteins. This indicates that the PERK-ATF4 branch of the ER stress was activated. In addition, IRE 1, EDEM1 and JNK were upregulated at mRNA level, indicating induction of ERAD and a possible link to apoptosis through JNK signaling. This is in line with previous studies by Jakobsen et al. (2008) who showed that DHA induces ER stress in the DHA sensitive human colon cancer cell line SW620 [16]. However, the effect of PUFA`s on ER stress-related genes are not restricted to cancer cells, as shown by a recent study by Myhrstad et al. (2014) who found elevated expression of genes related to cell cycle, ER stress and apoptosis in pheripheral blood mononuclear cells from healthy subjects after 7 weeks with fish oil intake [68]. ER stress and UPR were further established at protein level already 3 h after DHA treatment in DLD-1 cells. This was demonstrated by elevated protein levels of the PERK-eIF2α-ATF4 branch of UPR. In contrast, in the insensitive LS411N cells, the ER stress response was induced at later timepoints, and not to the same extent. Due to the central role of ATF4 having both a pro-survival and pro-apoptotic role, possibly depending on the degree of upregulation, the focus for this study was ATF4, its upstream inducers and downstream targets. A recent study, done on mouse embryo fibroblasts, found phosphorylated eIF2α to promote cell survival by limiting protein synthesis, while an upregulation of ATF4 and CHOP increased protein synthesis, causing ATP-depletion, oxidative stress and cell death. These findings indicate that cell survival depends on reduced protein synthesis, and not increased expression of ATF4 [45]. In light of these findings it seems that phosphorylated eIF2α are being transiently upregulated in response to ER stress, promoting cell survival by attenuating protein synthesis. Meanwhile, phosphorylated eIF2α induces the transcription of ATF4, which together with CHOP increases protein synthesis, leading to ROS and cell death

if ER homeostasis is not yet restored. Cancer cells have a very different metabolism, with high proliferation together with low vascularization, creating a hostile microenvironment with lower pH, oxygen, and nutrient supply than normal cells. The cells evolve ways to adapt to this stress and avoid ER stress-induced apoptosis. Studies have shown that the activity of PERK/eIF2α/ATF4 pathway is an important survival response of cancer during hypoxic stress, which is a very common stress factor in cancer cells, making it a potential therapeutic target (reviewed in [69]). ATF4 is found upregulated in many human tumors, and promotes survival through the upregulation of asparagine synthetase (ASNS) [70], which was induced at mRNA level in DLD-1 cells, and by negatively regulating genes involved in senescence [71]. Although the ER stress response is an important survival mechanism in cancer cells, prolonged and severe ER stress may exceed the capacity of this response, thereby turning into a pro-apoptotic signal. CHOP is a known mediator of ER stress-induced apoptosis, and was upregulated at protein level at all timepoints in DLD-1 cells.

## 4.3. DHA induces autophagy in the DHA sensitive DLD-1 cell line, but not in the DHA insensitive LS411N cell line

ATF4 is known to induce autophagy, and in correlation with results presented above showing an upregulation of ATF4, at both mRNA and protein level, autophagic flux seemed to be increased in the DLD-1 cells after DHA treatment at both 12 and 24 h, represented by an upregulation of lipidated LC3B (LC3B II), while it remained unchanged in the LS411N cells. TRIB3 is a negative regulator of the AKT pathway, and was found upregulated in DHA-treated DLD-1 cells, both on mRNA and protein level, indicating a possible connection between ER stress and autophagy. Several in vitro and in vivo studies have shown that DHA induces apoptosis in cancer cells (reviewed in [72]). Some previous studies have shown that conjugated DHA and EPA induce apoptosis in the DLD-1 cells [60] [61]. In line with our preliminary results, Jing et al. (2011) and Shin et  al. (2013) found that DHA induced autophagy in DHA sensitive human cancer cells [58, 73]. Jing et al. found that DHA-induced autophagy was accompanied by loss of p53, and an increase in autophagy was found when inhibiting p53, indicating that p53 could be a possible mediator of DHA-induced autophagy. Further findings showed the active form of AMP-activated protein kinase (AMPK) to be elevated along with reduced activity of mTOR, implicating that DHA induces autophagy through p53/AMPK/mTOR in cancer cells harboring wild type p53. Inhibition of autophagy was shown to suppress apoptosis, and induction of autophagy increased apoptosis in DHA-treated human cancer cells, indicating that apoptosis and autophagy occurred simultaneously,

both contributing to the DHA mediated cytotoxicity [73]. Shin et al. recently found that DHA induced apoptosis and autophagy by reducing phosphorylated AKT and phosphorylated mTOR in prostate cancer cells, independent of p53 status. The effect was almost completely blocked by adding the antioxidant N-acetyl-cysteine (NAC), suggesting that the DHA-induced suppression of the AKT-mTOR pathway was mediated by ROS [58]. Basal levels of autophagy is necessary for maintaining cellular homeostasis, while to high autophagy may help cell survival by rendering resistance to stress, or cause cell damage by degrading essential components of the cell. Autophagy may also act as an energy source to apoptosis, which is an ATP-dependent process [73]. Both DLD-1 and LS411N cell lines have mutations in p53, although DLD-1 still express p53, while LS411N cells have no trace of p53 [74]. Although these results are preliminary, these data indicate differences between the two cell lines in their ability to induce autophagic flux, which may influence their sensitivity towards DHA.

## 4.4. Significance of ATF4 and ER stress on survival in DLD-1 cells

As mentioned, ATF4 was found to be highly expressed at both mRNA and protein level after DHA treatment in DLD-1 cells. Since ATF4 is important for survival after induction of ER stress, or induction of apoptosis when ER stress is severe, it was exciting to try to knock down ATF4 using siRNA. Results from the ATF4 knockdown experiment, showed the importance of ATF4 and its downstream targets on growth of DLD-1 cells. ATF4 siRNA reduced the growth of DLD-1 control cells, but did not seem to influence the degree of DHA-mediated growth inhibition. The reduced growth in DLD-1 cells after knocking down ATF4 is in agreement with another study by Ye et al. (2010), which found a similar growth reduction in DLD-1 using short hairpin RNA (shRNA) to knock down ATF4. They found that knocking down ATF4 in DLD-1 cells led to $G_1/S$ arrest and apoptosis, when cultivated without non-essential amino acids (NEAA). Both $G_1$ arrest and apoptosis were reversed by adding NEAA, indicating that ATF4 knockdown induced amino acid starvation, causing reduced proliferation and apoptosis. A reduction in ASNS was found by knocking down ATF4, and by overexpressing ASNS or supplementing with asparagine, they were able to almost abolish the growth reduction in cancer cells, proving the importance of the GCN2-eIF2α-ATF4 in maintaining metabolic homeostasis in cancer cells [70]. Although our preliminary results may indicate that activation of the PERK/eIF2α/ATF4 arm of UPR may not be the main cause of DHA-induced growth inhibition in DLD-1 cells, the growth inhibitory effect of DHA may still be mediated by ER stress. IRE1 is shown to induce apoptosis by stimulation of ASK1,

which activates JNK and P38 MAPK. P38 MAPK activates CHOP, while JNK promotes apoptosis by inactivation of anti-apoptotic Bcl-2 and activation of pro-apoptotic Bim. As mentioned, both IRE1 and JNK mRNA were found upregulated by 1.5 fold compared to control after 6h of DHA incubation using RT-PCR. The protein expression of CHOP, which may be induced by all three arms of UPR, was elevated at protein level at all timepoints in the DLD-1 cells. A study by Matsumoto et al. used siRNA to knock down ATF4 (the same siRNA used in this work) and CHOP to investigate the effect on ER-induced autophagy and apoptosis. They found that CHOP siRNA completely suppressed apoptosis, while autophagy was activated with enhanced ATF4 and reduced CHOP expression. When using ATF4 siRNA, the formation of autophagosomes was inhibited, indicating that ATF4 is the key signal to ER stress-induced autophagy. The authors concluded that the change over switch between apoptosis and autophagy is probably located between ATF4 and CHOP [56]. TRIB3 has been proposed by Ohoka et al. (2005) to be an important sensor of ER stress-induced apoptosis by blocking CHOP and ATF4 during mild ER stress, while leading to apoptosis during severe ER stress when TRIB3 is induced in excess. The CHOP/TRIB3 pathway may operate in response to other stress signals as well [30]. TRIB3 and CHOP were both induced in DLD-1 cells, and as shown by Ohoka et al., their induction may not be dependent on ATF4, which still makes the CHOP-TRIB3 pathway a potential inducer of apoptosis in DHA treated DLD-1 cells. Further work is needed to elucidate the role of ER stress in DHA-induced cytotoxicity. With CHOP being an important mediator of ER stress-induced apoptosis, the effect of knocking down CHOP mRNA on DHA mediated growth inhibition should be investigated.  Also, the effect on DHA-induced autophagy in DLD-1 cells transfected with siATF4 should be investigated, especially focusing on the AKT/mTOR signaling pathway, which has been found downregulated by DHA in previous studies.

## 4.5.   Lipid peroxidation does not seem to mediate the DHA-induced growth inhibition in DLD-1 cells

Lipid peroxidation has been proposed as a main mechanism for PUFA-mediated growth inhibition in human cancer cells.  Results from previous studies indicate however that there are differences between cell lines in regard to their sensitivity towards lipid peroxidation [18]. Also, cancer cells having deficiencies in the antioxidant defense system, like glutathione peroxidase (GSH-Px), seem more prone to oxidative damage induced by omega-3 PUFAs. Schønberg et al. (1997, 2006) reported an increase in malondialdehyde (MDA), a secondary lipid peroxidation product, in both DHA-sensitive and DHA-resistant cell lines after DHA-

and EPA-treatment for different time periods [18, 75]. The least n-3 PUFA sensitive cell line A-172 showed the highest level of MDA after 48 h compared to the most sensitive cell line A-427. Vitamin E reduced the level of MDA below that in control cultures in all cell lines tested. However, vitamin E was not able to restore cell growth in all cell lines in regard to n-3 PUFA-induced cytotoxicity. These results imply that there is no correlation between the amount of MDA produced by lipid peroxidation and PUFA-induced cytotoxicity in different cancer cells.

Vitamin E was not able to counteract the growth inhibitory effect of DHA in DLD-1 cells, and decreased the growth of cells supplemented with vitamin E only. Also, vitamin E reduced growth of LS411N cells alone and in combination with DHA. Studies have shown that different forms of vitamin E may have cytotoxic effects on some human cancer cell lines [76, 77]. The differences in the protein level of Nrf2 in DLD-1 and LS411N cells in response to DHA, may indicate differences in the antioxidant defense between the two cell lines. Also, since ATF4 induces target genes involved in antioxidant functions, by interacting with Nrf2 (reviewed in [25]), we wanted to examine the protein level of ATF4 and Nrf2 after treatment with DHA alone or in combination with vitamin E. Co-incubation of cells with DHA and vitamin E led to an upregulation of protein levels of ATF4 and Nrf2 in DLD-1 cells, and an increased level of ATF4 was also found when incubated with vitamin E only. Nrf2 was upregulated when co-incubated with DHA and vitamin E in LS411N cells, but ATF4 showed only a slight increase. These preliminary results are in line with recent findings showing that gamma-tocotrienol (γ-T3), a member of the vitamin E family, induces ER-stress and apoptosis in breast cancer cells, probably mediated through ATF4/CHOP [77-79]. This might also explain why LS411N cells were growth inhibited by co-treatment with DHA and vitamin E; with the highest growth reduction when both pre-incubated with vitamin E + co-incubated with DHA and vitamin E. Why there was no additional growth inhibitory effect of DHA in the DLD-1 cells when co-incubated with vitamin E, although ATF4 was more upregulated, may support our previous results from siATF4, indicating that the  growth inhibition by DHA is possibly not mediated only through ATF4.

# 5. Conclusions and future perspectives

DHA induced different growth response in two different human colon cancer cell lines, even though grown in the same culture medium. Unlike the DLD-1 cells, the LS411N cells did not show any growth inhibition upon DHA (70 µM) treatment. In DLD-1 cells, different ER stress-related proteins were induced at early timepoints, while in the LS411N cells these were only slightly upregulated at a later stage. This may indicate that differences in the ER stress response may be important regarding the differences in DHA sensitivity. However, the DHA-induced growth inhibition in DLD-1 cells was not influenced by knocking down ATF4, indicating that the PERK-eIF2α-ATF4 branch of the UPR is not alone responsible for the DHA-mediated growth inhibition. Preliminary results also indicate a possible difference between the two cell lines in the level of autophagic flux after DHA (70 µM) treatment; which seemed to be induced in DLD-1 cells, while remained unaffected in LS411N cells. This difference may possibly explain their different DHA-sensitivity. Furthermore, co-incubation with vitamin E did not counteract the DHA-induced growth inhibition in DLD-1 cells, suggesting that lipid peroxidation alone can not explain the DHA-mediated cytotoxicity.

The role of ER stress in DHA-mediated cytotoxicity should be further investigated. The effect of ATF4 knockdown on DHA-induced growth inhibition in DLD-1 cells must be confirmed. It would also be interesting to look at the effect of ATF4 knockdown on its downstream targets (CHOP, TRIB3, GADD34) after DHA treatment. The effect of DHA on other potential mediators of the ER stress response, like the IRE-JNK-CHOP and the ATF6 branches need to be further explored. Since ATF4 is known to induce autophagic mediators, the expression level of autophagy-related proteins, like LC3B II, should be examined after DHA treatment of DLD-1 cells in future ATF4 knockdown studies. Also, the experiments regarding autophagy should be repeated for both cell lines. Even though vitamin E did not counteract the DHA-induced growth inhibition, ROS may still be important for the effect of DHA. Future studies should include other antioxidants, such as NAC, since vitamin E only works on lipid peroxidation products. Regarding lipid peroxidation, the MDA level could also be examined in the DLD-1 and LS411N cell lines, to see whether lipid peroxidation is induced to different extents in the two cell lines. It would also be interesting to examine whether there are differences in the antioxidant defense between the two cell lines.
Only two types of FAs were used in this study, DHA (n-3 PUFA) and OA (n-9 PUFA), therefore the effect of other FAs, such as n-6 PUFAs, should be investigated, to ensure n-3

PUFA-specific responses. Normal cell lines should also be included in future studies to make sure the effect of DHA is cancer specific.

# References

1.      Bang, H.O., J. Dyerberg, and H.M. Sinclair, *The composition of the Eskimo food in north western Greenland.* Am J Clin Nutr, 1980. **33**(12): p. 2657-61.
2.      Skender, B., A.H. Vaculova, and J. Hofmanova, *Docosahexaenoic fatty acid (DHA) in the regulation of colon cell growth and cell death: a review.* Biomed Pap Med Fac Univ Palacky Olomouc Czech Repub, 2012. **156**(3): p. 186-99.
3.      Calviello, G. and S. Serini, *Dietary Omega-3 Polyunsaturated Fatty Acids and Cancer.* 2010.
4.      Harris, A.W.C.C., *Multistage carcinogenesis*. 6th ed. Holland-Frei cancer medicine, ed. P.R. Kufe DW, Weichselbaum RR. 2003: BC Decker Inc.
5.      Hanahan, D. and R.A. Weinberg, *Hallmarks of cancer: the next generation.* Cell, 2011. **144**(5): p. 646-74.
6.      [http://kreftregisteret.no/no/Generelt/Publikasjoner/Cancer-in-Norway/Cancer-in-Norway-2011/](http://kreftregisteret.no/no/Generelt/Publikasjoner/Cancer-in-Norway/Cancer-in-Norway-2011/).
7.      Ratnayake, W.M. and C. Galli, *Fat and fatty acid terminology, methods of analysis and fat digestion and metabolism: a background review paper.* Ann Nutr Metab, 2009. **55**(1-3): p. 8-43.
8.      Richard Harvey, D.F., *Lippincott`s illustrated reviews: Biochemistry*. Fifth ed. Lippincott`s illustrated reviews, ed. R.A. Harvey. 2008.
9.      Tvrzicka, E., et al., *Fatty acids as biocompounds: their role in human metabolism, health and disease--a review. Part 1: classification, dietary sources and biological functions.* Biomed Pap Med Fac Univ Palacky Olomouc Czech Repub, 2011. **155**(2): p. 117-30.
10.     Arild C Rustan, C.D., *Fatty Acids: Structures and Properties.* Encyclopedia of life sciences, 2005.
11.     Chaves, V.E., D. Frasson, and N.H. Kawashita, *Several agents and pathways regulate lipolysis in adipocytes.* Biochimie, 2011. **93**(10): p. 1631-40.
12.     Russell, F.D. and C.S. Burgin-Maunder, *Distinguishing health benefits of eicosapentaenoic and docosahexaenoic acids.* Mar Drugs, 2012. **10**(11): p. 2535-59.
13.     *Fats and fatty acids in human nutrition. Report of an expert consultation.* FAO Food Nutr Pap, 2010. **91**: p. 1-166.
14.     Cockbain, A.J., G.J. Toogood, and M.A. Hull, *Omega-3 polyunsaturated fatty acids for the treatment and prevention of colorectal cancer.* Gut, 2012. **61**(1): p. 135-49.
15.     Zand, H., et al., *Docosahexaenoic acid sensitizes Ramos cells to Gamma-irradiation-induced apoptosis through involvement of PPAR-gamma activation and NF-kappaB suppression.* Mol Cell Biochem, 2008. **317**(1-2): p. 113-20.
16.     Jakobsen, C.H., et al., *DHA induces ER stress and growth arrest in human colon cancer cells: associations with cholesterol and calcium homeostasis.* J Lipid Res, 2008. **49**(10): p. 2089-100.
17.     Calviello, G., et al., *n-3 PUFAs reduce VEGF expression in human colon cancer cells modulating the COX-2/PGE2 induced ERK-1 and -2 and HIF-1alpha induction pathway.* Carcinogenesis, 2004. **25**(12): p. 2303-10.
18.     Schonberg, S.A., et al., *Closely related colon cancer cell lines display different sensitivity to polyunsaturated fatty acids, accumulate different lipid classes and downregulate sterol regulatory element-binding protein 1.* Febs j, 2006. **273**(12): p. 2749-65.
19.     Calviello, G., S. Serini, and E. Piccioni, *n-3 polyunsaturated fatty acids and the prevention of colorectal cancer: molecular mechanisms involved.* Curr Med Chem, 2007. **14**(29): p. 3059-69.
20.     Dupertuis, Y.M., M.M. Meguid, and C. Pichard, *Colon cancer therapy: new perspectives of nutritional manipulations using polyunsaturated fatty acids.* Curr Opin Clin Nutr Metab Care, 2007. **10**(4): p. 427-32.
21.     Mukutmoni-Norris, M., N.E. Hubbard, and K.L. Erickson, *Modulation of murine mammary tumor vasculature by dietary n-3 fatty acids in fish oil.* Cancer Lett, 2000. **150**(1): p. 101-9.

22.     Chakrabarti, A., A.W. Chen, and J.D. Varner, *A review of the mammalian unfolded protein response.* Biotechnol Bioeng, 2011. **108**(12): p. 2777-93.

23.     Schroder, M., *Endoplasmic reticulum stress responses.* Cell Mol Life Sci, 2008. **65**(6): p. 862-94.

24.     Gorman, A.M., et al., *Stress management at the ER: regulators of ER stress-induced apoptosis.* Pharmacol Ther, 2012. **134**(3): p. 306-16.

25.     Ameri, K. and A.L. Harris, *Activating transcription factor 4.* Int J Biochem Cell Biol, 2008. **40**(1): p. 14-21.

26.     Wang, W.A., J. Groenendyk, and M. Michalak, *Endoplasmic reticulum stress associated responses in cancer.* Biochim Biophys Acta, 2014.

27.     Ding, W.X., S. Manley, and H.M. Ni, *The emerging role of autophagy in alcoholic liver disease.* Exp Biol Med (Maywood), 2011. **236**(5): p. 546-56.

28.     Miyoshi, N., et al., *Abnormal expression of TRIB3 in colorectal cancer: a novel marker for prognosis.* Br J Cancer, 2009. **101**(10): p. 1664-70.

29.     Jousse, C., et al., *TRB3 inhibits the transcriptional activation of stress-regulated genes by a negative feedback on the ATF4 pathway.* J Biol Chem, 2007. **282**(21): p. 15851-61.

30.     Ohoka, N., et al., *TRB3, a novel ER stress-inducible gene, is induced via ATF4-CHOP pathway and is involved in cell death.* Embo j, 2005. **24**(6): p. 1243-55.

31.     Cullinan, S.B., et al., *Nrf2 is a direct PERK substrate and effector of PERK-dependent cell survival.* Mol Cell Biol, 2003. **23**(20): p. 7198-209.

32.     Komatsu, M., et al., *The selective autophagy substrate p62 activates the stress responsive transcription factor Nrf2 through inactivation of Keap1.* Nat Cell Biol, 2010. **12**(3): p. 213-23.

33.     Darling, N.J. and S.J. Cook, *The role of MAPK signalling pathways in the response to endoplasmic reticulum stress.* Biochim Biophys Acta, 2014.

34.     Pettersen, C.H., *The effect of omega-3 polyunsaturated fatty acids on human colon cancer cells.* 2012, NTNU: Trondheim, Norway.

35.     Sano, R. and J.C. Reed, *ER stress-induced cell death mechanisms.* Biochim Biophys Acta, 2013. **1833**(12): p. 3460-70.

36.     Schroder, M. and R.J. Kaufman, *The mammalian unfolded protein response.* Annu Rev Biochem, 2005. **74**: p. 739-89.

37.     Mizushima, N., et al., *Autophagy fights disease through cellular self-digestion.* Nature, 2008. **451**(7182): p. 1069-75.

38.     Salazar, M., *Endoplasmic reticulum stress in health and disease.* ER stress as modulator of autophagy pathways. 2012: Springer science. 163-184.

39.     Li, J., et al., *The unfolded protein response regulator GRP78/BiP is required for endoplasmic reticulum integrity and stress-induced autophagy in mammalian cells.* Cell Death Differ, 2008. **15**(9): p. 1460-71.

40.     Samuels, Y., et al., *Mutant PIK3CA promotes cell growth and invasion of human cancer cells.* Cancer Cell, 2005. **7**(6): p. 561-73.

41.     Bjorkoy, G., et al., *p62/SQSTM1 forms protein aggregates degraded by autophagy and has a protective effect on huntingtin-induced cell death.* J Cell Biol, 2005. **171**(4): p. 603-14.

42.     Mizushima, N. and T. Yoshimori, *How to interpret LC3 immunoblotting.* Autophagy, 2007. **3**(6): p. 542-5.

43.     Wong, R.S., *Apoptosis in cancer: from pathogenesis to treatment.* J Exp Clin Cancer Res, 2011. **30**: p. 87.

44.     Li, X., K. Zhang, and Z. Li, *Unfolded protein response in cancer: the physician's perspective.* J Hematol Oncol, 2011. **4**: p. 8.

45.     Han, J., et al., *ER-stress-induced transcriptional regulation increases protein synthesis leading to cell death.* Nat Cell Biol, 2013. **15**(5): p. 481-90.

46.     Mosmann, T., *Rapid colorimetric assay for cellular growth and survival: application to proliferation and cytotoxicity assays.* J Immunol Methods, 1983. **65**(1-2): p. 55-63.

47.     Technologies, N., *ND-1000 Spectrophotometer, V3.1.1 Users manual*. 2005, USA.

48.     Qiagen, *RT<sup>2</sup> Profiler PCR Array Handbook*. 2012, USA.

49.     Bio-Rad, *Bio-Rad Protein Assay, instruction manual*. USA.

50.     Ogata, M., et al., *Autophagy is activated for cell survival after endoplasmic reticulum stress.* Mol Cell Biol, 2006. **26**(24): p. 9220-31.

51.     Yorimitsu, T., et al., *Endoplasmic reticulum stress triggers autophagy.* J Biol Chem, 2006. **281**(40): p. 30299-304.

52.     Hoyer-Hansen, M. and M. Jaattela, *Connecting endoplasmic reticulum stress to autophagy by unfolded protein response and calcium.* Cell Death Differ, 2007. **14**(9): p. 1576-82.

53.     Yorimitsu, T. and D.J. Klionsky, *Endoplasmic reticulum stress: a new pathway to induce autophagy.* Autophagy, 2007. **3**(2): p. 160-2.

54.     Kouroku, Y., et al., *ER stress (PERK/eIF2alpha phosphorylation) mediates the polyglutamine-induced LC3 conversion, an essential step for autophagy formation.* Cell Death Differ, 2007. **14**(2): p. 230-9.

55.     B'Chir, W., et al., *The eIF2alpha/ATF4 pathway is essential for stress-induced autophagy gene expression.* Nucleic Acids Res, 2013. **41**(16): p. 7683-99.

56.     Matsumoto, H., et al., *Selection of autophagy or apoptosis in cells exposed to ER-stress depends on ATF4 expression pattern with or without CHOP expression.* Biol Open, 2013. **2**(10): p. 1084-90.

57.     Singleton, D.C. and A.L. Harris, *Targeting the ATF4 pathway in cancer therapy.* Expert Opin Ther Targets, 2012. **16**(12): p. 1189-202.

58.     Shin, S., et al., *The omega-3 polyunsaturated fatty acid DHA induces simultaneous apoptosis and autophagy via mitochondrial ROS-mediated Akt-mTOR signaling in prostate cancer cells expressing mutant p53.* Biomed Res Int, 2013. **2013**: p. 568671.

59.     Chapkin, R.S., et al., *Immunomodulatory effects of (n-3) fatty acids: putative link to inflammation and colon cancer.* J Nutr, 2007. **137**(1 Suppl): p. 200s-204s.

60.     Tsuzuki, T., et al., *Conjugated EPA activates mutant p53 via lipid peroxidation and induces p53-dependent apoptosis in DLD-1 colorectal adenocarcinoma human cells.* Biochim Biophys Acta, 2007. **1771**(1): p. 20-30.

61.     Igarashi, M. and T. Miyazawa, *Do conjugated eicosapentaenoic acid and conjugated docosahexaenoic acid induce apoptosis via lipid peroxidation in cultured human tumor cells?* Biochem Biophys Res Commun, 2000. **270**(2): p. 649-56.

62.     Hossain, Z., M. Hosokawa, and K. Takahashi, *Growth inhibition and induction of apoptosis of colon cancer cell lines by applying marine phospholipid.* Nutr Cancer, 2009. **61**(1): p. 123-30.

63.     Noding, R., et al., *Effects of polyunsaturated fatty acids and their n-6 hydroperoxides on growth of five malignant cell lines and the significance of culture media.* Lipids, 1998. **33**(3): p. 285-93.

64.     Griffiths, G., et al., *Effect of n-6 polyunsaturated fatty acids on growth and lipid composition of neoplastic and non-neoplastic canine prostate epithelial cell cultures.* Prostate, 1997. **31**(1): p. 29-36.

65.     Maehle, L., et al., *Effects of n-3 fatty acids during neoplastic progression and comparison of in vitro and in vivo sensitivity of two human tumour cell lines.* Br J Cancer, 1995. **71**(4): p. 691-6.

66.     Diggle, C.P., *In vitro studies on the relationship between polyunsaturated fatty acids and cancer: tumour or tissue specific effects?* Prog Lipid Res, 2002. **41**(3): p. 240-53.

67.     Vistica, D.T., et al., *Tetrazolium-based assays for cellular viability: a critical examination of selected parameters affecting formazan production.* Cancer Res, 1991. **51**(10): p. 2515-20.

68.     Myhrstad, M.C., et al., *Fish oil supplementation induces expression of genes related to cell cycle, endoplasmic reticulum stress and apoptosis in peripheral blood mononuclear cells: a transcriptomic approach.* J Intern Med, 2014.

69.     Martinon, F., *Targeting endoplasmic reticulum signaling pathways in cancer.* Acta Oncol, 2012. **51**(7): p. 822-30.

70.     Ye, J., et al., *The GCN2-ATF4 pathway is critical for tumour cell survival and proliferation in response to nutrient deprivation.* EMBO J, 2010. **29**(12): p. 2082-96.

71. Horiguchi, M., et al., *Stress-regulated transcription factor ATF4 promotes neoplastic transformation by suppressing expression of the INK4a/ARF cell senescence factors.* Cancer Res, 2012. **72**(2): p. 395-401.

72. Serini, S., et al., *Dietary polyunsaturated fatty acids as inducers of apoptosis: implications for cancer.* Apoptosis, 2009. **14**(2): p. 135-52.

73. Jing, K., et al., *Docosahexaenoic acid induces autophagy through p53/AMPK/mTOR signaling and promotes apoptosis in human cancer cells harboring wild-type p53.* Autophagy, 2011. **7**(11): p. 1348-58.

74. Liu, Y. and W.F. Bodmer, *Analysis of P53 mutations and their expression in 56 colorectal cancer cell lines.* Proc Natl Acad Sci U S A, 2006. **103**(4): p. 976-81.

75. Schonberg, S.A., et al., *Evidence that changes in Se-glutathione peroxidase levels affect the sensitivity of human tumour cell lines to n-3 fatty acids.* Carcinogenesis, 1997. **18**(10): p. 1897-904.

76. Schwartz, J. and G. Shklar, *The selective cytotoxic effect of carotenoids and alpha-tocopherol on human cancer cell lines in vitro.* J Oral Maxillofac Surg, 1992. **50**(4): p. 367-73; discussion 373-4.

77. Patacsil, D., et al., *Gamma-tocotrienol induced apoptosis is associated with unfolded protein response in human breast cancer cells.* J Nutr Biochem, 2012. **23**(1): p. 93-100.

78. Wali, V.B., S.V. Bachawal, and P.W. Sylvester, *Endoplasmic reticulum stress mediates gamma-tocotrienol-induced apoptosis in mammary tumor cells.* Apoptosis, 2009. **14**(11): p. 1366-77.

79. Park, S.K., B.G. Sanders, and K. Kline, *Tocotrienols induce apoptosis in breast cancer cell lines via an endoplasmic reticulum stress-dependent increase in extrinsic death receptor signaling.* Breast Cancer Res Treat, 2010. **124**(2): p. 361-75.

# Appendix

## Appendix A. Equipments and chemicals.

### Cell cultivation:

- Cellcultivation flasks (25 cm², 75 cm² and 175 cm²), Costar (USA).
- 6 and 12 well plates, Costar (USA).
- Tissue Culture dish, 150x20 mm, SPL Lifescience Co., Ltd (Korea).
- Clinical tube, 50 ml, SPL Lifescience Co., Ltd (Korea).
- Cellstar® tubes, 15 ml, greiner bio-one.
- Disposable Serological Pipettes (1 ml, 5 ml, 10 ml, 25 ml), Costar (USA).
- RPMI 1640 Medium, Gibco (England).
- Fetal bovine serum (FBS), Gibco (England).
- Phosphate buffered saline (PBS), Oxoid (England)
- Trypsin solution (0.25 %) with EDTA (0,02%), Lonza (Belgium)
- Gentamincin, 10 mg/ml, Gibco (England).

### Treatments:

- Docosahexaenoic acid (DHA, 50 mg in 200 µ EtOH), Lot: 0444840-9, Cayman (Ann Harbor, MI)
- Oleic Acid (OA, 500mg/ 1 ml EtOH), Lot: 0423813-6, Cayman (Ann Harbor, MI)
- Ethanol (Absolute alcohol prima), Arcus (Oslo, Norway)
- Thapsigargin (TG, 650,75 g/mol), Lot: 052M4144V, Sigma-Aldrich (USA)
- Vitamin E, α-tocopherol, Sigma-Aldrich (USA)
- Bafilomycin A1 (Baf A1, 0.16 mM) B1793-10UG, Sigma-Aldrich (USA)

### MTT assay:

- MTT, Sigma-Aldrich (USA)
- Isopropanol prima (2-propanol), Arcus (Norway)

### Imaging:

- Axiovert 200 microscope with confocal module LSM 510 Meta and a 63x1.2 W objective (Carl Zeiss)

- Zeiss LSM Image Examiner Software version 4.2.0.121

**Quantification of total RNA:**

- NanoDrop-1000 Spectrophotometer (ND-1000), NanoDrop Technologies (USA)

**Quality assessment of total RNA:**

- 2100 expert BioAnalyzer, Agilent Technologies

**Protein isolation:**

- EDTA (1M), Sigma-Aldrich (USA)
- Biorad protein assay dye reagent concentrate, Bio-Rad laboratories (USA)

**RNA-isolation:**

- RNeasy$^R$ Mini Kit, Qiagen
- RNase-Free DNase set, Qiagen

**Reverse transcriptase PCR:**

- RT² Profiler PCR Array, Qiagen
- RT² SYBR$^R$ Green ROX$^{TM}$ qPCR Mastermix, Qiagen
- RT² First Strand Kit, Qiagen
- AB1 StepOnePlus$^R$ instrument, Applied Biosystems (USA)

**Western blotting:**

- NuPAGE reducing agent, Life Technologies (USA)
- NuPAGE Sample buffer, Life Technologies (USA)
- NuPAGE Novex Bis-Tris gels, Life Technologies (USA)
- NuPAGE MOPS Running buffer, Life Technologies (USA)
- NuPAGE Antioxidant, Life Technologies (USA)
- NuPAGE transfer buffer, Life Technologies (USA)
- XCell Mini-Cell, Life Technologies (USA)
- XCell II Blot Module, Life Technologies (USA)

- PDVF membrane, Millipore (USA)

- Odyssey$^R$ protein  molecular weight marker, 928-40000, LI-COR biosciences (USA)

**Immunostaining:**

- Odyssey blocking buffer, LI-COR biosciences (USA)

**Transfection with siRNA:**

- Lipofectamine RNAiMax transfection reagent, Life Technologies (USA)

- ATF4 (#SI03019345, Qiagen)

- AllStars Hs Cell Death control, (#1027298, Qiagen)

- AllStars Negative Control (#1027280, Qiagen)

- SignalSilence control siRNA (Fluorescein conjungate, #6201, Cell Signaling)

# Appendix B. Buffers and solutions used for protein isolation and western blotting

**NuPAGE MOPS Running Buffer (1 L)**
50 mL 20xNuPAGE MOPS running buffer
950 mL dH2O

**NuPAGE Transfer Buffer (1 L)**
850 mL dH2O
100 mL methanol
50 mL NuPAGE Transfer Buffer

**Phosphate buffered saline (PBS) washing buffer (1 L)**
1 L dH2O
20 PBS tablets
(Add 10 mL Tween20 to make PBST)

**10xTris-buffered saline (TBS)**
200 mM (0.2 mol/L) Tris (hydroxymethyl)-aminomethan
1369 mM (1.369 mol/L) NaCl
*Making 1 L*
Mix 900 mL dH2O, 24.2 g Tris(hydroxymethyl)-aminomethan and 80 g NaCl. Adjust the pH to 7.6 by using concentrated HCl or NaOH. Add dH2O to get a total volume of 1 L.

**Tris-buffered saline (TBS) washing buffer (1 L)**
100 mL 10xTBS
900 mL dH2O
(Add 10 mL Tween20 to make TBST)

**Blocking buffer:**
50 % TBST + 50 % Odyssey blocking buffer

**Primary- and secondary antibody solution:**
Blocking buffer + primary/secondary antibody in appropriate dilution

**Table B.1**. Lysisbuffer used for isolation of total proteins.

| 8 M Urea lysisbuffer | Concentration | | In buffer | | 1000 µL | |
|---|---|---|---|---|---|---|
| **Urea** | 60.06 | g/mol | 8 | M | 0.48 | g |
| **Triton-X** | 100 | % | 0.50 | % | 5 | µL |
| **DTT** | 1 | M | 0.1 | M | 100 | µL |
| **PI / Complete** | 25 | X | 1 | X | 40 | µL |
| **PIC2** | 100 | X | 2 | X | 20 | µL |
| **PIC3** | 100 | X | 2 | X | 20 | µL |
| **MQ water** | | | | | 815 | µL |

**Table B.2**. Lysisbuffer used for isolation of phosphorylated proteins.

| Reagent | Amount | Consentration |
|---|---|---|
| **1 M NaCl** | 75 | 0.15 M |
| **1 M HEPES, pH 7,5** | 10 | O.02 M |
| **Glycerol 50 %** | 100 | 10 % |
| **Triton X-100** | 5 | 1 % |
| **O,5 M EDTA** | 1 | 0.001 M |
| **NaF 1 M** | 50 | 0.1 M |
| **0,3 M β-glycerol fosfat** | 29.2 | 0.0175 M |
| **Phosphatase inhibitor cocktail 1** | 10 | 2 % |
| **Phosphatase inhibitor cocktail 2** | 10 | 2 % |
| **Protease inhibitor** | 40 | 4 % |
| **MQ water** | 169.8 | 37.96 % |
| **Total** | 500 | |

**Table B.3.** Phosphate buffered saline (PBS) washing buffer used to isolate phosphorylated proteins, supplemented with Phosphatase inhibitors (PI) from the Nuclear extract kit (AMI).

| Reagent | $3{,}2 \times 10^6$ cells |
|---|---|
| **10 x PBS** | 0.4 ml |
| **Distilled water** | 3.4 ml |
| **Phosphatase inhibitors(from** | O.2 ml |
| **Total amount** | 4.0 ml |

# Appendix C. Buffers and anyibody solutions for immunofluorescent staining

**Blocking buffer:**

3 % Goat serum

97 % 1xPBS

**Primary/secondary antibody solution:**

1 % Goat serum

99 % 1xPBS

Primary/ secondary antibody (appropriate dilutions)

# Appendix D. Results from total RNA isolation

**Table D.1.** An overview of the concentrations and quality assessment of total RNA by measuring rRNA ratios and RIN values of samples from DLD-1 cells receiving different treatments; control (EtOH, 70 µM), DHA (70 µM) or TG (1 µM) for 3, 6 , 12 and 24 h.

| Sample | ND 1000 ng/µl | ND 1000 A260/A280 | ND 1000 A260/A230 | RIN | 28S/18S |
|---|---|---|---|---|---|
| **3 h control** | 602.4 | 2.1 | 1.9 | 10.0 | 2.5 |
| **3 h DHA (70 µM)** | 565.6 | 2.0 | 2.2 | 9.8 | 2.5 |
| **3 h TG (1 µM)** | 600.7 | 2.1 | 2.2 | 9.5 | 2.6 |
| **6 h control** | 567.4 | 2.1 | 2.2 | 9.2 | 2.2 |
| **6 h DHA (70 µM)** | 560.9 | 2.0 | 2.2 | 9.2 | 2.0 |
| **6 h TG (1 µM)** | 658.7 | 2.1 | 2.2 | 8.9 | 2.1 |
| **12 h control** | 711.8 | 2.1 | 2.1 | 10.0 | 2.3 |
| **12 h DHA (70 µM)** | 871.8 | 2.1 | 2.1 | 9.4 | 2.4 |
| **12 h TG (1 µM)** | 842.0 | 2.1 | 2.2 | 9.8 | 2.2 |
| **24 h control** | 688.9 | 2.1 | 2.1 | 9.3 | 2.1 |
| **24 h DHA (70 µM)** | 605.8 | 2.1 | 2.1 | 8.0 | 1.5 |
| **24 h TG (1 µM)** | 453.5 | 2.1 | 2.1 | 7.4 | 1.3 |

# Appendix E. Protein ladders
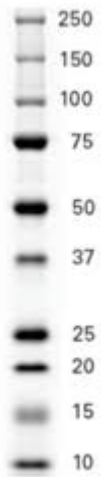


**Picture:** Odyssey protein molecular weight marker, 928-40000 (LI-COR biosciences)